12-19-2008

Abrupt Climate Change and Storm Surge Impacts in Coastal Louisiana in 2050

Jay Ratcliff
University of New Orleans

Abrupt Climate Change and Storm Surge Impacts in Coastal Louisiana in 2050

A Dissertation

Submitted to the Graduate Faculty of the
University of New Orleans
in partial fulfillment of the
requirements for the degree of

Doctor of Philosophy
In
Engineering and Applied Science

By

Jay Ratcliff

B.S. Tulane University, 1979
M.E. University of New Orleans, 1994

December 2008

To my mother

ACKNOWLEDGMENTS

My storm surge modeling team members, especially Dr. Joannes Westerink, provided me constant guidance and assistance in working with large finite element meshes and in understanding and executing the ADCIRC storm surge model. Vann Stutts and Dr. Don Resio first introduced me to the vast arena of statistical modeling and risk analyses. Andy Cox and Vince Cardone of Ocean Weather, Inc for use of their PBL wind model. I would also like to acknowledge my committee members help and support including Dr. George Ioup, Dr. Ioannis Georgiou, D. Martin Guillot, Dr. Donald Barbe, Dr. Bhaskar Kura, Dr. Joannes Westerink, and Dr. Alex McCorquodale. Dr. Alex McCorquodale has taught me over the years and allowed me to complete this research under his guidance. I will also be forever grateful to Dr. Alim Hannoura who has been and will always be my teacher, mentor, and friend.

Table Of Contents

List of Figures

List of Tables

List of Abbreviations

ADCIRC……Advanced Circulation Model
AR4……..… Fourth Assessment Report
CLEAR……..… Coastal Louisiana Ecosystem and Restoration
FAR…….. First Assessment Report
FEMA……. Federal Emergency Management Association
Ft……feet
GCM…….……... Global Climate Model
GFDL……. Geophysical Fluid Dynamics Laboratory
GWCE…….. Generalized Wave Continuity Equation
HWM…….. High Water Mark
IPCC…….. International Panel on Climate Change
IPET…….. Interagency Performance Evaluation Task
km……..…….…… kilometers
LACPR…… Louisiana Coastal Protection and Restoration
Ma…….……... Million years ago
mb…….…….…… millibars
MPI……...… Maximum Potential Intensity
nm…….…….…… nautical miles
PBL…… Planetary Boundary Layer
PDI……..…….. Power Dissipation Index
Prob……. probability
SAR……..… Second Assessment Report
SLR…….. Sea Level Rise
SPM……... Summary for Policy Makers
SRES……...… Special Report on Emission Scenarios
SST……...…… Sea Surface Temperature
sq…….…… square
TC……..…… Tropical Cyclone
THC……. Thermohaline Circulation
TAR……..... Third Assessment Report
USACE……...United States Army Corps of Engineers
USGS……..….. United States Geological Survey

Abstract

The most critical hazards impacting the world today are the affects of climate change and global warming. Scientists have been studying the Earth's climate for centuries and have come to agreement that our climate is changing, and has changed, many times abruptly over the history of our planet. This research focuses on the impacts of global warming related to increased hurricane intensities and their surge responses along the coast of the State of Louisiana. Surge responses are quantified for storms that could potentially occur under present climate but 50 years into the future on a coast subjected to current erosion and local subsidence effects. Analyses of projected hurricane intensities influenced by an increase in sea surface temperatures (SSTs) are performed. Intensities of these storms are projected to increase by 5% per degree of increase in SSTs. A small suite of these storms influenced by global warming and potentially realized by abrupt climate changes are modeled. Simulations of these storms are executed using a storm surge model. The surges produced by these storms are significantly higher than surges produced by present-day storms. These surges are then compared to existing surge frequency distributions along the Louisiana coast.

KEYWORDS: abrupt climate change, global warming, hurricanes, storm surge

Chapter 1 Introduction

1.1 Background

On the 29th August 2005 the world changed. Katrina was by far "the storm of the century" for the Gulf Coast. Then on the 24th September, less than a month later, Rita struck western Louisiana and eastern Texas. Not one, but two immense storms struck in relatively close proximity within less than one month. Katrina caused well over an estimated $100 billion in economic damages alone. But these storms were only two of a total of twenty six named storms of the year 2005. This was the very first year the alphabetical list of names was not long enough (the list has only 21 names since it excludes those beginning in Q, U, X, Y or Z). There were three Category 5 storms (Katrina, Rita, and Wilma) in one year. The last year to record 3 Category 5 storms was 1851. In 2005 Wilma was the most intense storm ever recorded in Gulf of Mexico.

Katrina devastated the city of New Orleans and the surrounding metropolitan area. Levees were breached in many locations in areas of St. Bernard and Plaquemines Parish, but the major New Orleans city flooding was due to the overtopping and breaks in the now infamous 17th Street and London Avenue Canal floodwalls. This catastrophe was not supposed to happen. Levees were breached in many of the surrounding areas including St. Bernard and New Orleans East. The floodwalls along the 17th Street Canal were estimated to have failed about 9:45 am on the 29th August, and the water could not

be stopped. The storm and flooding caused so much destruction and the tragedy that it became imperative to resolve the in detail the entire reasons and sequence of events that enabled such calamity to occur.

1.2 IPET

The Chief of Engineers, U.S. Army Corps of Engineers (USACE), established the Interagency Performance Evaluation Task (IPET) Force on October 10, 2005, by memorandum to the Director of Civil Works. IPET was sanctioned by the Secretary of Defense in a directive to the Secretary of the Army on October 19, 2005. The IPET mission was to provide credible and objective scientific and engineering answers to fundamental questions about the performance of the hurricane protection and flood damage reduction system in the New Orleans metropolitan area. This information is being used as it is developed to assist in the reconstitution of hurricane protection in New Orleans in the ongoing repair phase and to form a foundation for more effective hurricane protection in the future in New Orleans and in other parts of the nation that face similar threats.

The IPET was composed of 10 tasks, of which Task 4 was the Storm Surge Modeling and Wave Analyses. Task 4 scientists and engineers used the Advanced Circulation (ADCIRC) model for storm surge computations. (Luettich et. al. 1992; Westerink et al. 1992) ADCIRC is a state of the art program for solving the equations of motion of moving fluid on a rotating earth. Essentially, ADCIRC computes water surface elevations and currents in coastal oceans, estuaries, lakes, and rivers. Information on the ADCIRC model is provided in Chapter 2. Congress also directed the Corps of

Engineers, New Orleans District, in partnership with the State of Louisiana, to initiate a 24-month endeavor, the Louisiana Coastal Protection and Restoration (LACPR) Project. The LACPR project was mandated to identify, describe and propose a full range of flood control, coastal restoration, and hurricane protection measures for South Louisiana. Components of this project include characterization of a Saffir-Simpson Category 5 storm which is a 1-5 rating based on the hurricane's wind speed and intensity. This dissertation work will complement LACPR efforts and perform simulations some of the storm characteristics defined by LACPR project.

In addition to the impact to the people of the coast, the storms of 2005 caused great injury to the already disappearing Louisiana coastal wetlands. These wetlands and barrier islands reduce storm surge and help protect coastal cities and infrastructure. (Suhayda, 1997). The Louisiana Coastal Area (LCA) Study Report (USACE, Nov 2004) documents much of the history of the causes and disappearance of the wetlands. LCA Study Report, Appendix B, is the Historic and Projected Coastal Louisiana Land Changes 1978 – 2050. The USGS documents in Appendix B, the land loss (and some gain) from 1956 through 2000. Additionally, the USGS projected land loss rates through 2050. According to this report, the projected land loss from 2000 to 2050 is 674 sq miles (1,746 sq km) and land gain of 161 sq miles (417 sq km). All land loss and gain features, existing and projections, were encoded as layers in a Geographic Information System (GIS). This study was completed prior to Katrina and Rita, and did not consider such devastation as caused by the record storms of 2005.

1.3 Global Climate Change

Katrina increased the debate over the global climate change caused by man made "green house gases" (TIME, August 2005). People wanted to know if Katrina and the other very powerful storms could have been caused by human induced global climate warming. Ultimately, it is fundamentally impossible to prove an individual storm was caused by human (CO_2) induced global climate change. Our weather each day is one realization of an infinite number of possibilities created by the many forces that form and create our climate. The weather is semi-random by nature and conversely, it would not be defensible to say a specific single event as Katrina was caused by the long-term natural climate cycle alone.

There is much evidence that the scientific community has agreed that natural cycles alone cannot explain recent ocean warming (IPCC AR4, 2007). Due to human activities such as burning fossil fuels, clearing forests, etc., today's carbon dioxide (CO_2) levels in the atmosphere are significantly higher than at any time during the past 400,000 years. CO_2 and other heat-trapping emissions act like insulation in the lower atmosphere, warming land and ocean surface temperatures (Houghton et al. 2001). Oceans have absorbed most of this excess heat, raising sea temperatures by almost one degree Fahrenheit since 1970. September sea surface temperatures in the Atlantic over the past decade have risen far above levels documented since 1930 (Online at http://www.ncdc.noaa.gov accessed April, 2006). Increases in both the horizontal and temporal characteristics of ocean changes over the last 45 years have been closely replicated by the state-of-the-art Parallel Climate Model (PCM) forced by observed and

estimated anthropogenic gases. (Barnett et al., 2001) The PCM results provide credible weight for claims that an anthropogenic signal has been detected in the global climate model system.

Although scientists agree that global warming is underway, there is significant controversy over the relation between hurricanes and climate change. Research over the past few years has indicated potential links between global warming and hurricane size and energy (Emanuel, (2005, 2005a); Mann and Emanuel, 2006). Hurricanes are a complex phenomena and their formation is affected by sea surface temperature, wind speeds and directions, humidity, and other ocean and atmospheric conditions. A 2004 study analyzed the relationships of today's storms with simulated storms for increased concentrations of CO_2 (the primary greenhouse gas) (Knutson and Tuleya, 2004). A total of nine different global climate models were executed, all with the same amount of increased CO_2, a +1% yr^{-1} for 80 years. These GCM results formed boundary conditions for an idealized hurricane model, the Geophysical Fluid Dynamics Laboratory (GFDL) R30 coupled model. Approximately 1300 5-day simulations were performed with a high resolution GFDL R30 model. Results from all of the simulations were aggregated and averaged. They indicate a 14% increase in central pressure fall, a 6% increase in maximum surface wind speed, and an 18% increase in average precipitation rate within 100 km of the storm center. Current hurricane potential intensity theories were also applied to the climate model environments in this study. These theories show an average increase in intensity (pressure fall) of 8% (Emanuel convective parameterization model) to 16% (Holland model) or the high-CO_2 environments. Convective available potential

energy (CAPE) is 21% higher on average in the high-CO_2 environments. One implication of these results is that if the frequency of tropical cyclones remains the same over the coming century, a greenhouse gas–induced warming may lead to a gradually increasing risk in the occurrence of highly destructive category-5 storms.

Even more recently, a 2005 study demonstrated a statistical link of global warming to an increase in storm intensity and duration. (Emanuel, 2005) The study suggests intensity and duration relationships to increased sea surface temperatures associated with global warming, specifically during the past 10 years. During this time global average sea surface temperatures were at record levels (Online at http://www.ncdc.noaa.gov accessed April, 2006). The destructive power of storms can be measured by the total power dissipation (PD). (Emanuel, 1998). The PD is defined as

$$\mathrm{PD} = 2\pi \int_0^{\tau} \int_0^{r_0} C_D \rho |\mathrm{V}|^3 r \mathrm{d}r \mathrm{d}t \qquad \text{Eq. (1.3.1)}$$

where C_D is the surface drag coefficient, ρ the surface air density, $|V|$ is the magnitude of the surface wind, and the integral is over radius to an outer storm limit given by r_0 and over τ , the lifetime of the storm. Due to the difficulty in evaluating these integrals and other reasons, Emanuel defined a simplified Power Dissipation Index (PDI) as

$$\mathrm{PDI} \equiv \int_0^{\tau} V_{\max}^3 \mathrm{d}t \qquad \text{Eq. (1.3.2)}$$

where V_{max} is the maximum sustained wind speed at the 10 meter altitude. The PDI was computed for all storms since 1950. It is a combination of each storm's maximum wind speeds and storm duration. It was found that during the last 30 years, the destructive

power of storms, the PDI, has doubled in the Atlantic and Pacific. But Emanuel did not just find the upward trend of storm intensity. What he also found startled the climate community. In the area of the Atlantic where most hurricanes start, the power released during the lifetimes of the storms is "spectacularly well correlated with sea surface temperatures" (Kerr, 2006). Figure 1 displays Emanuel (2005) results for the North Atlantic. Emanuel (2005) has shown that the hurricane intensity and sea surface temperatures have risen over the last 45 years. Many scientists now believe that the warming of the Atlantic may be driven at least in part by rising greenhouse gases.

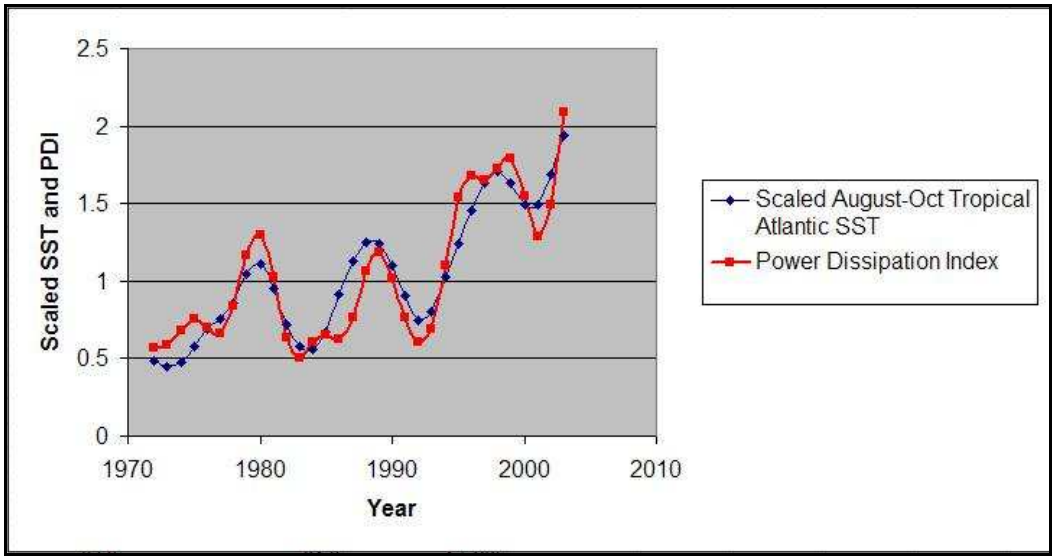

Figure 1 SST versus Power Dissipation Index from (Emanuel, 2005)
Both SST and PDI have been scaled using a constant offset for ease of comparison.
SST Scaled August-October temperatures and PDI is meters^3 / seconds^2

However, to date, science has not been able to acceptably link worldwide storm frequency with global warming (Webster et.al, 2005). Each ocean basin has its multiyear cycles of storm activity. While the total number of storms in the tropics remained similar through time, one study suggests that the percentage of category 4 and 5 hurricanes have increased over the past 30 years (Trenberth, 2005). Trenberth states that despite the enhanced activity, there is still no sound theoretical basis for defining if and/or how

anthropogenic climate change affects hurricane numbers or tracks, and if they hit land. This issue was so intense, that the leading US meteorologist Chris Landsea resigned from the IPCC, complaining that Trenberth had supported a link between warming and storms in a previous press conference (Schiermeier, 2005).

Landsea (2005) in review of Emanuel (2005) results presented three critical issues. The first issue was the plotting of unfiltered end points of the PDI time series which should have been deleted. Emanuel plotted these end points which suggested the strong increase in PDI over the last few years. If the unfiltered end points were removed the indexes are similar to those previous to the 1950s. The second issued concerned the method of bias removal which reduced the tropical cyclone winds for the Atlantic by 2.5 – 5.0 m/s for the 1940s- 1960s. Landsea (2005) argued that the hurricane winds should be used as is with no adjustments. The third issue was the difficulty to interpret an anthropogenic signal in the Atlantic storms due to the large natural multi-decadal oscillations and the short time period of the reliable data record. He presented a PDI for 1901-2004 for only US land falling tropical cyclones which showed no evidence of long term trends (Figure 2).

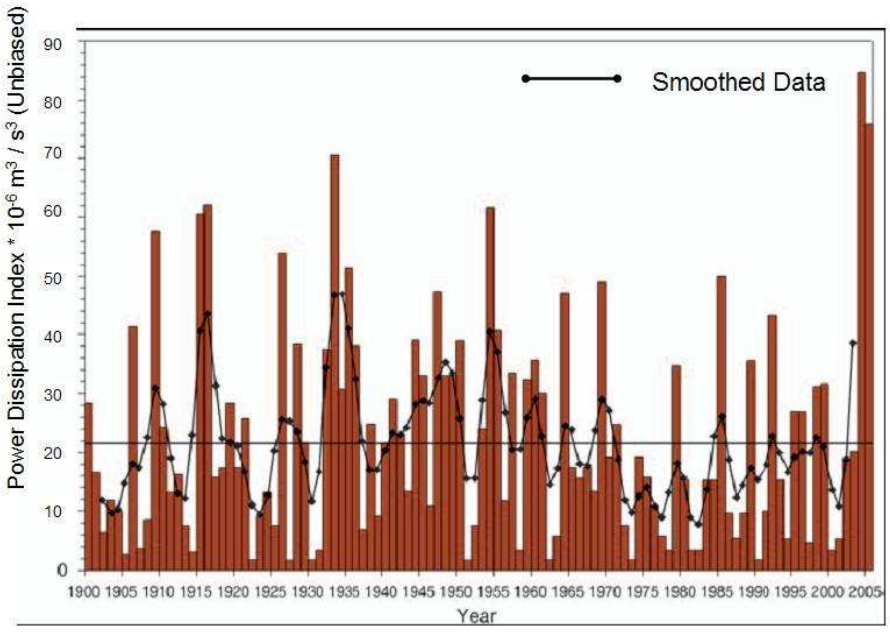

Figure 2 Power dissipation index landfalling storms from Landsea (2005)

Given the rapidly changing topology and land characteristics in Southern Louisiana, as well as the possible fundamental changes in climate, this research proposes to investigate the impact on Southern Louisiana through detailed hydrodynamic model studies. In light of the above background, research tasks and goals are outlined in the following sections.

1.4 Abrupt Climate Change

What is “abrupt” climate change? Alley defines abrupt as a change that occurs when the climate system is forced to cross some threshold, triggering a transition to a new state at a rate determined by the climate system itself and faster than the cause (Alley, 2002). Although this is accurate for a scientific definition, most people see abrupt change as any type of climate change that lasts for years or longer and has significant

impact on their lives. These include change in intensity, duration, or frequency of extreme events which persist. Thus, for example, a persistent change, may be seen as an increase in the number of floods or the number and intensity of storms.

"Large, abrupt climate change have repeatedly affected much or all of the earth, locally reaching as much as 10ºC change in 10 years. Available evidence suggests that abrupt climate changes are not only possible but likely in the future, potentially with large impacts on ecosystems and societies." (Alley, 2002). Our climate changes rapidly when being forced either naturally, or, as being postulated today, by human induced greenhouse warming which may increase the possibility of abrupt, regional or global events.

Before the 1990s, most scientists believed the climate changed very slowly, with gradual swings of the ice ages over tens of thousands of years or longer. But over the last few decades, geologic evidence has undisputedly shown that the climate can and has changed abruptly (NRC, 1998). Changes of up to 16^{o}C and a factor of 2 in precipitation have occurred in some places in periods as short as a few years or decades (Alley, Clark, 1999). Sedimentary and other "proxy" methods have demonstrated widespread abrupt climate changes over the last 100,000 year and beyond. The period called the "Younger Dryas" is the best known cold interval. The Younger Dryas (YD) began about 12,800 years ago as an interruption to the gradual global warming trend following the last ice age. The YD event ended abruptly about 11,600 years ago. Analysis of the Greenland ice cores (Alley, 2000) showed that cooling occurred in a few decade long steps, but

warming at the end, happened in one large step of about 8°C in about 10 years. Even so, additional studies of the Greenland ice core data have indicated the YD was only one of many large, abrupt, widespread climate changes. Scientists around the world give recognition to these abrupt state changes but only a small amount of knowledge and information is understood about the reasons for the abrupt state changes. We do not fully know under what conditions state changes are possible either under modern or near-future climate conditions. But from the evidence, we know they can be abrupt.

No one has yet identified the exact cause of the YD but many scientists have associated drastic changes in the Atlantic thermohaline circulation (THC) as playing a central role in this event as well as many other past abrupt climate changes. Some theories suggest large influxes of fresh water into the North Atlantic reduced the ability of its waters to sink. This reduction in heat transport to the north allowed heat to remain in the south, thus a reduction in the THC. The implications of fluctuations in the Atlantic THC have received much attention and many efforts are being conducted to more fully understand the THC and how the ocean heat transport affects the climate.

Most GCM models suggest that for the THC, or sometimes called the "conveyor belt" to shut down, a 4 – 5°C global warming is required. But the current warming trend is at 0.3ºC per decade for the period 1990 through 2005 (IPCC AR4, 2007). The current rate is approximately 0.2ºC per decade and is remain the same for the next two decades. GCM models show that the THC flow may be expected to slow by an average of 25% by the end of the twenty-first century, but not to shut down completely. An inter-model

comparison analysis (Gregory et al. 2005), specifically on the THC, also confirmed these results under various IPCC increased CO_2 concentration scenarios. However, recent observations (Bryden et al. 2002) have estimated a 30% weakening in the overturning circulation within the last few decades. These results came as a surprise to many scientists because of the disparity with other factors such as changes in salinity, deep convection, or lack of observed cooling in the North Atlantic.

Some scientists believe that natural cycles in the THC (rather than human induced changes) are responsible for the increase in Atlantic hurricane activity in recent decades. Dr. William Gray, in a statement to the US Senate Committee on Environment and Public Works (September, 2005) stated that an *increase* in the intensity of the Atlantic Thermohaline circulation over recent decades was entirely responsible for this increase in hurricane activity. "The Atlantic has large multi-decadal variations in major (category 3-4-5) hurricane activity. These variations are observed to result from multi-decadal variations in the North Atlantic Thermohaline Circulation (THC). When the THC is strong, it causes the North Atlantic to have warm or positive Sea Surface Temperature Anomalies (SSTA) and when the THC is weak, cold SSTAs prevail." By Gray's reasoning, there should have been a *downturn* in activity, and not the observed *upturn* if Bryden et al. results are correct.

There have been attempts to relate SST with hurricane intensity, however, Emanuel states that there is no theoretical relationship between SST and hurricane intensity. The underlying causes of the SST needs to be understood. This area is called

"Potential Intensity (PI) theory. However, within this area, increasing destructiveness of tropical cyclones over the past 30 years has been theorized (Emanual, 2005). These results indicate the very real possibilities of increased tropical cyclone destructive capability.

1.5 Scope and Objectives of Research

The overall objective of this research is to quantify potential future storm surges, as well as storm frequency, taking into consideration global warming and in particular abrupt climate change. This research will have 3 primary objectives:

(1) Quantify storm surges for the Louisiana Coast with wetland loss as projected by the USGS in the year 2050.

(2) Project the impacts of abrupt climate change through creation and modeling of storms of increasing maximum intensities possible under such change to estimate future surge levels.

(3) Estimate frequencies of future storms based upon minimum central pressure and radius to maximum wind, and compare surge results obtained from these future storms, to published storm surge return period levels.

1.5.1 2050 Storm Surge Simulations.

In order to quantify storm surges for the Louisiana Coast with wetland loss as projected by the USGS in the year 2050, the Advanced CIRCulation (ADCIRC) model will be used to perform all storm surge computations. The ADCIRC mesh representing 2050 future degraded conditions of the Louisiana zone will be used. This mesh is the same mesh created for use in the USACE Louisiana Coastal Protection and Restoration

(LACPR) study. The Coastal Louisiana Ecosystem And Restoration (CLEAR) group projected land loss/gain rates and future topography based upon historic relative regional and local subsidence rates (Twilley, et al. 2008). This topography represents the future topography and bathymetry in 2050 and was transferred onto an ADCIRC mesh. The pre-Katrina topography and levee system is represented in the LACPR 2007 ADCIRC mesh. A post-Katrina, ADCIRC mesh with topography representing the Louisiana coast of 2050, will be encoded with all levee heights set to the published Corps of Engineers 100-year level of protection elevations. ADCIRC executions will be performed to simulate Katrina, as well as the Category 5 storm characteristics defined by the USACE Louisiana Coastal Protection Restoration Study. Simulations of these storms will be performed on these grids which represent the Louisiana coast in 2050, to quantify surges that could occur with the predicted future land loss.

The final results of these simulations will provide a quantitative assessment of future storm surges in the 2050 projected land configuration by the USGS. Areas of inundation can be compared to 2005 Katrina flooded locations. This will demonstrate the locations of more severe flooding and those with less flooding, based on an event similar to Katrina, and a potential Category 5 storm striking the Louisiana coast in 2050.

1.5.2 Abrupt Climate Change.

The second objective of this research is to project the impacts of abrupt climate change through modeling of storms of increasing maximum intensities. Future physically realistic storms with maximum potential intensity (Holland, 1997) and Emanuel (1987)

that can be attributed to abrupt climate change will be created. Simulations of these storms will be performed and the results analyzed for impacts to the Gulf Coast, specifically the state of Louisiana and the New Orleans area.

An important question in any climate change scenario is will the Atlantic THC remain stable under the global warming conditions occurring over the next few decades and beyond. If slowing of the THC occurs, how will the ice sheets and continental glaciers respond? Recent analyses of the Greenland ice sheets have indicated the flow of several large glaciers is accelerating. Changes in the THC, combined with increased melting, suggest that previous estimates of future sea-level rise, of about 0.5 +/- 0.4 m this century (IPCC, 2001a) are too low (Dowdeswell, 2006). These results indicate a contribution from the Greenland Ice Sheet of more than 0.5 mm $year^{-1}$ to the global sea-level rise. These more than double previous estimates of losses from the ice sheet to the oceans. If these numbers are correct, large influxes of fresh water will decrease the salinities and may trigger a slow down in the thermohaline circulation.

Even without the affects of a THC slow down, a major consequence of abrupt climate change could be a significant rise in sea level due to glacier and ice sheet melting. This research will review relevant published results from coupled ocean-atmosphere model simulations of 20th - 22nd century climate collected for the 4th Assessment Report of the Intergovernmental Panel on Climate Change (AR4). The 4th IPCC Report model sea level rise (SLR) projections will be reviewed as well as more recent publications to quantify a possible range of SLR under abrupt climate change (ACC) forcing. An

overview of ADCIRC simulations is shown in Table 1. Results from the simulations will be used to capture ACC impacts on surges along the Louisiana coast and the Gulf of Mexico.

For the purposes of evaluating this objective, "abrupt" change will be interpreted as a rise in sea surface temperature (SST) of 6ºC during the period from the present to 2050. For comparison if the current trend of SST persists (0.2ºC for 2 decades until 2027, then 0.4 ºC per decade) without an abrupt change the SST would increase by approximately (2 * 0.2) + (2 * 0.4) = 1.2ºC by 2047. For the "A1F1" high emissions scenario (IPCC 2001a), global mean temperature increase is estimated to be 4ºC by 2100, or 2ºC by 2050.

1.5.3 Frequency Analyses.

Storms projected to form under abrupt climate change conditions will have different characteristics than those of the current climate. These most likely include higher intensities in terms of stronger wind speeds and lower central pressures. Consequently these storms will produce higher surges. Analyses will be conducted to determine how these storms and surges fit into relations published for future climate conditions.

Table 1 Overview of Storm Simulations

2050 and Abrupt Climate Change Storm Simulations

2050 Current Climate

Mesh	Simulations
2007 Topography & Authorized Levees	High Cat 5 Storms
2050 Topography and 100 year Levees	High Cat 5 Storms, Katrina

Abrupt Climate Change

Mesh	Simulations
2050 Topography and 100 year Levees	Increased Intensity Storms

Chapter 2 Storm Surge Models Literature Review

2.1 Historic Storm Surge Models

Numerical estimates of surges due to hurricanes began in the late 1950s. Conner et. al. (1957) created a methodology to estimate storm surge tides that began with the difference between ambient and minimum central pressures. He used the formula:

$$\eta_{max} = 0.867(p_a - p_0)^{0.618} \qquad (2.1)$$

Where η_{max} is the maximum surge, p_a is the ambient pressure (millibars), and p_0 is the minimum central pressure (millibars). Conner et. al. (1957) then revised this equation after analyzing historical observed surges from land-falling Gulf of Mexico tropical cyclones and developed a regression equation: $\eta_{max} = 0.154(1019 - p_0)$. Ambient pressure was defined as 1019mb. It was later understood that pressure differences alone could not quantify the total surge and Hoover (1957) concluded that Conner equations underestimated maximum surge heights and computed his own regression equations, one for the Atlantic coast, and a separate one for the Gulf of Mexico: $\eta_{max} = 0.151(1032 - p_0)$. These methodologies were superseded in the 1960's when Harris (1963) created a somewhat computer assisted empirical model which included five parameters: (1) pressure forcing (called the barometer effect) which is the result of lower pressure of the storm causing a "bubble" of water to be forced upward; (2) direct wind (wind setup); (3) Coriolis force; (4) waves; and (5) rainfall. Harris presented that the first four parameters were proportional to wind stress, and that rainfall is correlated with below normal pressures.

Jelesnianski et. al. (1972) improved computer based modeling with advances in computer hardware and software that enabled the creation complex computer code which was called “SPLASH”. SPLASH had three basic steps to compute the maximum surge. The first step calculated a maximum surge based on the empirical formulas derived by Conner et. al. (1957) and Harris (1963). There were five constraints: (1) radius of maximum winds is constant; (2) for each set of storms, only the pressure drop is varied; (3) all storms have steady motions, 15 mph and the track is normal to the coast; (4) a standard simplified coast is used for all storms; (5) all storms make landfall at 30ºN. The second step was an adjustment to the first computation by introducing a shoaling factor to correct for local coastal bathymetry. The third step was to correct for storm direction and storm speed. The final equations established were:

$$\text{Max Surge} = S_p \times F_G \times F_M \quad \text{(Gulf Coast)} \quad (2.2)$$

$$\text{Max Surge} = S_p \times F_E \times F_M \quad \text{(Atlantic Coast)} \quad (2.3)$$

where S_p is the preliminary maximum surge estimate, F_G and F_E are the Gulf and East coast shoaling factors, and F_M is the correction factor for storm motion.

During the mid 70’s, the FEMA SURGE model was created by Tetra Tech, Inc. and called TTSURGE (Camp Dresser et. al. 1985). TTSURGE later became known as the FEMA SURGE model after several updates and applications. It was used extensively to map the coastal flood inundation and hazard zones for Flood Insurance Rate Maps (FIRMs). TTSURGE employs an explicit, 2D, space-averaged, finite-difference scheme to simulate hurricane surges. TTSURGE has two parts, the hurricane storm model and the

hydrodynamic model. The hurricane is defined by its barometric pressure field and corresponding wind field over it rectangular grid domain. The two fields are parameterized by the radius to maximum winds and central pressure depression. The fields are defined in time by the forward storm velocity and the computed stress and pressure gradients provide the forcing for the hydrodynamic model. This model uses the principles of mass and momentum conservation to simulate the water surface response to hurricanes. A Manning's n coefficient and bed elevation are specified for all grid cells and water surface elevations are computed for each cell. This FEMA SURGE model was used in historic Joint Probability Method analyses to determine return periods of surge elevations (Massey et. al. 2007). The late 1980's was the last time the FEMA SURGE model was used in new or updated flood insurance studies to revise FIRMs (Massey et. al. 2007). Although in the early 1990's coastal engineering firms were updating the model to run on desktop computer platforms.

The 1990's saw the development of the SLOSH model by Techniques Development Laboratory of the National Weather Service (Jelesnianski et. al., 1992). SLOSH is a 2D numerical-dynamical tropical storm surge model created for real time forecasting of hurricane storm surges. Since its creation it has been extensively used by the National Hurricane Center to provide decision makers quantitative surge estimates to base critical decisions for emergency evacuations. Originally, SLOSH used a curvilinear grid, but has been updated to employ elliptical and hyperbolic grids to allow for finer cell size near the shore and coarser sizes in less important locations. SLOSH does include wetting and drying algorithms and surface wind coefficients based on land topography.

Barriers such as roads, dunes, levees, and small channels are represented as sub-grid elements. Most often hypothetical storms are modeled to create Maximum Envelope of Water (MEOW) and Maximum of MEOWs (MOMs). A MEOW is the maximum surge height at each cell of all sets of storms within the same category, forward speed, direction of motion, and parallel tracks. A MOM is the maximum of all MEOWs with storms of the same category. When used for real time forecasting, only the storm forecasted track, radius to maximim winds, and pressure intensity are entered. Wind fields are computed based on pressure differentials and wind stresses are computed for each cell upon which the resultant surge elevations are calculated.

2.2 ADCIRC

ADCIRC will be used to perform all storm surge modeling. ADCIRC was developed by Dr. Joannes Westerink and Dr. Richard Luettich for the US Army Corps of Engineers as part of the Dredging Research Program (Luettich, et. al. 1992). The purpose was: (a) to provide a means of generating a database of harmonic constituents for tidal elevation and current at discrete locations along the east, west, and Gulf of Mexico coasts, and (b) to utilize tropical and extratropical global boundary conditions to compute frequency indexed storm surge hydrographs along the US coasts. The database was to provide site-specific hydrodynamic boundary conditions for use in analyzing the long-term stability of existing or proposed dredge material disposal sites.

ADCIRC was developed to simulate hydrodynamic circulation along shelves, coasts, and within estuaries. To allow long numerical simulations (over one year) over

very large computational domains (for example the entire east coast of the United States, including the Gulf of Mexico), ADCIRC was designed to have high computational efficiency and has been extensively tested for both hydrodynamic accuracy and numerical stability (USACE New Orleans District, ITR, 2003); Westerink, et. al. 2004).

Since its inception in the early 1990s, ADCIRC has evolved in many ways that range from its modeling capabilities, numerical algorithms, and computational efficiencies. Today it is a state of the art finite element model that enables the use of highly flexible, unstructured, and large domain meshes (or grids). Many agencies and organizations are using ADCIRC for a wide range of applications including modeling tides and wind driven circulation, analyzing hurricane storm surge and flooding, dredging and material disposal studies, estuarine hydrodynamic studies, as well as larval transport studies, and near shore marine operations.

An important aspect of the model is that it can simulate tidal circulation and storm-surge propagation over very large computational domains while simultaneously providing high resolution in areas of complex shoreline configuration and bathymetry. The mesh domains for hurricane simulations within the Gulf of Mexico extend from the mid Atlantic and North from Nova Scotia, cover the entire Gulf of Mexico and south past Venezuela. Figures 3, 4, and 5 provide a visual of the entire ADCIRC domain and also the high element resolution along the south shore of Lake Pontchartrain.

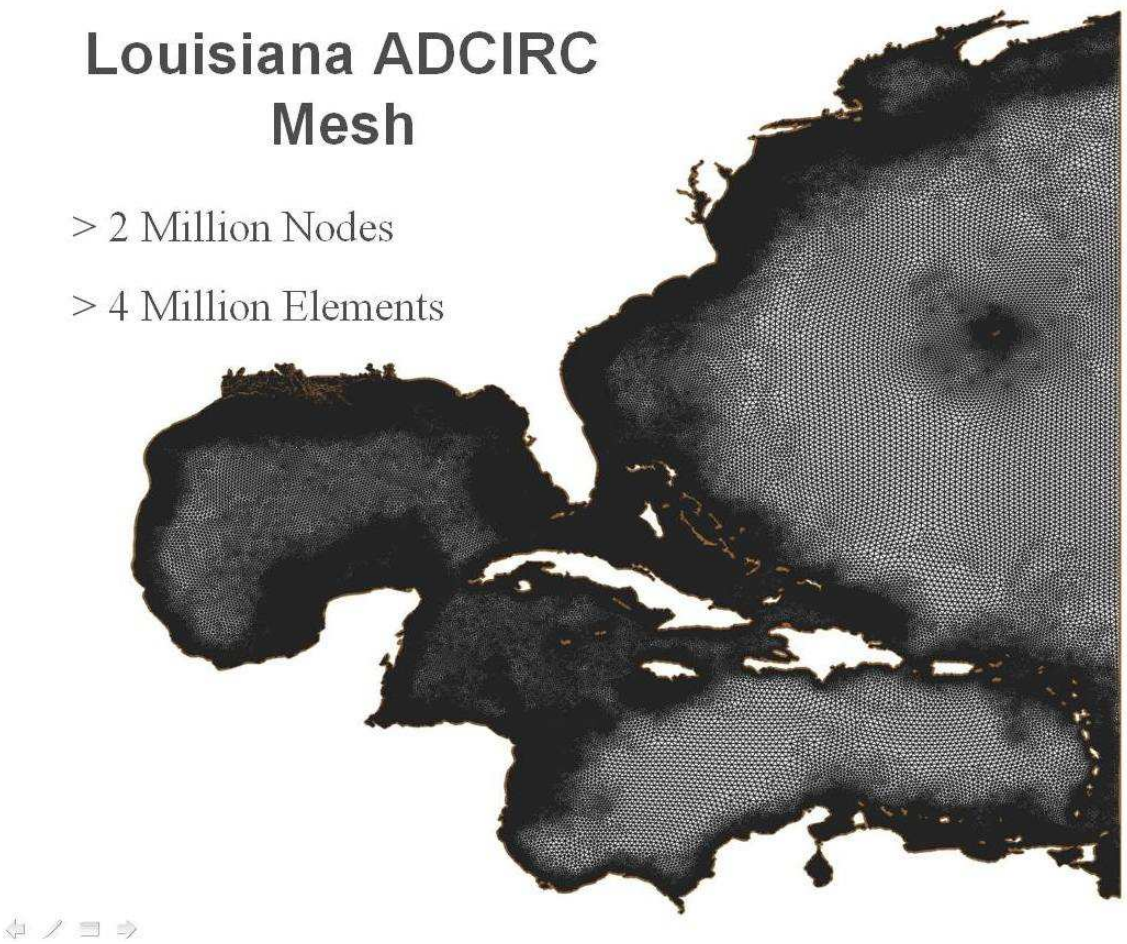

Figure 3 ADCIRC Finite Element Mesh used for Louisiana surge modeling

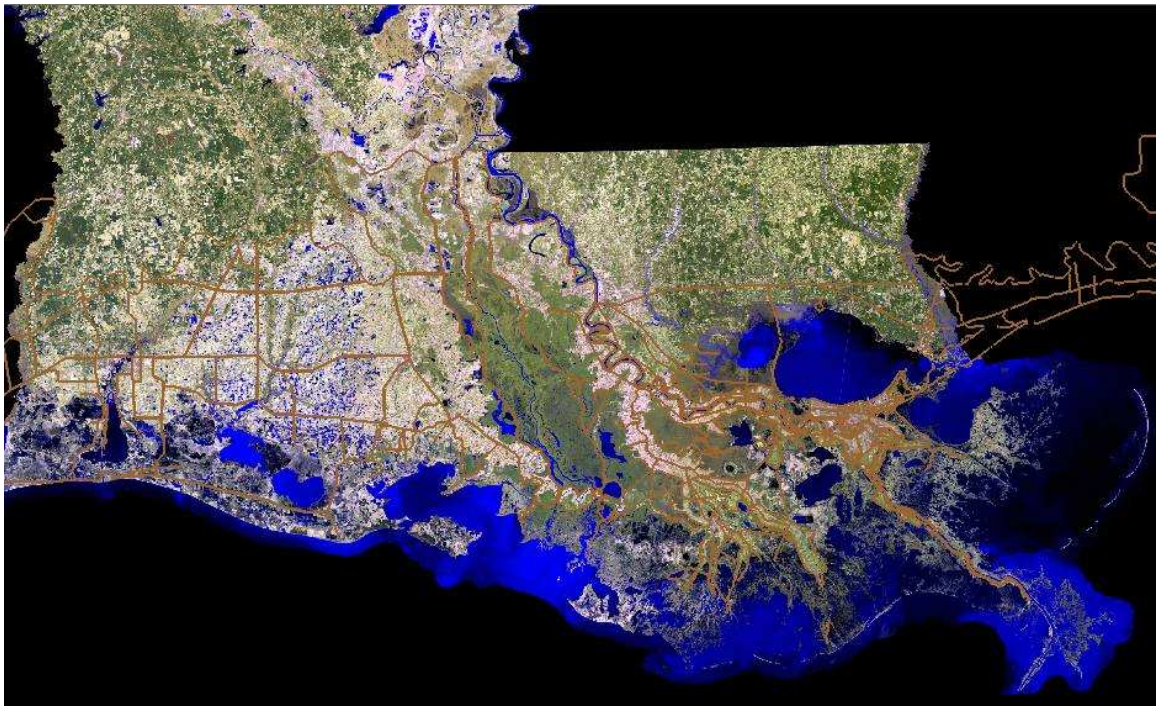

Figure 4 ADCIRC Mesh Internal Boundaries for Coastal Louisiana
Louisiana Oil Spill Coordinator's Office (LOSCO), 1998, Thematic Mapper Image of Louisiana

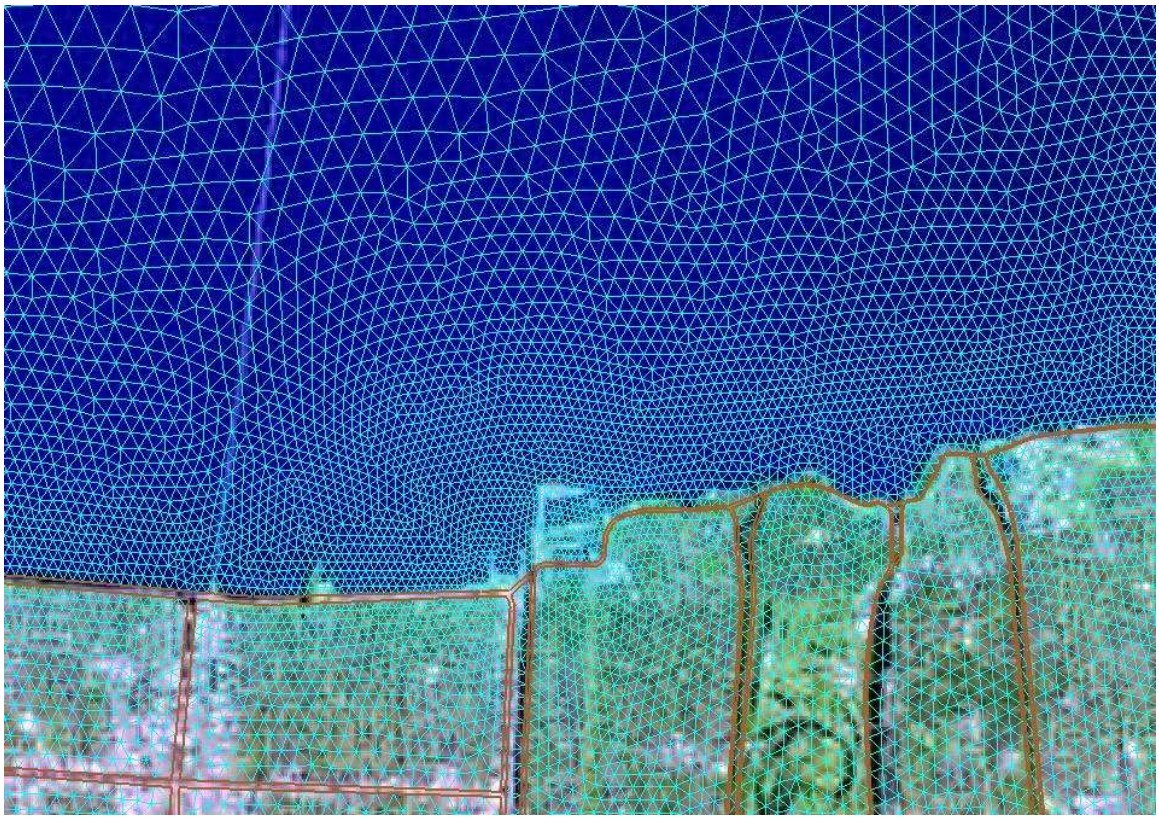

Figure 5 ADCIRC Mesh Detail Lake Pontchartrain

In 2002 FEMA accepted ADCIRC to predict return periods of storm surges for use in Flood Insurance Studies (FIS). ADCIRC was then used to define the limit of inland flooding and as a base for calculating wave heights for mapping coastal zone hazard areas for the new Digital Flood Insurance Rate Maps (DFIRMS). In 2007 the USACE completed the Joint FEMA/USACE Louisiana Coastal Storm Surge Study. This study used ADCIRC for all storm surge modeling and in a new statistical methodology called the Modified Joint Probability Method with Optimal Sampling (JPM-OS). The USACE computed all storm surge return periods using the JPM-OS methodology for Louisiana. Storm surge return periods were also completed using ADCIRC and the JPM-OS methodology by a team of private entities for the Mississippi State coast in 2007.

2.2.1 Model Formulation

In two dimensions, the model is formulated using the depth-averaged shallow water equations for conservation of mass and momentum. Furthermore, the formulation assumes that the water is incompressible, hydrostatic pressure conditions exist, and that the Boussinesq approximation is valid. Using the standard quadratic parameterization for bottom stress and neglecting baroclinic terms, the following equations are implemented in primitive, non-conservative form, and expressed in a spherical coordinate system, and incorporated into the model (Flather 1988; Kolar et al. 1993; Luettich and Westerink, 2004).

$$\frac{\partial U}{\partial t} + \frac{1}{r\cos\phi} U \frac{\partial U}{\partial \lambda} + \frac{1}{R} V \frac{\partial U}{\partial \phi} - \left[\frac{\tan\phi}{R} U + f \right] V = - \frac{1}{R\cos\phi} \frac{\partial}{\partial \lambda} \left[\frac{p_s}{\rho_0} + g(\zeta - \eta) \right] + \frac{\tau_{s\lambda}}{\rho_0 H} - U\tau \tag{2.4}$$

$$\frac{\partial V}{\partial t} + \frac{1}{r\cos\phi} U \frac{\partial V}{\partial \lambda} + \frac{1}{R} V \frac{\partial V}{\partial \phi} - \left[\frac{\tan\phi}{R} U + f \right] U =$$

$$- \frac{1}{R} \frac{\partial}{\partial \phi} \left[\frac{p_s}{\rho_0} + g(\zeta - \eta) \right] + \frac{\tau_{s\lambda}}{\rho_0 H} - V\tau \qquad (2.5)$$

$$\frac{\partial \zeta}{\partial t} + \frac{1}{R\cos\phi} \left[\frac{\partial UH}{\partial \lambda} + \frac{\partial (VH)\cos\phi}{\partial \phi} \right] = 0 \qquad (2.6)$$

where

t = time,

λ and φ = degrees longitude (east of Greenwich is taken positive) and degrees latitude (north of the equator is taken positive),

ζ = free surface elevation relative to the geoid,

U and V = depth-averaged horizontal velocities in the longitudinal and latitudinal directions, respectively,

R = the radius of the earth,

$H = \zeta + h$ = total water column depth,

h = bathymetric depth relative to the geoid,

$f = 2\Omega \sin\varphi$ = Coriolis parameter,

Ω = angular speed of the earth,

p_s = atmospheric pressure at free surface,

g = acceleration due to gravity,

η = effective Newtonian equilibrium tide-generating potential parameter,

ρ_0 = reference density of water,

$\tau_{s\lambda}$ and $\tau_{s\varphi}$ = applied free surface stresses in the longitudinal and latitudinal directions, respectively, and

τ = bottom shear stress and is given by the expression $C_f(U^2 + V^2)^{1/2}/H$ where C_f is the bottom friction coefficient.

The momentum equations (Equations 2.4 and 2.5) are differentiated with respect to λ and τ and substituted into the time differentiated continuity equation (Equation 2.6) to develop the following Generalized Wave Continuity Equation (GWCE):

$$\frac{\partial^2\zeta}{\partial t^2} + \tau_0\frac{\partial\zeta}{\partial t} - \frac{1}{R\cos\phi}\frac{\partial}{\partial\lambda}\left[\frac{1}{R\cos\phi}\left(\frac{\partial HUU}{\partial\lambda} + \frac{\partial(HUV\cos\phi}{\partial\phi}\right) - UVH\frac{\tan\phi}{R}\right]$$

$$\left[-2\omega\sin\phi\,HV + \frac{H}{R\cos\phi}\frac{\partial}{\partial\lambda}\left(g(\zeta - \alpha\eta) + \frac{p_5}{l}p_0\right) + \tau_* HU - \tau_0 HU - \tau_{s\lambda}\right]$$

$$-\frac{1}{R}\frac{\partial}{\partial\phi}\left[\frac{1}{R\cos\phi}\left(\frac{\partial HVV}{\partial\lambda} + \frac{\partial HVV\cos\phi}{\partial\phi}\right) + UUH\frac{\tan\phi}{R} + 2\omega\sin\phi\,HU\right] \quad (2.7)$$

$$+\frac{H}{R}\frac{\partial}{\partial\phi}\left(g(\zeta - alfa\eta) + \frac{p_s}{\rho_0}\right) + \tau_* - \tau_0 HV - \frac{\tau_{s\lambda}}{\rho_0}]$$

$$-\frac{\partial}{\partial t}[\frac{VH}{R}\tan\phi] - \tau_0[\frac{VH}{R}\tan\phi] = 0$$

The ADCIRC-2DDI model solves the GWCE in conjunction with the primitive momentum equations given in Equations 2.4 and 2.5. The GWCE-based solution scheme eliminates several problems associated with finite-element programs that solve the primitive forms of the continuity and momentum equations, including spurious modes of oscillation and artificial damping of the tidal signal. Forcing functions include time-

varying water-surface elevations, wind shear stresses, atmospheric pressure gradients, and the Coriolis affect.

The ADCIRC model uses a finite-element algorithm in solving the defined governing equations over complicated bathymetry encompassed by irregular sea/ shore boundaries. This algorithm allows for extremely flexible spatial discretizations over the entire computational domain and has demonstrated excellent stability characteristics. The advantage of this flexibility in developing a computational grid is that larger elements can be used in open-ocean regions where less resolution is needed, whereas smaller elements can be applied in the near shore and estuary areas where finer resolution is required to resolve hydrodynamic details.

2.2.2 ADCIRC Louisiana mesh validation

The Louisiana ADCIRC mesh has approximately 80% of the nodes and elements along the Louisiana coast and highly resolved topographic and bathymetry definition extends from portions of Texas, through Louisiana, Mississippi, and into Mobile Bay. All ridge features such as levees, roads, railways, and raised linear features which can impede flow are either specifically represented in the finite elements or by internal boundaries. Internal boundaries were modeled as weirs and represent a non-hydrostatic flow scenario. Once water levels overtopped these barrier heights, the flow across the crest is computed using the standard weir formula. All Federal levees are captured, as well as numerous state, local, and private levees. The computational grid (Figures 3,4, and 5) has been constructed to provide sufficient resolution for the tidal, wind, atmospheric pressure, and

riverine flow forcing functions from the ocean basins to the coastal floodplain. A minimum spacing of 100 feet was used since a 0.5 Courant, Fredrichs, Levy parameter is best for the ADCIRC model. An optimum time step equal to 1 second was used for all storm simulations using the Louisiana mesh. The mesh was validated using 3 historic storms: Katrina, Rita, and Andrew. Water levels and time series results for each of these storms were compared against measured high water marks (HWMs) and observed hydrographs captured for these events. Tidal validation simulations were also performed and consistently produced R^2 values greater than 0.9 for the Louisiana, Mississippi-Alabama coast (FEMA and USACE 2008). HWMs for Katrina and comparison results are documented in the IPET report (USACE, 2007). A straight line fit through all of the USACE HWMs produced a slope of 1.0007. Thus, the model was over predicting surge by only 0.07%. The average error is -0.14 foot while the average absolute error is 1.31 feet. A correlation coefficient (R^2) equal to 0.9317 was achieved. A group of additional HWMs were collected by URS, Inc. for FEMA and when using all of these HWMs the slope of the line through all data points was equal to 1.0315. This indicates the model is on average over-predicting surge by 3.15 percent. The average error was 0.45 foot while the average absolute error was 1.24 feet. The correlation coefficient (R^2) was equal to 0.9460. Results for Rita and Andrew are also well correlated with HWMs and hydrographs from these storms. Detailed results for Katrina and Rita simulations are in "Flood Insurance Study: Southeastern Parishes, Louisiana, Intermediate Submission 2, FEMA and the U.S. Army Corps of Engineers (USACE) New Orleans District, 2008.

2.2.3 ADCIRC Numerical Implementation

The ADCIRC model and Louisiana mesh validation results (Section 2.2.2) demonstrate the local accuracy of the ADCIRC model even though it is globally but not locally mass conservative. But, there is no standard or consensus on the best way to check local mass conservation. ADCIRC implements a rigorous method that directly integrates the continuity equation over a control volume that coincides with a finite element or an entire cluster of finite elements. This method provides diagnostics and ability to determine if transport computations driven with these flows will result in localized mass losses/gains that result in artificial oscillations. With this tool, local mass balance errors have been effectively minimized and hence local truncation errors (FEMA and the USACE, 2008). Local mass conservation is minimized by use of a local "τ_0" or Generalized Wave-Continuity Equation (GWCE) weighting factor that weights the relative contribution of the primitive and wave portions of the GWCE. Local mass conservation was checked at the element level for the Louisiana mesh and it was found that over 93% of the domain had a relative error of less than 0.01% in magnitude and 72% of the domain had a relative error of less than 0.001% in magnitude (FEMA and the USACE, 2008). These errors are within tolerances normally associated with modeling of these complex systems.

The GWCE in ADCIRC is implemented by combining the differentiated momentum equation in its conservative form with the temporally differentiated continuity equation multiplied by a numerical parameter τ_0 (Kolar and Westerink, 2000). The GWCE and the momentum equations are solved sequentially. The finite element solution is implemented using Lagrange linear finite elements in space and 3 and 2 level schemes in time for the GWCE and momentum equations respectively. Details of the

discretization and solution techniques used in ADCIRC are given in Luettich and Westerink, 1992; Westerink, 1993; Luettich and Westerink, 2004.

Wetting and drying processes are implemented based on a combination of nodal and elemental criteria (Luettich and Westerink, 1999; Dietrich et. al. 2005). The following is a brief overview of the wetting and drying algorithm following from (FEMA and USACE, 2008). "All nodes within an element must be wet in order for that element to be included in the hydrodynamic computations. Two parameters are used to define the wetting/drying criteria. The first parameter, *H0* defines the nominal water depth for a node to be considered wet. The second parameter is a minimum velocity, *Umin*, that must be exceeded for water to propagate from a wet node to a dry node. Nodes are defined as initially dry if they lie above the defined starting water level or if they are below the starting water level but are within pre-defined regions, such as ring levees as in protected areas of New Orleans. Wetting is accomplished by examining each dry element with at least two wet nodes with depth greater than 1.2 *H0* (ensuring sufficient water depth to sustain flow to the adjacent node). The velocity of the flow from the wet nodes toward the dry node along each element edge is computed based on a force balance between the free surface gradient and the bottom friction. If this velocity exceeds *Umin*, then the third node and the element are wetted. Finally, a check is made for elements that are surrounded by wet elements to ensure sufficient water column height (greater than 1.2 *H0* at all flow originating nodes) to allow flow to occur through these elements. While a purely nodal wetting scheme will allow these elements to wet, the elemental check may prevent this from occurring. For hurricane storm surge inundation, wet/dry parameters that are relatively unrestrictive have been found to be most effective: *H0* = 0.10 m, and

Umin = 0.01 m/s. It is critical that all wet/dry checks be done at a small enough time interval so that the wetting/drying algorithm is not Courant surpassing. This latter condition artificially retards the wetting front as the surge progresses inland and the surge height will excessively build up behind the wetting front. Practically, this implies performing wet/dry checks at each model time step." (FEMA and USACE, 2008)

2.2.4 ADCIRC Input and Forcing Functions

ADCIRC can be forced by various methods which are described online at http://www.adcirc.org as well as all specific input and output formats. Input geometry is specified by the finite element mesh for which the Louisiana mesh shown in Figures 3, 4, and 5 was used for this work. Forcing functions applied in this effort included both river and atmospheric (winds) forcing. The Mississippi and Atchafalaya Rivers were forced with steady flows of 181,000 cfs and 79,000 cfs respectively. Atmospheric forcing included both wind speed and atmospheric pressure every 15 minutes at each node on a 0.05º longitude and 0.05º latitude rectangular grid. Wind speed and atmospheric pressure are computed by an updated version of the TC-96 Planetary Boundary Layer (PBL) wind model (Thompson and Cardone, 1996). Additional input requirements are wind surface reduction factors, Manning's n roughness coefficients, and sea surface submergence state. These parameter definitions and formats can be found at http://www.adcirc.org. Other primary ADCIRC parameters such as time step and tidal factors are specified and defined in a "control" file which is also described on the ADCIRC web site.

Chapter 3 Global Climate Change

3.1 Introduction

Only within the past century or so have we come to fully realize how much the earth's climate has changed over the long time scales of our planet's evolution. Many scientists and people of all walks of life have labored and endeavored to understand our climate. A complete history of these efforts and results would take volumes. This chapter will focus primarily on the summaries and results of the reports produced by the International Panel on Climate Change (IPCC) of which the first was published in 1990. A very brief outline of major advances in this effort are covered within the next few paragraphs.

Throughout history some people believed that humans could affect climate in some way or another but had no way of actually proving any theories. In the early 19th century many Americans believed cutting down forests brought more rain to a region. Discovery of the ice ages opened the eyes of many scientists and demonstrated that the earth's climate did change and very drastically. However, it was thought that the time scales were over tens to thousands of years, and no one knew why or what forced these changes. It occurred to several scientists that one of these could be the composition of the atmosphere. Joseph Fourier was one of the first to realize that energy in the form of light from the sun penetrates the atmosphere to heat up the surface but could not as easily escape back into space. (Online at http://www.aip.org/history/climate/index.html) He

theorized the air absorbed invisible heat rays (infrared radiation) from the surface. Once heated, the warmer air radiates heat back down to the surface thus keeping it warm. This effect later came to be called the "greenhouse effect".

The question of the explanation of the ice ages intrigued other scientists such as John Tyndall who later (1850's) identified several gases (water vapor, carbon dioxide) that he proved in his laboratory did trap heat rays. Following Tyndall, Svante Arrhenius also sought to solve the mystery of the ice ages and calculated that by cutting the amount of CO_2 in the atmosphere in half, could lower the temperature in Europe by 5–7 ^{O}C or approximately 7-9 ^{O}F, which was the temperature of the ice ages. (Online at http://www.aip.org/history/climate/index.html) But this answer was a solution to the mystery only if the large changes in the atmospheric composition were actually possible. In looking for this answer, Arrhenius brought up the possibility that as humans burned coal that added carbon to the atmosphere, the atmosphere would heat up and raise the average temperature of the earth. But scientists found many reasons to doubt that human emissions could actually raise the temperature of the earth and if possible, it would take thousands of years.

During the 1930's scientists and most people realized that the U.S. and North America had warmed significantly during the last 50 years. Most thought is was a natural cycle except for Guy Stewart Callendar who insisted that is was the greenhouse warming effect and the warming would continue.

In the 1950's scientists performed more detailed research into the questions raised by Callendar, and did so with better techniques and calculations (and funding from the military). Results showed that accumulation of carbon dioxide in the atmosphere could result in increased global warming. Then in 1960, exact and careful measurements were performed by Charles David Keeling both in Antarctica and on top the Mauna Loa volcano in Hawaii. Continued measurements and subsequent publications proved inexorably that carbon levels were becoming noticeably higher each year. The now famous "Keeling curve" has become one of the most iconic symbols of the greenhouse effect. Over the next decade scientists created simple mathematical models of the climate that showed feedbacks which could make the climate very variable. The field of paleoclimatology was born with people finding ways to retrieve ancient temperatures using ancient pollens and fossils. They found evidence the climate had changed in a small a span as a few centuries. The new general circulation climate models were even able to reproduce these climates and the models themselves were the results of significant efforts to predict the weather. However, altogether scientists saw no need for political or policy actions but just the need for more understanding and research efforts.

Environmentalism of the 1970's brought ideas on the tremendous negative effects humans had on the earth and our climate. The media seized upon reports by scientists that showed the dust and smog particles being put into the atmosphere could block sunlight and cause general cooling. There became confusion with some reports predicting large scale warming with the ice caps melting, and others which pointed to a doomsday

view to a new ice age. All scientists agreed that much more research was needed because we clearly did not fully understand the climate system.

Research began a great pace to obtain detailed measurements and observations of all aspects of the climate and our environment. The world soon began to realize the climate was an amazingly complex system which was influenced by very many factors. These included volcanic eruptions, solar flares, and subtle changes in the Earth's orbit. It became apparent that even small changes might initiate large and severe shifts over to new climate regimes. The now famous "chaos" theory, developed by Lorenz (1963) explained that the most insignificant change of initial conditions might randomly bring a huge change in the future climate. "Climate may or may not be deterministic," he concluded. "We shall probably never know for sure." (Lorenz, 1963) These theories were later supported by analyzes of the Greenland and Antarctica ice cores which showed large and abrupt temperature changes throughout the history of our climate.

The 1980's and 1990's brought about significant advancements in computer hardware and software technology. This enabled tremendous improvements in numerical climate models. These models showed just how fast changes could occur in the atmosphere and ocean and also predicted storms, droughts, sea level rise and other disasters. However, the models did not capture all climate aspects equally. Assumptions and parameterizations had to be made about clouds and other factors which prominent scientists pointed out to dispute the reliability of the results. There was a need for more coherent and organized approach but the research remained disparate and unorganized.

During this time the unexpected discovery of other gases levels in the atmosphere were rising and were related to depletion of the ozone layer. Also, in the 1980's global temperatures were being observed to be on the rise again. It was 1988 that scientist's claim first caught high public attention as 1988 was claimed the hottest summer on record (now since exceeded by several years in the 1990's and 21st century). There was a constant and highly aggressive debate on what actions to take and how much governments should intervene. Eventually, the world's governments created a panel to provide the most reliable possible advice obtained from thousands of climates experts and scientists. This became the International Panel on Climate Change who established a consensus that it was *much more likely than not* that our world in fact is in a global warming state.

3.2 International Panel on Climate Change (IPCC) 1st through 3rd Assessments

The World Meteorological Organization (WMO) and the United Nations Environment Programme (UNEP) created the IPCC in 1988 with the task of assessing the scientific, technical, and socioeconomic information relevant for understanding the risk of human-induced climate change. The original mandate for the IPCC was extensive: '(a) Identification of uncertainties and gaps in our present knowledge with regard to climate changes and its potential impacts, and preparation of a plan of action over the short-term in filling these gaps; (b) Identification of information needed to evaluate policy implications of climate change and response strategies; (c) Review of current and planned national/international policies related to the greenhouse gas issue; (d) Scientific

and environmental assessments of all aspects of the greenhouse gas issue and the transfer of these assessments and other relevant information to governments and intergovernmental organizations to be taken into account in their policies on social and economic development and environmental programs.' (IPCC, 2007) The IPCC has three Working Groups and a Task Force. Working Group I (WGI) assesses the scientific aspects of the climate system and climate change, while Working Groups II (WGII) and III (WGIII) assess the vulnerability and adaptation of socioeconomic and natural systems to climate change, and the mitigation options for limiting greenhouse gas emissions, respectively. The Task Force is responsible for the IPCC National Greenhouse Gas Inventories Programme. (IPCC, 2007) A primary activity of the IPCC is to provide on a timely basis an assessment of the state of knowledge on climate change. This section will focus on a summary of the key advances and accomplishments of the First (FAR), Second (SAR), and Third (TAR) Assessments Reports.

The IPCC reviews and synthesizes the scientific literature to create its reports to base them upon the best available science. In doing this work, the IPCC also contributes by identifying key uncertainties and coordinating focused research to address and answer specific important climate change questions. However, climate scientists cannot perform controlled experiments on the Earth and easily observe results. Earth science disciplines are similar to astronomy and cosmology. But to their credit, thousands of empirical tests of various hypotheses have built a large body of Earth science knowledge. By combining both models and observations, tests can be made to test planetary-scale hypotheses. Consider the example of global cooling resulting from the eruption of Mt. Pinatubo

which provided important tests of specific aspects of some climate models (Hansen et al., 1992). Another example is the subsequent measurements and observations of temperatures compared to the projections of the FAR, SAR, and TAR. Figure 6 shows that FAR model projections were higher than the SAR and TAR, and also higher than actual observations. The actual observations were above the SAR but within and near the upper range of the TAR (IPCC, 2001a).

Over the years IPCC efforts were required to increase dramatically to keep pace with the ever increasing amount of climate related research. Between 1965 and 1995, the number of articles published each year in atmospheric science journals tripled (Geerts, 1995). Stanhill (2001) found that the climate change science literature grew approximately exponentially with a doubling time of 11 years during the period 1951 to 1997. Additionally, 95% of all the climate change science literature since 1834 was published after 1951. (IPCC, 2007)

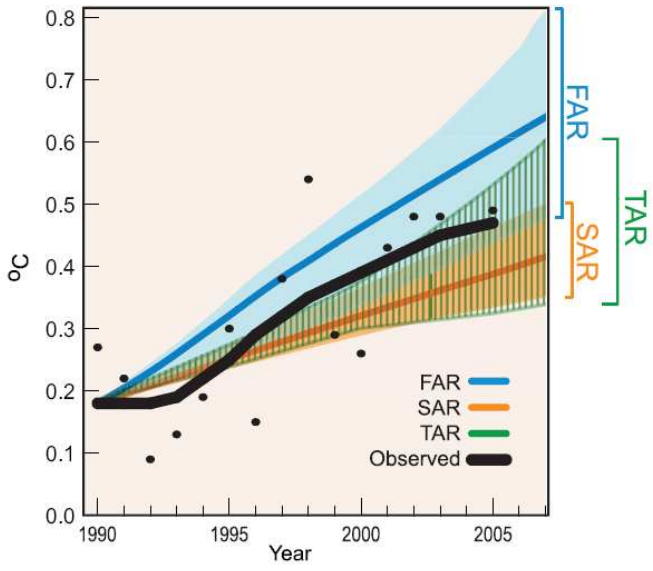

Figure 6 Yearly Global Average Surface Temperatures (IPCC, 2007)

Yearly Global Average Surface Temperatures from (IPCC, 2007, AR4WG1_Ch01, Figure 1.1) Temperatures are relative to the mean 1961 to 1990 values, and as projected in the FAR (IPCC, 1990), SAR (IPCC, 1996) and TAR (IPCC, 2001a). The "best estimate" model projections from the FAR and SAR are in solid lines with their range of estimated projections shown by shaded areas. The TAR did not have "best estimate" model projections but rather a range of projections. Annual mean observations are shown in black circles and the thick black line shows decadal variations obtained by smoothing the time series using a 13-point filter.

Over the years, collection of observed temperature data and analyses techniques have changed; however they all show a high degree of consistency. Figure 7 shows various published records of observed average global temperature with that of Brohan et al. (2006), being the longest. Most results agree but differences are greatest where the data is sparse. Willett's (1950) series agrees overall except prior to the 1880's where only 11 stations were used prior to 1850. The many different data sets and averaging techniques, and then the agreements and consistency of their results blends together to increase our confidence that the changes they demonstrate are real.

Knowledge of past and ancient climates has become increasingly important to help qualify the nature of ongoing changes and assist in the detection and attribution of those changes. Detection can be defined as the process of recognizing a change has occurred, usually in a statistical manner without out stating the reason for the change. Because we cannot perform laboratory experiments upon the Earth, attribution of anthropogenic climate change can only be obtained by: (a) detecting that the climate has changed (as defined above); (b) demonstrating that the detected change is consistent with computer model simulations of the climate change 'signal' that is calculated to occur in response to anthropogenic forcing; and (c) demonstrating that the detected change is not consistent with alternative, physically plausible explanations of recent climate change that exclude important anthropogenic forcings (IPCC, 2007). Results from the TAR

present evidence of many research results demonstrating model-predicted "fingerprints" of anthropogenic climate change and taken together these efforts clearly present the case for an identifiable human influence on the global climate.

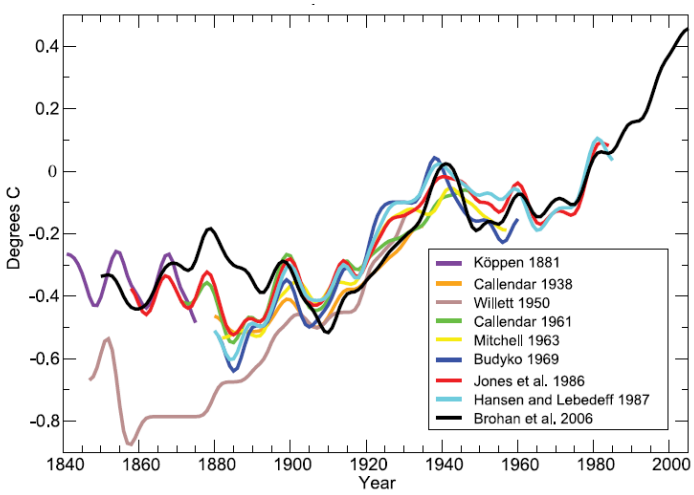

Figure 7 Global Average Temperature Series from (IPCC, 2007)

Figure 1.3. *Published records of surface temperature change over large regions. Köppen (1881) tropics and temperate latitudes using land air temperature. Callendar (1938) global using land stations. Willett (1950) global using land stations. Callendar (1961) 60°N to 60°S using land stations. Mitchell (1963) global using land stations. Budyko (1969) Northern Hemisphere using land stations and ship reports. Jones et al. (1986a,b) global using land stations. Hansen and Lebedeff (1987) global using land stations. Brohan et al. (2006) global using land air temperature and sea surface temperature data is the longest of the currently updated global temperature time series (Section 3.2). All time series were smoothed using a 13-point filter. The Brohan et al. (2006) time series are anomalies from the 1961 to 1990 mean (°C). Each of the other time series was originally presented as anomalies from the mean temperature of a specific and differing base period. To make them comparable, the other time series have been adjusted to have the mean of their last 30 years identical to that same period in the Brohan et al. (2006) anomaly time series.*

With increasing temperatures, the affects of the Greenland and Antarctica ice sheets, continental glaciers, snow, sea ice, river and lake ice, as well as permafrost, become even more important. Together, these features compose the "cryosphere" and have varying affects on the climate. Potential impacts on ocean circulation and sea level are very important and pose significant hazards to humans. A sea level rise of 5 meters was projected with the melting of the western Antarctic ice shelves and subsequent loss of the West Antarctic Ice Sheet to the ocean (Mercer, 1978).

With developments in the understanding of the oceanic and atmospheric circulations, scientists now better understand the strength and variability of global ocean

circulation but there is still debate to its complete role in the climate. To better understand the climate and these factors, climate scientists now rely heavily upon numerical models. Due to the speed and power of today's supercomputers, model complexity has also increased by including more and more components, increasing the length of simulations, as well as spatial resolutions. Figure 8 portrays spatial resolution advancements from the FAR through AR4. Since the work of Lorenz (1963) people have known that even simple models may display complex behavior because of their inherent nonlinearities. Additionally, it has been found that key processes (e.g. clouds, vegetation) that have significant control on climate sensitivity and abrupt climate change depend on very small spatial scales.

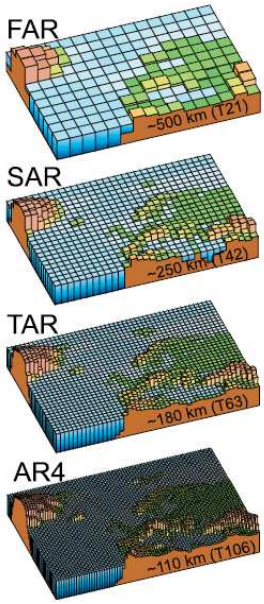

Figure 8 Spatial Model Resolutions from (IPCC, 2007)

Figure 1.4. *Geographic resolution characteristic of the generations of climate models used in the IPCC Assessment Reports: FAR (IPCC, 1990), SAR (IPCC, 1996), TAR (IPCC, 2001a), and AR4 (2007). The figures above show how successive generations of these global models increasingly resolved northern Europe. These illustrations are representative of the most detailed horizontal resolution used for short-term climate simulations. The century-long simulations cited in IPCC Assessment Reports after the FAR were typically run with the previous generation's resolution. Vertical resolution in both atmosphere and ocean models is not shown, but it has increased comparably with the horizontal resolution, beginning typically with a single-layer slab ocean and ten atmospheric layers in the FAR and progressing to about thirty levels in both atmosphere and ocean.*

3.3 International Panel on Climate Change (IPCC) 4th Assessment Report (AR4)

The Working Group I contribution to the IPCC AR4 describes in detail the human and natural drivers of climate change. This report is built upon the past IPCC work of the First (FAR), Second (SAR), and Third Assessment Reports (TAR), respectively. The IPCC AR4, released in the fall of 2007, captures new research and results spanning the six years after the TAR. The tremendous accomplishments of AR4 were so outstanding, the entire IPCC Board of Scientists along with climate change activist and former Vice President of the United States Al Gore, shared the 2007 Nobel Peace Prize for their efforts.

This chapter presents a brief summary of AR4 findings. However the AR4 provides new uncertainty guidance and the likelihood of a result or outcome. The standard terms used for levels of confidence are:

Table 2 IPCC Levels of Confidence Terminology (IPCC, 2007)

Confidence Terminology	Degree of confidence in being correct
Very high confidence	At least 9 out of 10 chance
High confidence	About 8 out of 10 chance
Medium confidence	About 5 out of 10 chance
Low confidence	About 2 out of 10 chance
Very low confidence	Less than 1 out of 10 chance

Standard terms to define the likelihood of an event are:

Table 3 IPCC Likelihood of Occurrence Terminology (IPCC, 2007)

Likelihood Terminology	Likelihood of the occurrence/ outcome
Virtually certain	> 99% probability
Extremely likely	> 95% probability
Very likely	> 90% probability
Likely	> 66% probability
More likely than not	> 50% probability
About as likely as not	33 to 66% probability
Unlikely	< 33% probability
Very unlikely	< 10% probability
Extremely unlikely	< 5% probability
Exceptionally unlikely	< 1% probability

The following are listing several of the primary findings of the IPCC AR4:

- Greenhouse gas concentrations of carbon dioxide, methane, and nitrous oxide have increased significantly due to human activities and now far exceed values obtained from ice cores spanning thousands of years. Carbon dioxide is the most important gas (Figure 9) and now exceeds a pre industrial level of 280 ppm to 379 ppm in 2005. Natural levels derived from ice cores range from 180 to 300 ppm over the last 650,000 years.
- Global warming is now undisputable as evident in measured increases in the average global air and ocean temperature as well as the world wide melting of glaciers and ice sheets, and the rise in average global sea level (Figure N.2).
- Numerous long term climate changes have occurred across continental and regional scales. These include widespread changes in precipitation, ocean salinity, wind patterns, and extreme weather including droughts, heavy precipitation, heat waves, and the intensity of tropical cyclones. (Figure 9 and Table 4 and 5).

- Since the TAR, major advancements have been realized in the assessment of climate change projections due to the significant improvements in numerical climate models, the broader range of models, and the larger number of simulations available. Model simulations cover a range of future scenarios including idealized emissions or concentrations. These include SRES[14] illustrative marker scenarios for the 2000 to 2100 year period, as well as concentrations held constant after year 2000 or 2100.
- For the next 20 years, a warming of about 0.2 ^{O}C per decade, or 0.4 ^{O}C by around 2027, for the range of SRES[14] scenarios. Continued greenhouse gas emissions at or above the current rates would cause *further* warming and induce many changes in the 21st century that would *very likely (>90% probability)* be larger than those of the 20th century. (Table 6 and Figure 10)
- Very likely of slow down of meridional overturning current or THC
- Anthropogenic warming and sea level rise would continue for centuries due to the time scales associated with climate processes and feedbacks, even if green gas concentrations were stabilized to those of today.

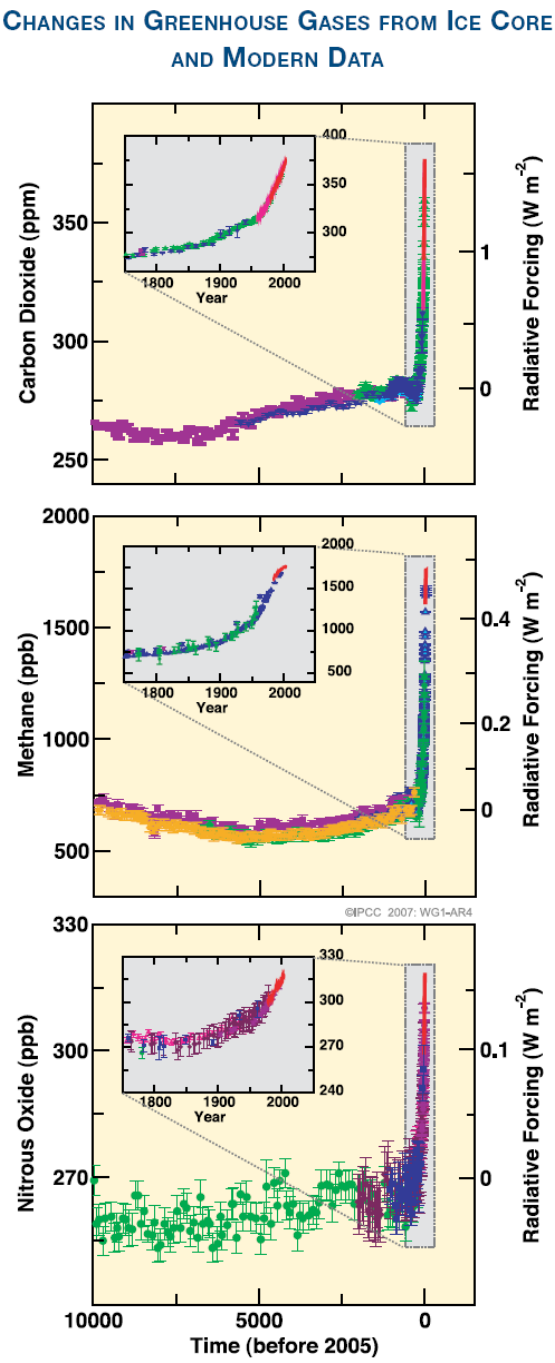

Figure 9 Atmospheric concentrations of green house gases 10,000 years to present (IPCC AR4 Figure SPM.1)

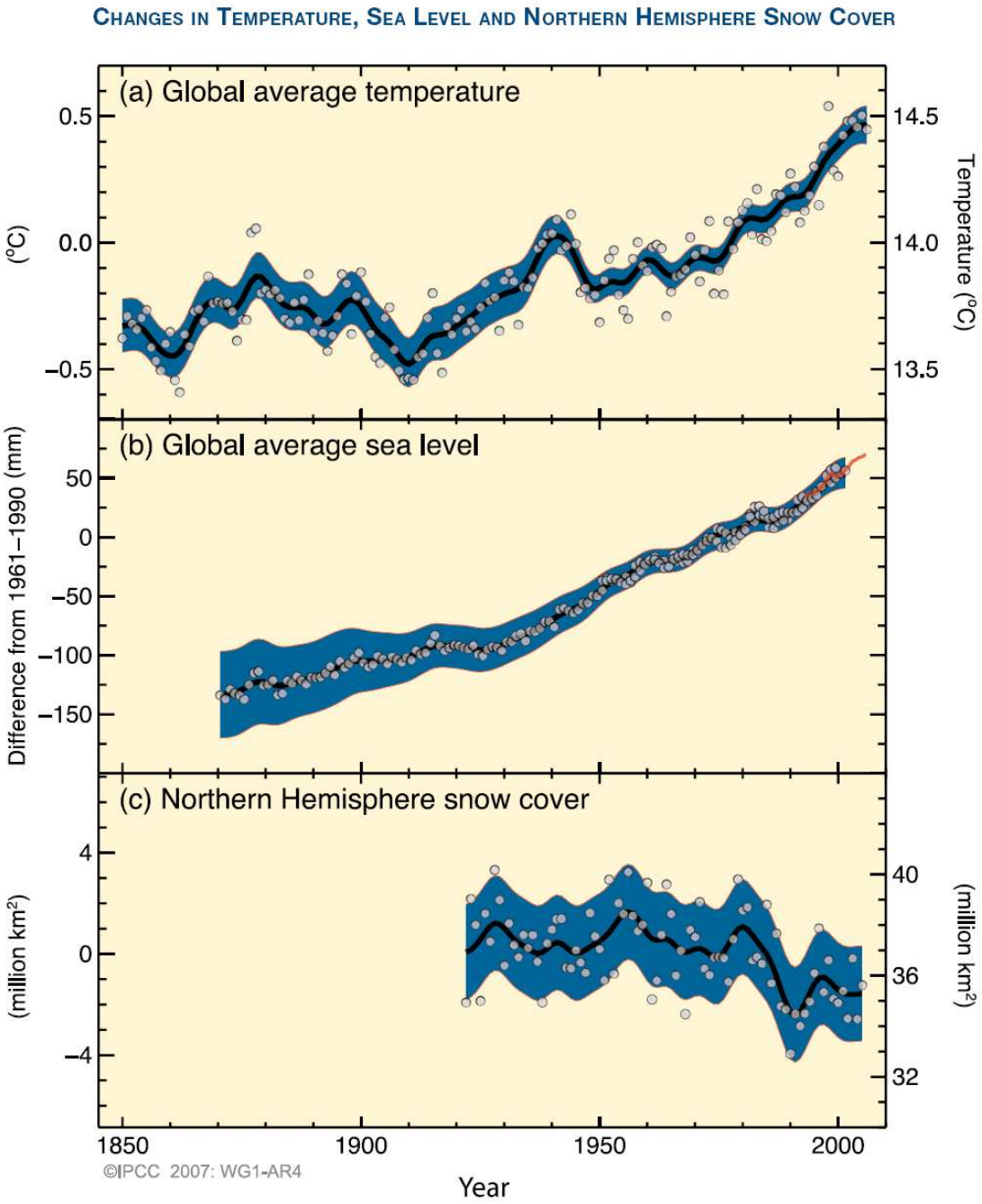

Figure 10 Observed changes in global temperatue, sea level, and snow cover
Observed changes in global average surface temperature, global average sea level, and Northern Hemisphere snow cover March through April. (IPCC AR4, SPM, Figure SPM.3)

Table 4 Sources of sea level rise (IPCC FAR, SPM Table SPM.1)

Source of sea level rise	Rate of sea level rise (mm per year) 1961–2003	1993–2003
Thermal expansion	0.42 ± 0.12	1.6 ± 0.5
Glaciers and ice caps	0.50 ± 0.18	0.77 ± 0.22
Greenland Ice Sheet	0.05 ± 0.12	0.21 ± 0.07
Antarctic Ice Sheet	0.14 ± 0.41	0.21 ± 0.35
Sum of individual climate contributions to sea level rise	1.1 ± 0.5	2.8 ± 0.7
Observed total sea level rise	1.8 ± 0.5[a]	3.1 ± 0.7[a]
Difference (Observed minus sum of estimated climate contributions)	0.7 ± 0.7	0.3 ± 1.0

Table 5 Recent trends and projections IPCC FAR

Recent trends, assessment of human influence on the trend, and projections of extreme weather events for which there is an observed 20th century trend. (IPCC FAR, Table SPM.2)

Phenomenon[a] and direction of trend	Likelihood that trend occurred in late 20th century (typically post 1960)	Likelihood of a human contribution to observed trend[b]	Likelihood of future trends based on projections for 21st century using SRES scenarios
Warmer and fewer cold days and nights over most land areas	*Very likely*[c]	*Likely*[d]	*Virtually certain*[d]
Warmer and more frequent hot days and nights over most land areas	*Very likely*[e]	*Likely (nights)*[d]	*Virtually certain*[d]
Warm spells/heat waves. Frequency increases over most land areas	*Likely*	*More likely than not*[f]	*Very likely*
Heavy precipitation events. Frequency (or proportion of total rainfall from heavy falls) increases over most areas	*Likely*	*More likely than not*[f]	*Very likely*
Area affected by droughts increases	*Likely* in many regions since 1970s	*More likely than not*	*Likely*
Intense tropical cyclone activity increases	*Likely* in some regions since 1970	*More likely than not*[f]	*Likely*
Increased incidence of extreme high sea level (excludes tsunamis)[g]	*Likely*	*More likely than not*[f,h]	*Likely*[i]

Table 6 Projected global average surface temperature and SLR

Case	Temperature Change (°C at 2090-2099 relative to 1980-1999)[a] Best estimate	*Likely* range	Sea Level Rise (m at 2090-2099 relative to 1980-1999) Model-based range excluding future rapid dynamical changes in ice flow
Constant Year 2000 concentrations[b]	0.6	0.3 – 0.9	NA
B1 scenario	1.8	1.1 – 2.9	0.18 – 0.38
A1T scenario	2.4	1.4 – 3.8	0.20 – 0.45
B2 scenario	2.4	1.4 – 3.8	0.20 – 0.43
A1B scenario	2.8	1.7 – 4.4	0.21 – 0.48
A2 scenario	3.4	2.0 – 5.4	0.23 – 0.51
A1FI scenario	4.0	2.4 – 6.4	0.26 – 0.59

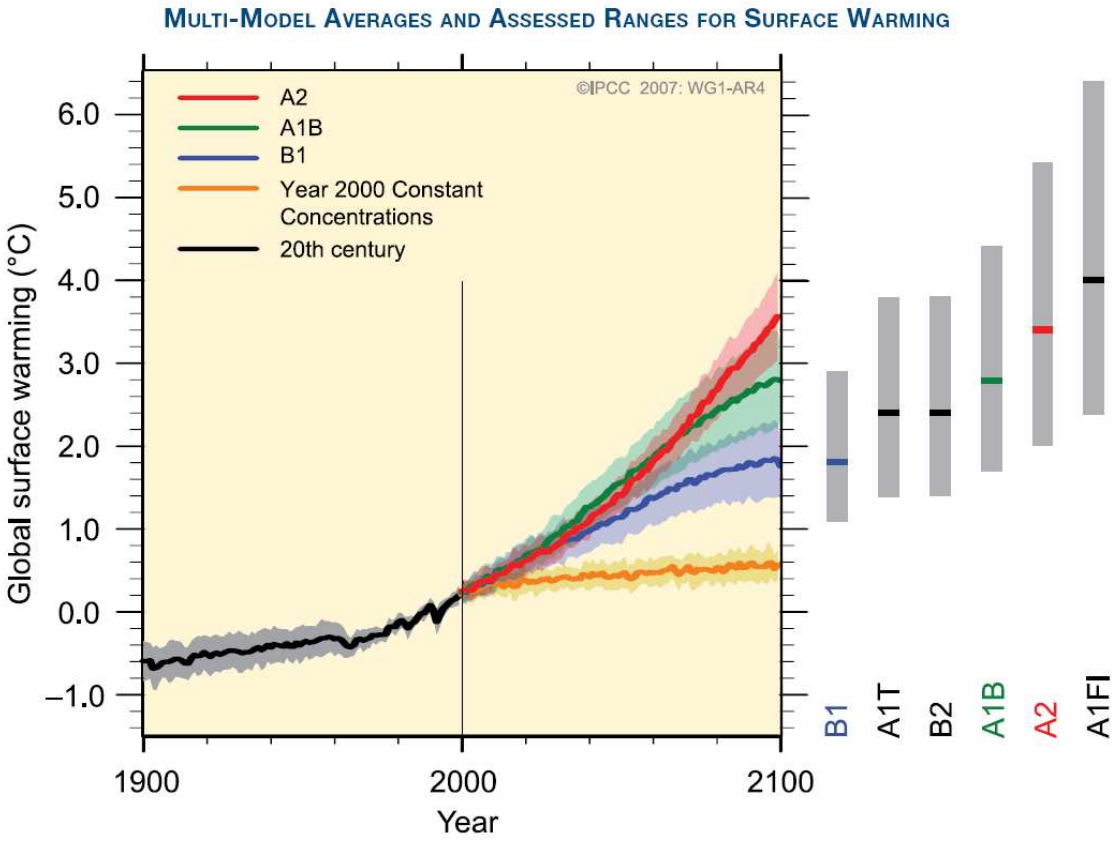

Figure SPM.5. *Solid lines are multi-model global averages of surface warming (relative to 1980–1999) for the scenarios A2, A1B and B1, shown as continuations of the 20th century simulations. Shading denotes the ±1 standard deviation range of individual model annual averages. The orange line is for the experiment where concentrations were held constant at year 2000 values. The grey bars at right indicate the best estimate (solid line within each bar) and the* ***likely*** *range assessed for the six SRES marker scenarios. The assessment of the best estimate and* ***likely*** *ranges in the grey bars includes the AOGCMs in the left part of the figure, as well as results from a hierarchy of independent models and observational constraints. {Figures 10.4 and 10.29}*

Figure 11 Projected average global surface temperatures (IPCC FAR, Figure SPM.5)

Table 7 SRES emission scenarios (IPCC, 2007 Special Report on Emission Scenarios)

THE EMISSION SCENARIOS OF THE IPCC SPECIAL REPORT ON EMISSION SCENARIOS (SRES)[17]

A1. The A1 storyline and scenario family describes a future world of very rapid economic growth, global population that peaks in mid-century and declines thereafter, and the rapid introduction of new and more efficient technologies. Major underlying themes are convergence among regions, capacity building and increased cultural and social interactions, with a substantial reduction in regional differences in per capita income. The A1 scenario family develops into three groups that describe alternative directions of technological change in the energy system. The three A1 groups are distinguished by their technological emphasis: fossil-intensive (A1FI), non-fossil energy sources (A1T) or a balance across all sources (A1B) (where balanced is defined as not relying too heavily on one particular energy source, on the assumption that similar improvement rates apply to all energy supply and end use technologies).

A2. The A2 storyline and scenario family describes a very heterogeneous world. The underlying theme is self-reliance and preservation of local identities. Fertility patterns across regions converge very slowly, which results in continuously increasing population. Economic development is primarily regionally oriented and per capita economic growth and technological change more fragmented and slower than other storylines.

B1. The B1 storyline and scenario family describes a convergent world with the same global population, that peaks in mid-century and declines thereafter, as in the A1 storyline, but with rapid change in economic structures toward a service and information economy, with reductions in material intensity and the introduction of clean and resource-efficient technologies. The emphasis is on global solutions to economic, social and environmental sustainability, including improved equity, but without additional climate initiatives.

B2. The B2 storyline and scenario family describes a world in which the emphasis is on local solutions to economic, social and environmental sustainability. It is a world with continuously increasing global population, at a rate lower than A2, intermediate levels of economic development, and less rapid and more diverse technological change than in the B1 and A1 storylines. While the scenario is also oriented towards environmental protection and social equity, it focuses on local and regional levels.

An illustrative scenario was chosen for each of the six scenario groups A1B, A1FI, A1T, A2, B1 and B2. All should be considered equally sound.

The SRES scenarios do not include additional climate initiatives, which means that no scenarios are included that explicitly assume implementation of the United Nations Framework Convention on Climate Change or the emissions targets of the Kyoto Protocol.

3.4 Abrupt Climate Change

Since the 1800's and through today a vast range of geomorphology and paleontology studies have provided knew knowledge of Earth's past climates going back to hundreds of millions of years. The Paleozoic Era (600 Ma) showed evidence of both warmer and colder climate than the present; while the Tertiary Period (6.5 to 2.6Ma) was

generally warmer, and the Quaternary Period (2.6 Ma to present) has shown oscillations between glacial and interglacial conditions (IPCC, 2007). Over the years people have become aware that long term climate observations can significantly advance the understanding of the physical mechanisms affecting the climate. Palaeoclimatic research has escalated over the last decade with a plethora of new techniques to retrieve numerous climate characteristics. With the discovery of past abrupt climate changes first discovered in Greenland (Dansgaard et al., 1984) and Antarctic ice cores, these efforts have become even more important. Within these contexts, 'abrupt' designates regional events of large amplitude, typically a few degrees Celsius, which occurred within several decades – much shorter than the thousand-year time scales that characterize changes in astronomical forcing (IPCC 2007). Further analyses of ice cores during the 1990's identified numerous changes (Dansgaard et al., 1993), that were abrupt (Alley et al., 1993) and of large magnitude. These changes are now called the Dansgaard-Oeschger events.

Now even more stunning evidence of really fast large climatic shifts within 1 to 3 years have been identified by analyzing new ice cores from the Northern Greenland Ice Core Project (Steffensen et al. 2008). The authors show that middle to high northern latitude atmospheric circulation changed within 1 to 3 years. They found deuterium excess, which is a proxy of Greenland precipitation moisture source, switched mode within 1 to 3 years and initiated a more gradual (50 year) change of Greenland air temperature. Along with deuterium excess, the authors used $\delta^{18}O$ (a proxy for local temperature), dust and calcium (originating at low-latitude Asian deserts), and sodium.

These enabled a high resolution record which allowed them to precisely define the shifts. Normally, ice core records are 'fuzzy' at these time scales and this is the first publication with such high resolution results.

In addition to ice cores, palaeoclimate studies use numerous types of physical records to reconstruct the past which include pollen records, insect and animal remains, oxygen isotopes and other geological data form lakes and ocean sediments and even cave stalagmites. A climate proxy is generally defined as a quantitative record, such as thickness and chemical composition of tree rings, oxygen isotopes, and pollen of different species. A "transfer function" is created based on physical principles and recent observed correlations between the two records.

Scientists are now using multiple types of climate proxies which complement each other. Steffensen et al., (2008) is an example of this type of effort because traditionally ice cores data is blurry at scales less than a decade. Stalactites and stalagmites have increasingly become valuable as high resolution proxies of prehistoric climates. They complement the ice core data by revealing climate information on the interior of continents away from ice sheets and glaciers. Stalagmites and stalactites are deposits of calcium carbonates called speleothems and of course form in caves. Fleitmann (2008) analyzed stalagmites from caves from Oman and Yemen to study climate of the Persian Gulf over the last 10,000 years. Speleothems are one of the exciting new proxies because of their great precision: from one year to decades. Treble et

al. (2007), found a very abrupt climate shift approximately 16,070 years ago using speleothems from Asia.

Paleotempestology is a relatively new field devoted specifically to the study of ancient storms using the geologic record. Liu (2004) examined the frequency of ancient Gulf Coast tropical cyclones by analyzing near shore sand over-wash deposits. Liu identified a Gulf Coast 'hyperactive period' about 3400 to 1000 yr ago during which catastrophic hurricanes struck 3 to 5 times more frequently than during the most recent millennium (Liu 2004). Paleotempestology records provide a better estimate of the 'worst case scenario' than conventional historical hurricane databases because very long records are more likely to sample very rare, catastrophic events with long recurrence intervals of hundreds to thousands of years (Frappier et al. 2007).

From this brief summary above, one can begin to see as we continue our efforts to retrieve prehistoric climate information, large scale abrupt climate changes abound throughout the earth's history. Accumulation of evidence points continues to point to abrupt changes that are possible within less than 10 years rather than on a scale of 100 to 1000 years as previously surmised.

Chapter 4 2050 Storm Surge Simulations with Present Climate

4.1 Introduction

Dating from the early 1940's significant efforts have been performed to map the northern Gulf Coast of Mexico and quantify not only the land loss and land gain but also the rich and changing ecosystem of the entire coast. The earliest land loss maps date from 1946 Corp of Engineers photography. Since then a series of mapping efforts coordinated and funded by several Federal and State agencies have quantified the coastal changes over time (Britsch, Dunbar, 1993). With the era of the satellites, the U.S. Geological Survey, the U.S. Army Corps of Engineers and Louisiana state agencies successfully used LANDSAT imagery to quantify land loss and gain from the 1970's through 2002 and used these historic rates to project coastal wetland areas in 2050 (Barras et al, 2007). This work was performed in conjunction with the Louisiana Coastal Area (LCA) project. The Corps of Engineers, USGS, and State of Louisiana quantified land loss rates for delineated sub domains, based on historical photos and satellite data to produce a projected land loss/gain for the year 2050. In support of LCA, the Coastal Louisiana Ecosystem and Restoration (CLEAR) Program performed additional analyses and produced datasets quantifying ecological and wetland changes for several future scenarios. The future landscapes were modeled based upon with state, federal, and local protection and restoration projects in place, as well as with "no increased actions" (Twilley et al., 2008). A 2050 landscape was created based on a "degraded" coastal zone. Using this degraded landscape, ADCIRC 2050 geometry was created as well as a

friction layer based on the Manning's n values of the wetland features. Figure 12 shows the difference between ADCIRC mesh which represents 2050 topography and the ADCIRC mesh which represents 2007 conditions in the south eastern Louisiana area. The "2007" denotes the configuration of the levee heights surrounding the New Orleans area and not specifically the topography. Topography and bathymetry encoded in the "2007" ADCIRC mesh were compiled from LIDAR collected from 2001 through 2005 and the most recent bathymetry available at the time of construction of the ADCIRC mesh. Generally, 2050 topography is approximately 1 to 3 feet lower than 2007 mesh topographic elevations but only in areas of high erosion or local subsidence. However there are some regions with land gain and 2050 topography is higher than present-day elevations. The 2050 geometry was delineated with 2007 levee heights and then a duplicate geometry was created but with 2057 levee heights. These ADCIRC geometries were used in the 2050 storm simulations. Having established the landscape of 2050, one can then ask "What are the results of a Katrina-like storm in 50 years?" A Planetary Boundary Layer wind model was used to create Katrina winds which were simulated with ADCIRC and the results of these simulations are detailed below. However, Katrina and Rita were not physically the most potentially high Category 5 storms making landfall on the coast. Questions now arise as to assuming today's climatology will be similar to the climatology 50 years in the future, what are the most physically possible storms, and what are the results if they were to strike the Louisiana coast.

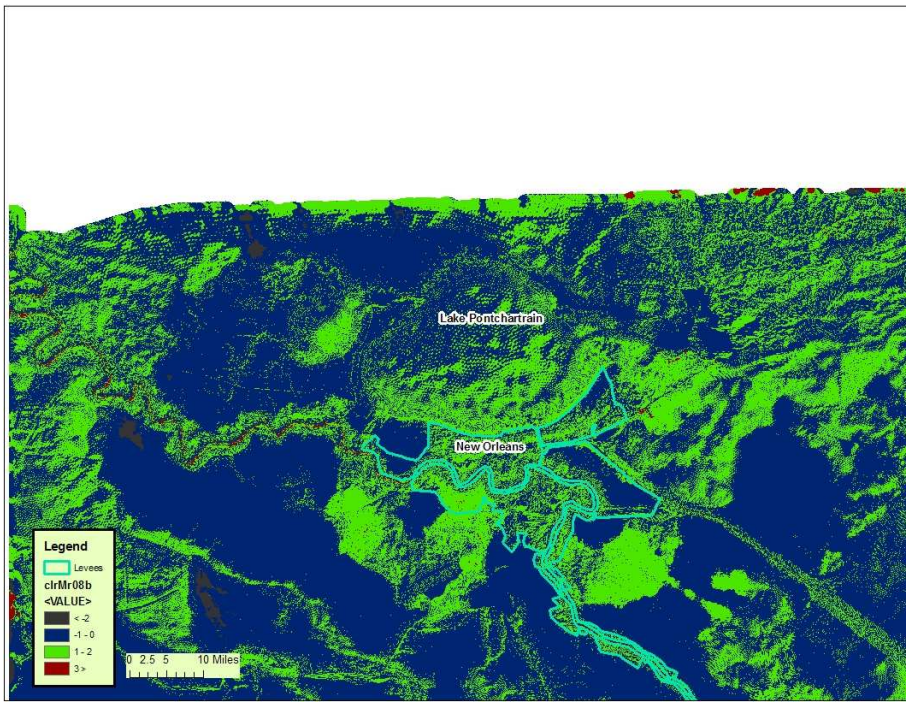

Figure 12 Difference Between 2050 topography and ADCIRC mesh topography of present-day topography with 2007 levee configuration

4.2 Analyses

What is potentially the most intense storm capable of striking the Louisiana coast? Much work has been done to answer this question. Emanuel (1987) was the first to introduce the concept of the maximum potential intensity for a tropical cyclone and link greenhouse gas-induced warming to potential intensity increases. The maximum potential intensity (MPI) can be defined as the upper limit of intensity that a TC can achieve based on conditions such as sea surface temperature, regional surface temperatures, and moisture content. But the MPI does not include dynamic effects such as wind shear. Given the today's climatology, a theoretical maximum potential intensity (MPI) was estimated as 880 mb (Resio, 2007). This MPI was obtained by combining the results of Tonkin *et al.* (2000) and Schade (2000). Tonkin *et al.* performed a comparison of the Emanuel (1986,1991) and Holland (1997) theoretical MPI models. Storms were

examined within three areas: 1) the Australian/southwest Pacific region, 2) the northwest Pacific region, and 3) the North Atlantic region. Figure 4.1 shows the comparison of these two models by Tonkin *et al.* This application used a climatological mean Sea Surface Temperature (SST) defined over the period 1950-1979. Figure 13 shows a strong relationship exists between climatological SST values and the lowest central pressures. In the range of SST values from 26^{o} to 28^{o} (C), the minimum central pressures of the Holland Model, the Emanuel model and the observed intensities are all in approximate agreement. However, above 28^{o} (C) the Holland model and the observations continue to show decreasing central pressures with increasing values of SST but the Emanuel model does not.

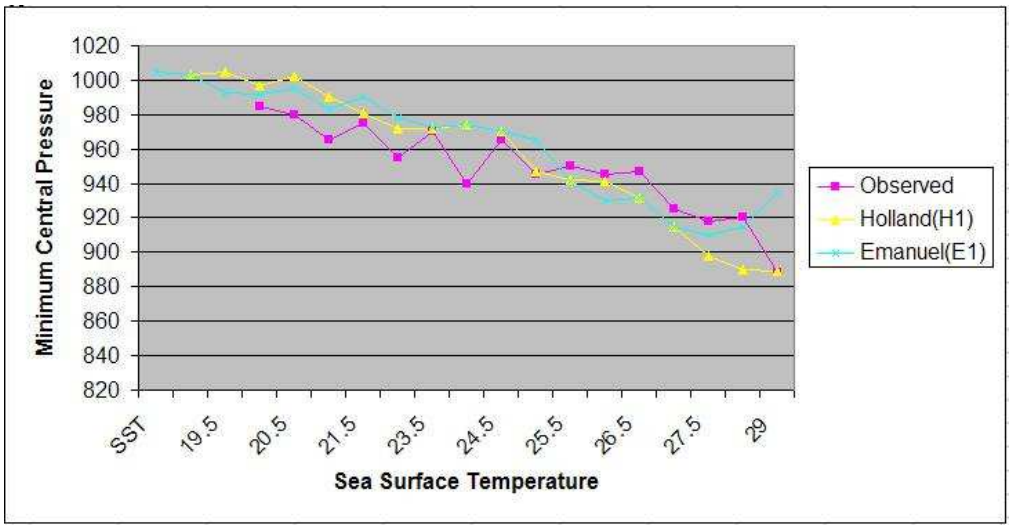

Figure 13 Relationship Observed MPI vs. Theoretical
Relationship between observed minimum central pressures (mb) and sea surface temperature (ºC) in the North Atlantic basin (from: Tonkin *et al.*, 2000).

Schade (2000) provides another method for computation and relation of the MPI to SST. Schade proposes that there are two primary effects of the SST field on tropical cyclone intensity. First, the large-scale ambient SST field "sets the stage for the tropical cyclone." Second, the intensity of a tropical cyclone is highly sensitive to the reduction

of the SST in the interior region of the storm due to the response of the ocean to surface winds. Thus, the interior SST which can be cooler can produce a negative feedback and essentially limit the decrease in central storm pressure. The highest average August-September SST for the Gulf of Mexico for the period 1940-2006 have varied from as low as 28.17^{o} C in 1984 to as high as 29.49^{o} C in 1962. (Resio, 2007) The dotted vertical line in Figure 14 shows this historical maximum plotted on top of Schade's results. The heavy solid line along the top of Figure 14 denotes the MPI value without consideration of any negative feedback of the type discussed by Schade. Thus, this value is expected to represent a maximum possible threshold for the MPI. Putting these results together one can deduce that a value of 880mb represents a sensible (perhaps slightly conservative) value for the MPI in the Gulf of Mexico. (Resio, 2007)

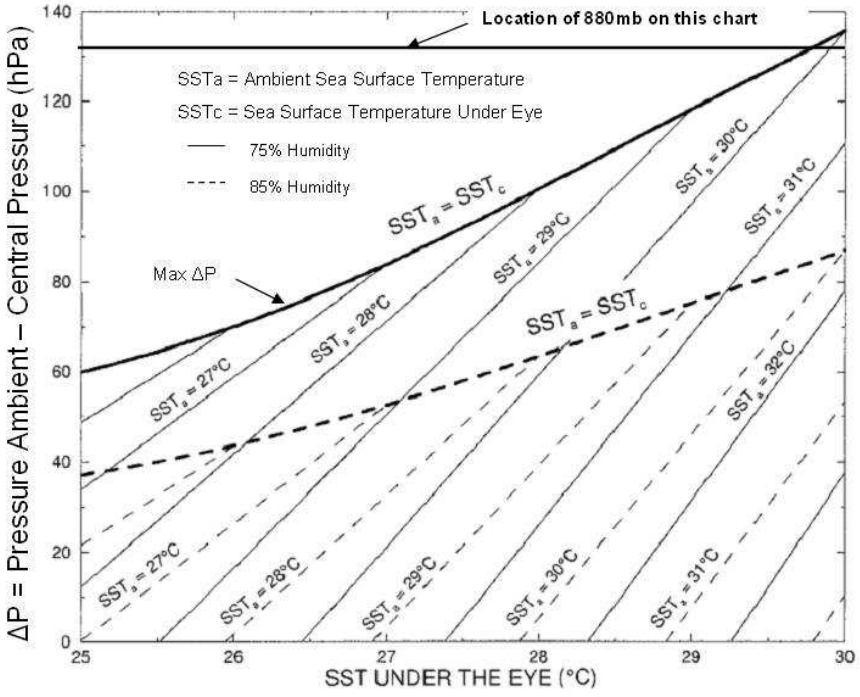

Figure 14 cyclone intensity as a function of the SST under the eye (Schade, 2000). The solid and the dashed lines correspond to ambient relative humidity of 75% and 85%, respectively. The heavy lines mark the maximum possible intensity that is realized neglecting (negative) SST feedback. The thin lines connect points with the same ambient SST.

4.3 Results

Using the theoretical maximum MPI of 880 mb, five storms (numbered 191 through 195) with a radius to max winds of 25 nautical miles, were simulated along five different tracks across southeast Louisiana shown in Figure 15. These tracks are labeled T1 through T5 and are the primary tracks used in the Corps of Engineers Louisiana Coastal Protection and Restoration (LACPR) storm surge study. Figures 16 through 19 show the peak surge levels for 2007 conditions for storms 192 through 195. Table 8 displays the parameters for each of these storms. These five storms were also simulated on the 2050 ADCIRC geometry and Figures 20 through 24 show the peak surge levels for these 2050 degraded coast conditions.

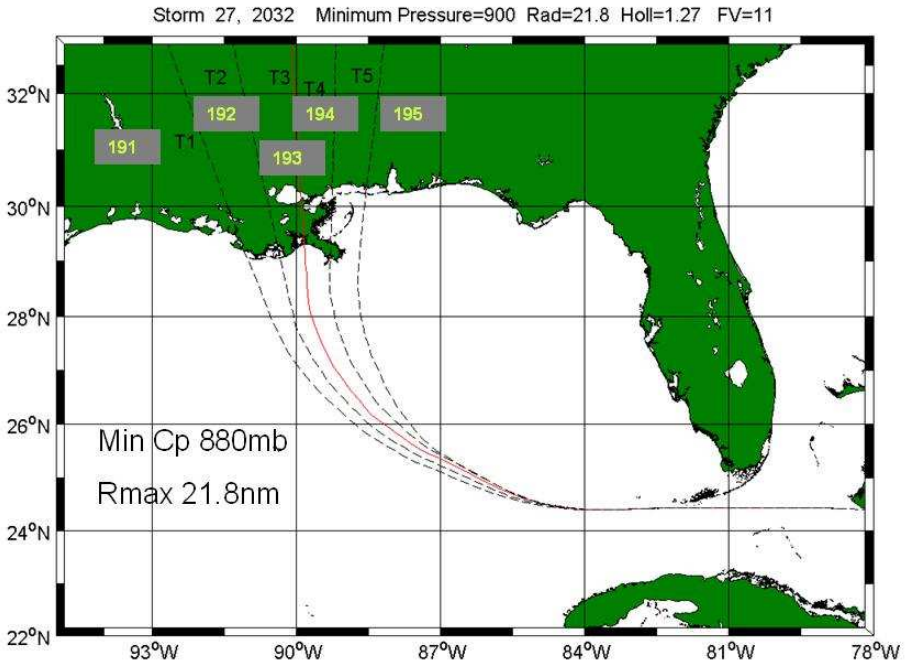

Figure 15 Storms 191 through 195 tracks

Table 8 Storms 191 through 195 parameters

Storm Number	MPI (mb)	Radius to Max Winds(nm)	Forward Velocity	Track Number
191	800	21.8	11	T1
192	800	21.8	11	T2
193	800	21.8	11	T3
194	800	21.8	11	T4
195	800	21.8	11	T5

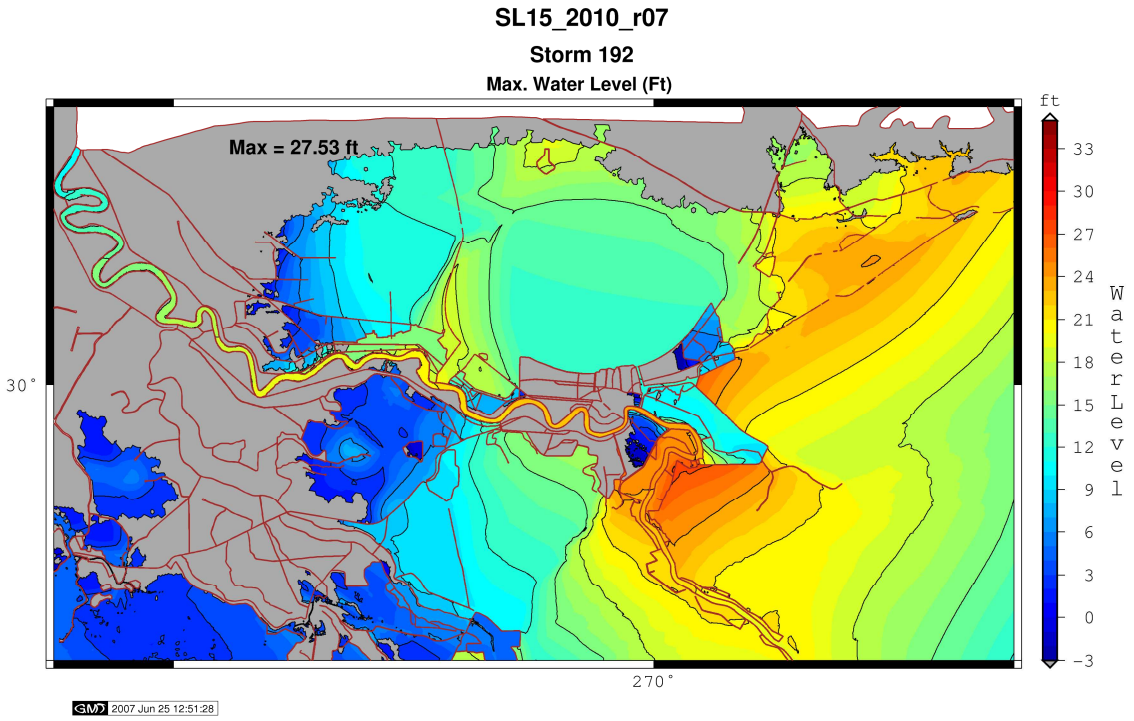

Figure 16 2007 Topography Storm 192 Surge Peaks (USACE, LACPR 2007 Tech Report)

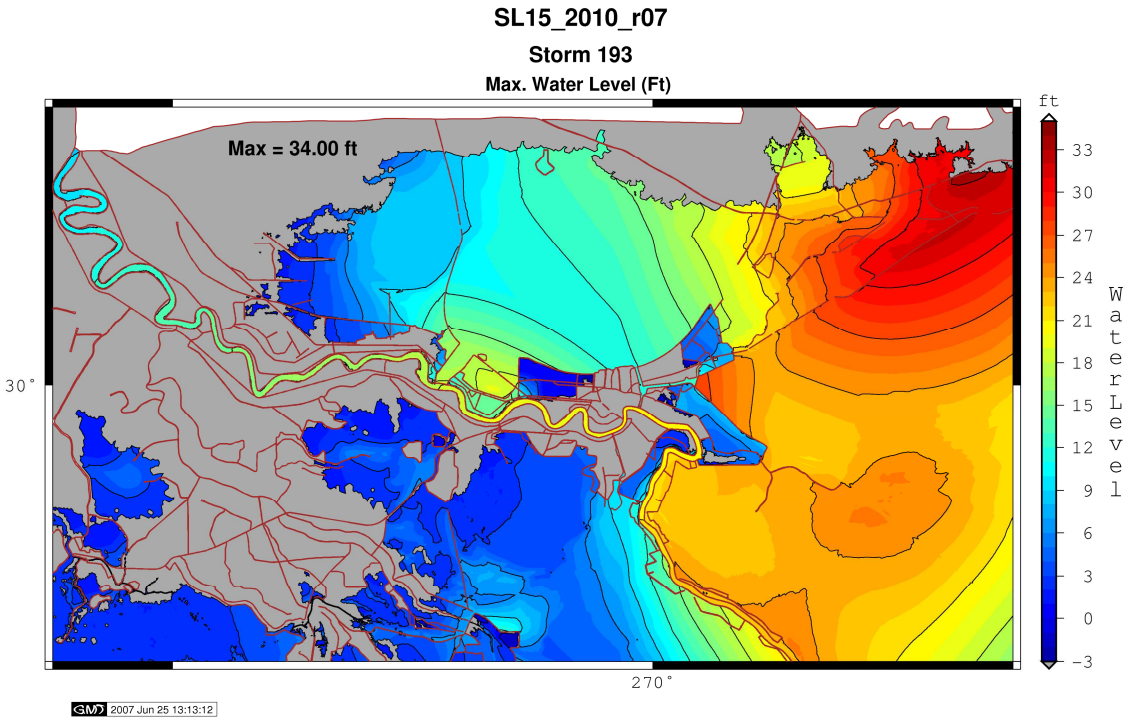

Figure 17 2007 Topography Storm 193 Surge Peaks (USACE, LACPR 2007 Tech Report)

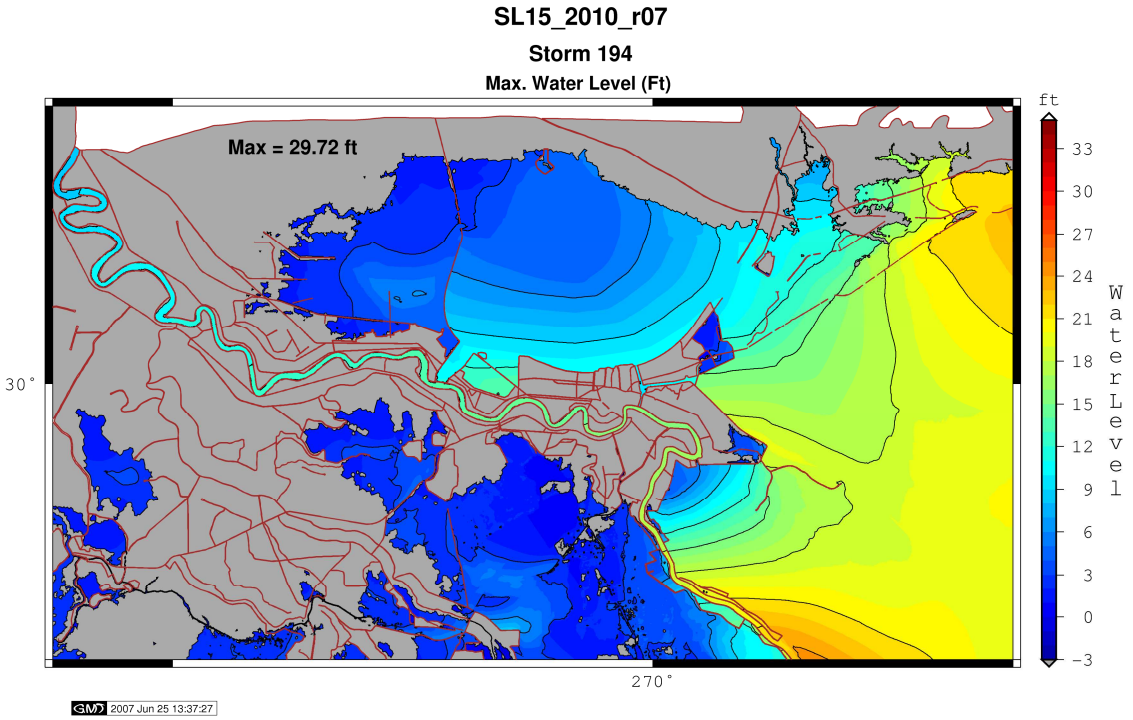

Figure 18 2007 Topography Storm 194 Surge Peak (USACE, LACPR 2007 Tech Report)

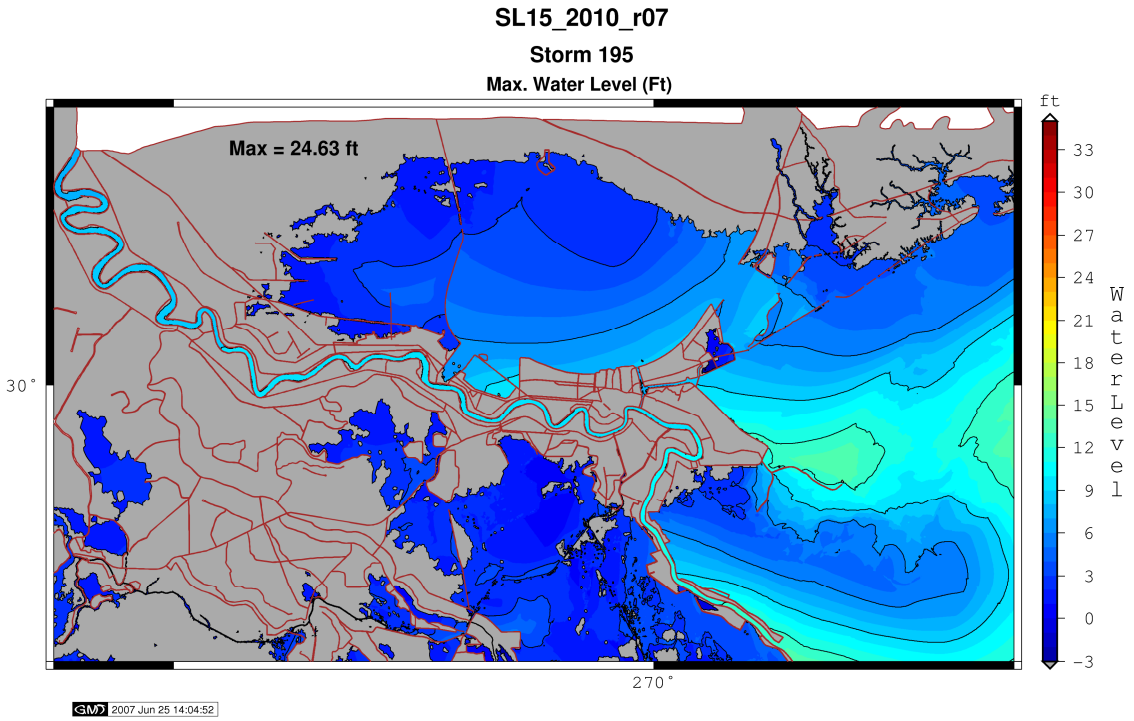

Figure 19 2007 Topography Storm 195 Surge Peak (USACE, LACPR 2007 Tech Report)

Storms 191 through 195 were also simulated with 2050 coastal topography using an ADCIRC 2050 geometry. The maximum surge elevations generated over the entire storm event, are shown for each storm in Figures 20 through 24.

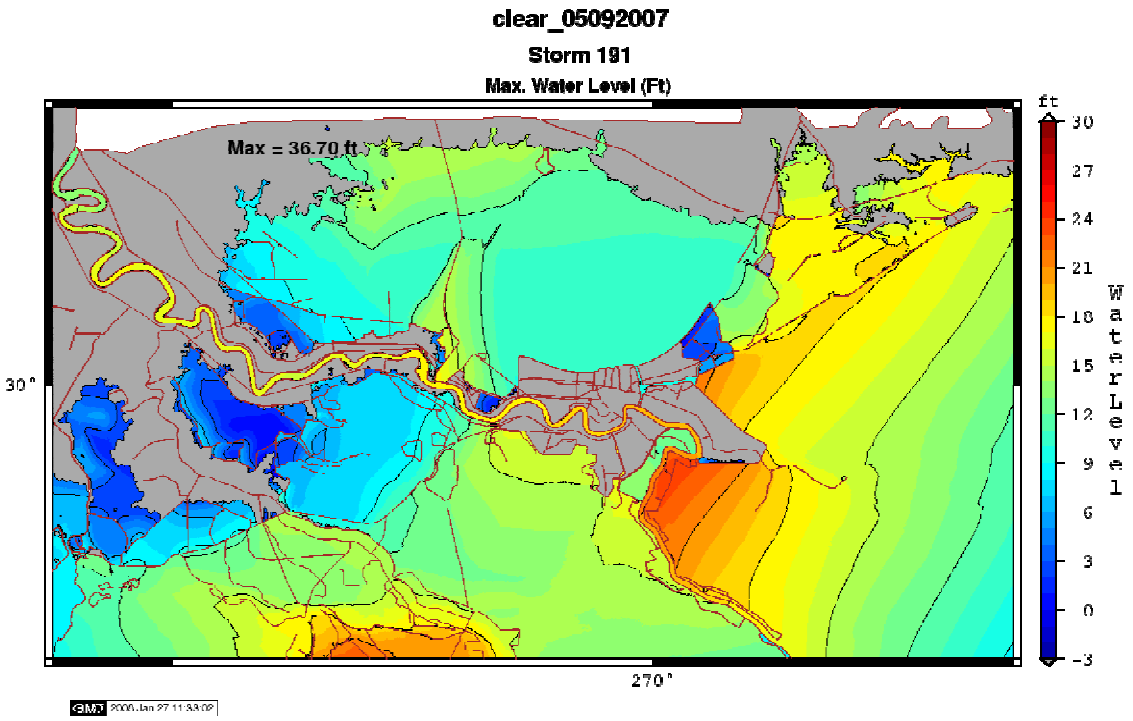

Figure 20 2050 Conditions Storm 191 peak surge elevations

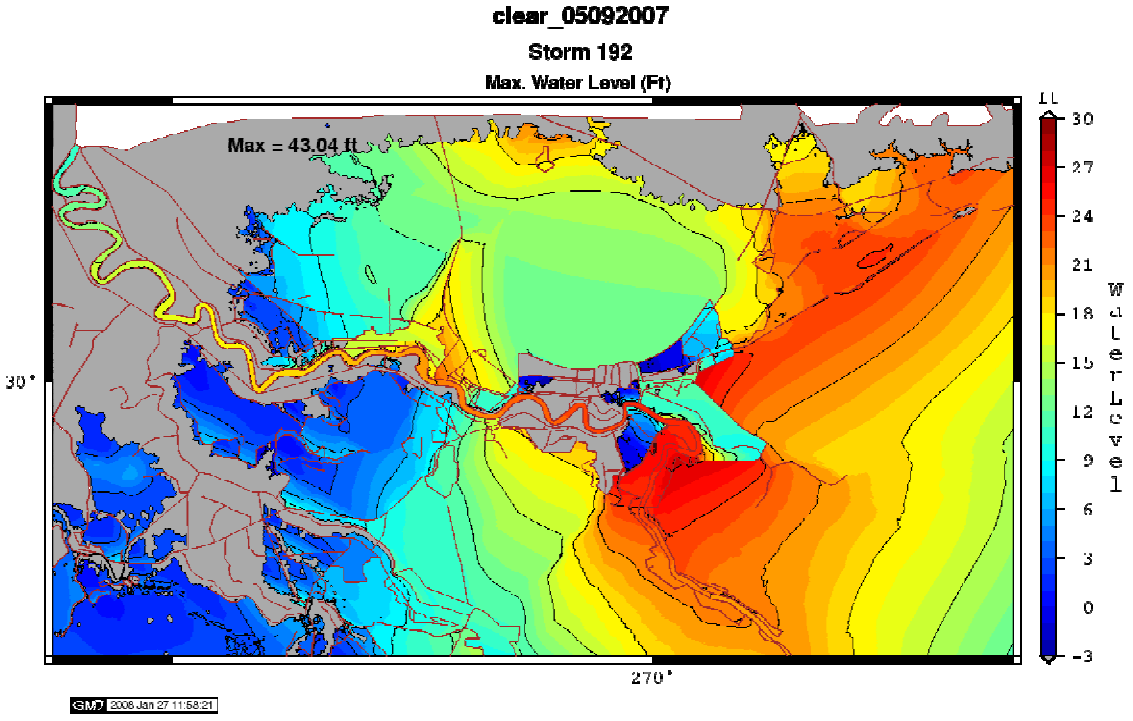

Figure 21 2050 Conditions Storm 192 peak surge elevations

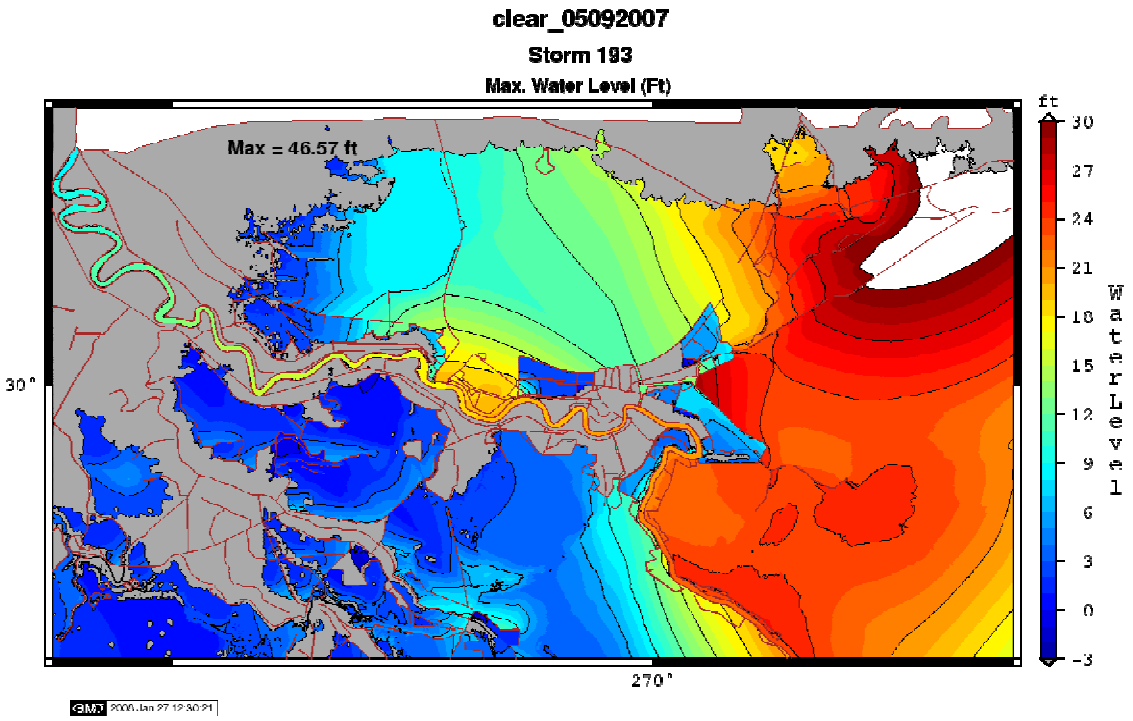

Figure 22 2050 Conditions Storm 193 peak surge elevations

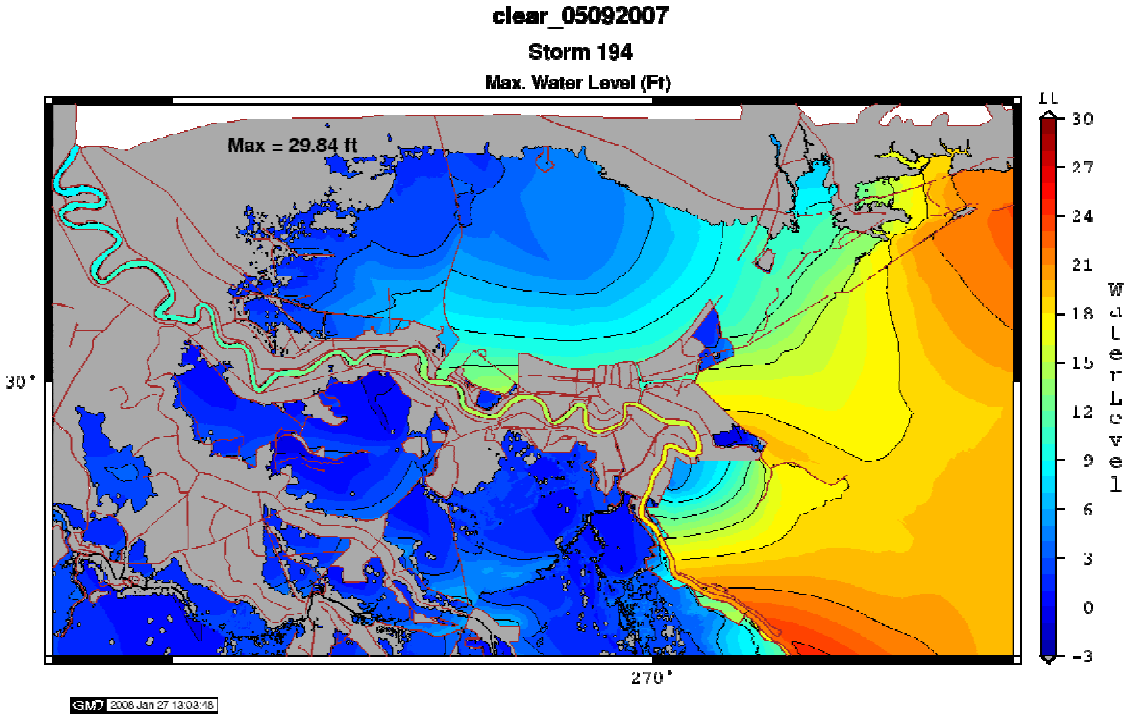

Figure 23 2050 Conditions Storm 194 peak surge elevations

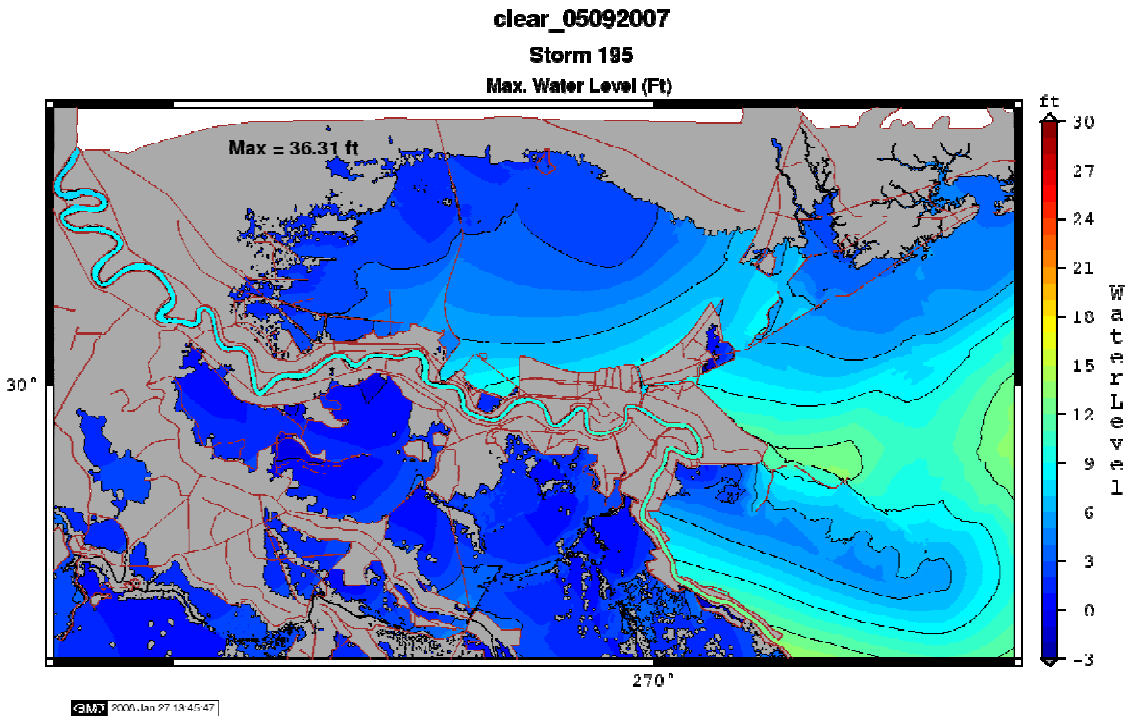

Figure 24 2050 Conditions Storm 195 peak surge elevations

Table 9 shows the comparison of peak surge for each storm for each condition. As can been seen, the peaks are all larger for the 2050 conditions. The peak maps show storm 193 with the highest surges and tremendous flooding occurs in St. Bernard, Orleans East, West Jefferson on south of Lake Pontchartrain, as well as inundation well inland on the north shore of the lake. One can see the impacts of a degraded coast where peak surges could range from a 1 to over 3 feet higher than existing conditions.

Table 9 Storm peaks for 2007 and 2050 conditions
Storm peaks for 2007 conditions and 2050 conditions for storms 191 through 195 for New Orleans and vicinity

Storm Number	Peak 2007 (ft)	Peak 2050 (ft)
191	27.00	~29.70
192	27.53	~30.40
193	34.00	~35.67
194	29.72	~29.84
195	24.63	~26.31

The U. S. Army Corps of Engineers (USACE) published 100 year level of protection levee heights (http://mvn.usace.army.mil) are show in Figure 25. The Corps will establish levees, floodwalls, and all pertinent structures to meet the 100 year level of protection by the 2011. An ADCIRC grid (2011_100yr.grd) was configured with levee heights matching this level of protection. Additionally, the proposed Inner Harbor Navigation Canal (IHNC) Closure Structure was placed into the model but was overtopped by many of the high intensity storms. This closure is still under design and the emphasis of this work is primarily to analyze overall climate and storm affects rather than specific future local results. For this reason the Mississippi River Gulf Outlent (MRGO) was left in place and not closed as it is scheduled to be closed by 2011. Katrina was simulated using this grid and the maximum peak water surface elevations are shown in Figure 26.

Figure 25 USACE 100 year level of protection levee heights

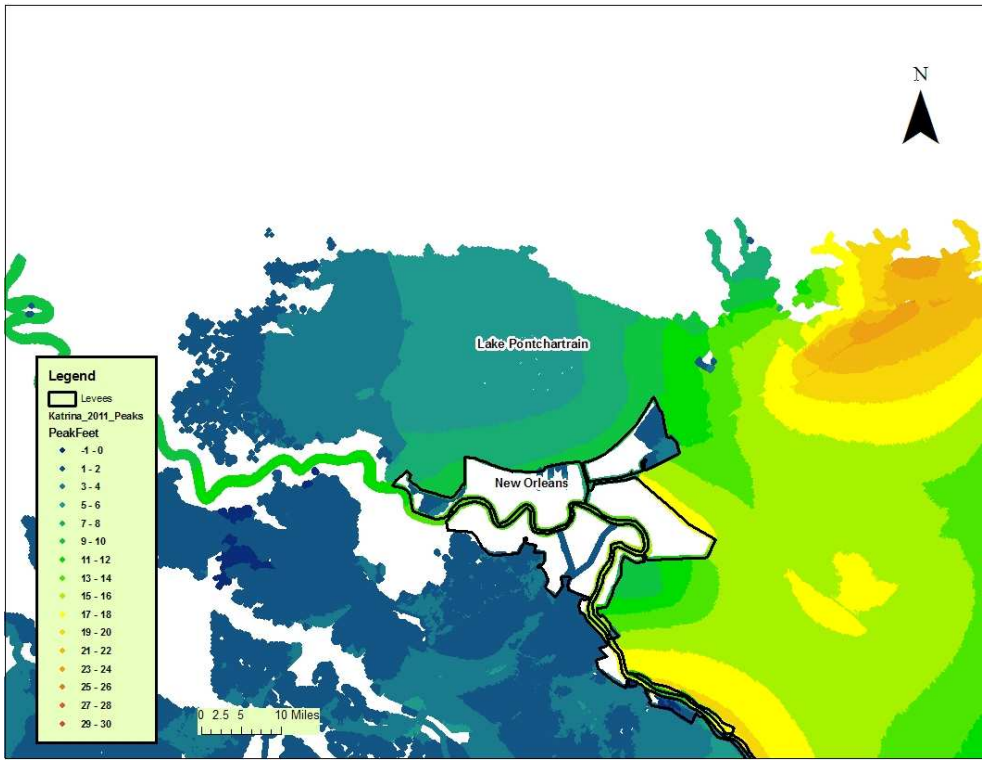

Figure 26 Maximum Katrina Storm Surge Peaks (Feet) with 2011 USACE 100 year levee heights

Katrina simulations for 2050 conditions result in somewhat higher surges; however there is essentially no overtopping of the USACE 100 year level of protection. Some overtopping occurred in the New Orleans East area due to a low levee height set in the mesh near the I-10 and levee junction. The low height was derived from levee height data that did not include the in-place structure height of 19 feet. This structure height would prevent overtopping in this location.

The storm simulations for 2050 conditions show a significant increase in surge heights for extremely intense storms. However, these storms represent the most intense events under the existing climate conditions of today. The following chapters will analyze potential intense storms under influence by increased warming from abrupt climate change.

Chapter 5 Abrupt Climate Change on Simulated Surges

5.1 Introduction

Maximum potential intensity refers to an upper-limit intensity that a tropical cyclone can attain for a given set of thermodynamic conditions (sea-surface temperature (SST), large-scale atmospheric temperature, and moisture) and does not consider effects of dynamical (e.g., related to motion or wind) influences such as wind shear on the intensity (Shepherd *et al*, 2007). Emanuel (1987) initially employed a simple model of a tropical cyclone as a Carnot engine. Figure 27 illustrates the Carnot cycle. Heat input is in the form of the latent heat of vaporization. At an outside radius, r_0, surface air begins to flow inward within a relatively small (1 to 2 km) frictional boundary layer. As the air moves inward at nearly a constant temperature, it acquires water vapor from the ocean which supplies the latent heat of vaporization. The rate of heat acquisition is a function of the near surface wind speeds. Heat is also added as the air moves inward due to isothermal expansion. Frictional dissipation is greatest during this inward motion. At a small radius the air abruptly turns upward and ascends the clouds that form the eye-wall. During ascent, total heat is approximately conserved, with little frictional loss of energy. The air eventually flows outward at the top of the storm and loses heat to long wave radiation to space. This simple model was later modified Emanuel (1988) to form exact equations governing pressure fall in steady tropical cyclones.

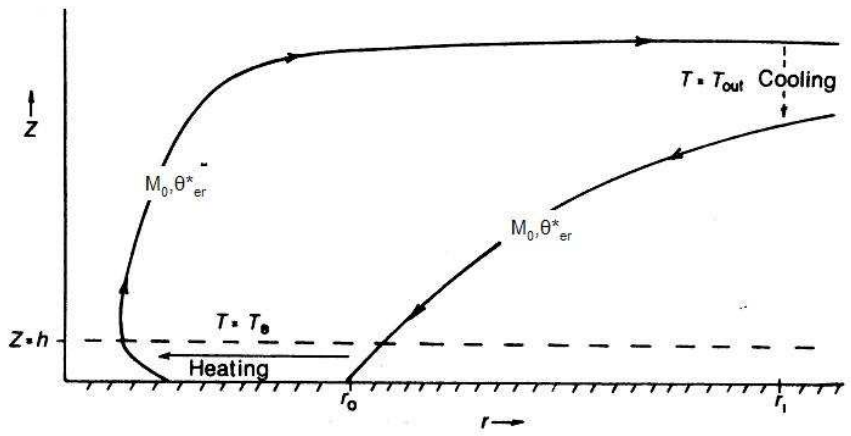

Figure 27 Carnot Engine Model for Tropical Cyclones
Carnot Engine Model for Tropical Cyclones from (Emanuel, 1987). Air movement begins inward at radius r_0 and M_o represents absolute angular momentum per unit mass, θ^*_{er} is moist entropy at radius r, T_B is temperature of inward airflow and within a thin boundary layer, M is angular momentum, θ^*_e is moist entropy, and T_{out} is mean outflow temperature.

Emanuel's was the first work which proposed a link between greenhouse gas induced warming to a possible future increase in potential tropical cyclone intensities.

Taking a different approach, Holland (1997) created a model that calculates the potential minimum central pressure of the storm based on the degree of warming in the atmospheric column above the storm center. This is relative to the local conditions in the tropical cyclone environment. Warming is achieved through latent heat release in the eyewall and subsidence in the eye. The degree of latent heat release in the eyewall is determined by a feedback process. This process is defined by falling surface pressures which cause an increase in the surface equivalent potential temperature, which in turn enhance the atmospheric warming (Tonkin et al., 2000). Holland's theory also predicted increasing potential intensities in warming climates.

Maximum potential intensity is very different from the realized actual intensity observed in historic hurricanes. Actual intensity is reduced due to negative feedbacks such as wind shear and landfall. Emanuel (2000) concludes from a statistical analysis that once a storm reaches minimal hurricane intensity, it has approximately a fifty percent chance of eventually achieving any intensity in the range between minimum and its upper maximum potential intensity. There are dynamical factors that have negative affects on storm intensity, wind shear, as one of the primary factors. Goldenberg et al. (2001) demonstrated a strong statistical relation between major hurricane counts in the Atlantic basin and a vertical wind shear index in the tropical Atlantic "Main Development Region" for tropical cyclones. Other factors affecting the potential intensity are the large scale ambient sea surface temperatures (SST) and the local sea surface temperatures under the eye which are reduced due to the surface winds of the storm. Schade (2000) created a theory for the maximum possible reduction of the SST directly under the eye of a tropical cyclone. This theory was tested against model data. The results imply a much higher sensitivity of tropical cyclone intensity to the SST under the eye of the storm than to the large-scale SST field. Thus, it underlines a greater importance of the SST feedback effect on the intensity of tropical cyclones. Scientists are still debating the relative importance of thermodynamic factors versus dynamical factors influence on the potential storm intensities. The location of the loop current in the Gulf of Mexico seems to modulate the strength of Gulf hurricanes as evidenced by the changes in storms such as Lilli and Gustav.

5.2 Analyses

Emanuel's (1987) theory predicts roughly a 5 percent increase in potential intensity per degree Celsius SST warming (e.g., Emanuel 2005a). His conclusions were later supported by a similar potential intensity theory proposed by Holland (1997) as applied to several climate models of greenhouse warming scenarios (Tonkin et al. 1997). Holland (1997) concluded a rapid increase in MPI of 30 hPa per degree Celsius SST warming up to 30 ºC. For SST > 30 ºC, a slower rate of increase in MPI occurs which may suggest a physical limit. Global average temperature increase projected by the IPCC TAR ranged from 1.4 to 5.8 ºC for the period from the present to 2100. This increase is projected to occur over the 100 years but nevertheless SST's could increase by 5 to 6 ºC. IPCC AR4 now has even broadened the range of temperature increases for the next 100 years. The AR4 range starts at 1.4 ºC for the lowest emissions scenario to an even higher 6.8 ºC for the highest emissions scenario. Emanuel (1988) created the theoretical basis for the maximum intensity of hurricanes and demonstrated the existence of critical conditions for which no solution for the minimum central pressure exists and defined storms within this supercritical regime as "hypercanes". Emanuel (1988) showed these hypercanes would extend high into the stratosphere and either have very large outer radii or very small eyes. These hypercanes require higher sea surface temperatures and other environmental conditions. It is possible that abrupt climate change may bring about some of these conditions, specifically higher SSTs. Emanual (1988) calculated several possible minimum central pressures, radius to max winds, and max wind speeds as shown in Table 9. These values are computed and shown in Table 9 along with radius to maximum winds

(r_m) and forward velocity (Vm). Results are for two different sea surface temperatures and for p_a = 1013 mb, relative humidity of 80%, and outflow temperature = -73 ºC.

Table 10 - MPI for theoretical hypercanes from Emanuel (1988)

Ts ºC	r_a(km)	p_c(mb)	pm(mb)	V_m(ms-1)	r_m(km)
30	700	894	917	80	26
35	700	762	788	96	2
35	1500	762	788	96	64

Given the IPCC projections and considerable evidence of past abrupt climate changes, this work constructs potential hurricanes for each degree of global warming increase up to 6 ºC. This complements the work of Lynas, 2008 which identified large scale impacts of climate change for each degree of global warming. Starting with an MPI of 880 mb for today's climate and SST's, one can tabulate approximate MPI values for each degree of global warming. These values are approximately a 3% change in MPI per degree of warming. Historic observations to date have shown that MPI values are usually not reached by a storm. However, one may consider that climate change factors including increase in CAPE (Knutson and Tuleya, 2004) could lend more possibility to closer realization of storm MPI values. With this in mind, 11 storms were designed assuming that under abrupt climate change conditions, storms could realize at least 80% of these MPI values. Three radiuses to max wind values were combined with these MPI values and are as shown in Table 10. Note that additional radius to maximum wind values were used for the 900mb MPI storms which were simulated for the USACE LACPR study. Storm numbers 27 and 193 were defined in the Corps of Engineers Louisiana Coastal Protection and Restoration (LACPR) study. Storms designed for abrupt climate change simulations were assigned a number relevant to the MPI and radius to maximum winds. Storm 800 represents a storm with an MPI of 800mb and a radius to maximum

winds of 25.8 nautical miles (nm). Storms 830, 850, and 870 also follow this convention with MPI values of 830, 850, and 870 respectively, all with a radius to maximum winds of 25.8 nm. Storms 871, 851, 831, and 881 have an MPI value of 1 less than their respective storm number. Thus Storm 871 has an MPI of 870 mb, storm 851 an MPI of 850 mb, etc. Storms 871, 851, 831 and 881 have radius to maximum winds of 6.0 nm.

Table 11 Abrupt Climate Change Storms

StormNumber	Average SST	Maximum Potential Intensity	80% MPI	MPI Used In ACC Simulations	Radius to Max Winds
(27)	30.00	880.00	**907**	**900**	**(21.8,14.9, 6.0)**
(193,881)	31.00	856.00	**888**	**880**	**(45.6,35.6, 25.8, 6.0)**
(870,871)	32.00	832.00	**869**	**870**	**(25.8, 6.0)**
(850,851)	33.00	808.00	**849**	**850**	**(25.8, 6.0)**
(830,831)	34.00	784.00	**830**	**830**	**(25.8, 6.0)**
(800)	35.00	760.00	**811**	**800**	**(25.8)**

One can ask are these MPI values realistic? Figure 28 shows the results of MPI observed and theoretical values computed from Tonkin et al, 2000. Shown are two pertinent Gulf of Mexico station MPI estimates calculated from Emanuel (1986) (E1), and Holland (1997) (H1) along with maximum observed intensities for each month.

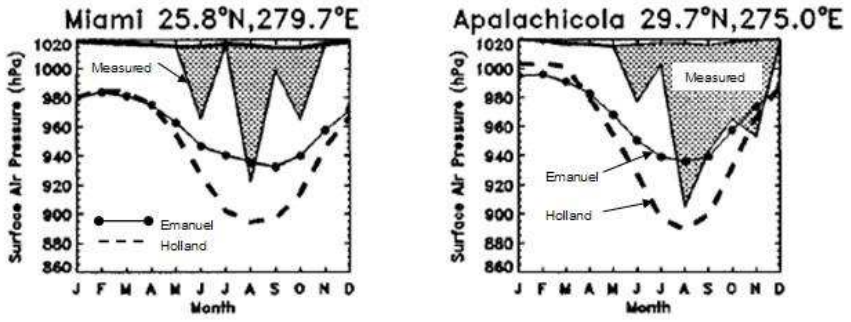

Figure 28 MPI theoretical estimates
MPI theoretical estimates calculated from E1 and H1compared to maximum observations for each month. (From Tonkin et al., 2000)

Using the results which are the stations most relevant to the Gulf of Mexico, one can compute the average MPI attained based on each theoretical model, H1 and E1. Table 11 shows these results.

Table 12 MPI percentages Attained from theoretical computed values

Miami	MPI	% H1 MPI	% E1 MPI
E1	930		111.11%
H1	892	78.13%	
OBS	920		
Apalachicola	MPI	% H1 MPI	% E1 MPI
E1	935		138.82%
H1	890	90.77%	
OBS	902		

Emanuel (1988) (E1) values underestimated observed values for both stations, however generally agreed with observations at other stations. Holland (1997) (H1) results were more intense than observed values which was the case for other stations as concluded by Tonkin et al., 2000. The average percentage MPI attained by the H1 model for these two stations is 84.5%. Thus, a value of approximately 80% theoretical MPI was used for the design of the storms.

5.3 Results

Considering the analyses above, these storms were designed with MPI values and a radius to maximum winds as shown in Table 12. Storms were simulated along one track to reduce the total number of variations and enable effective comparisons between storm results. An ADCIRC grid of the Louisiana coast in 2050 with the USACE 100 year levee design elevations in place. Figure 29 shows 100 year level of protection levee heights as set in the ADCIRC mesh.

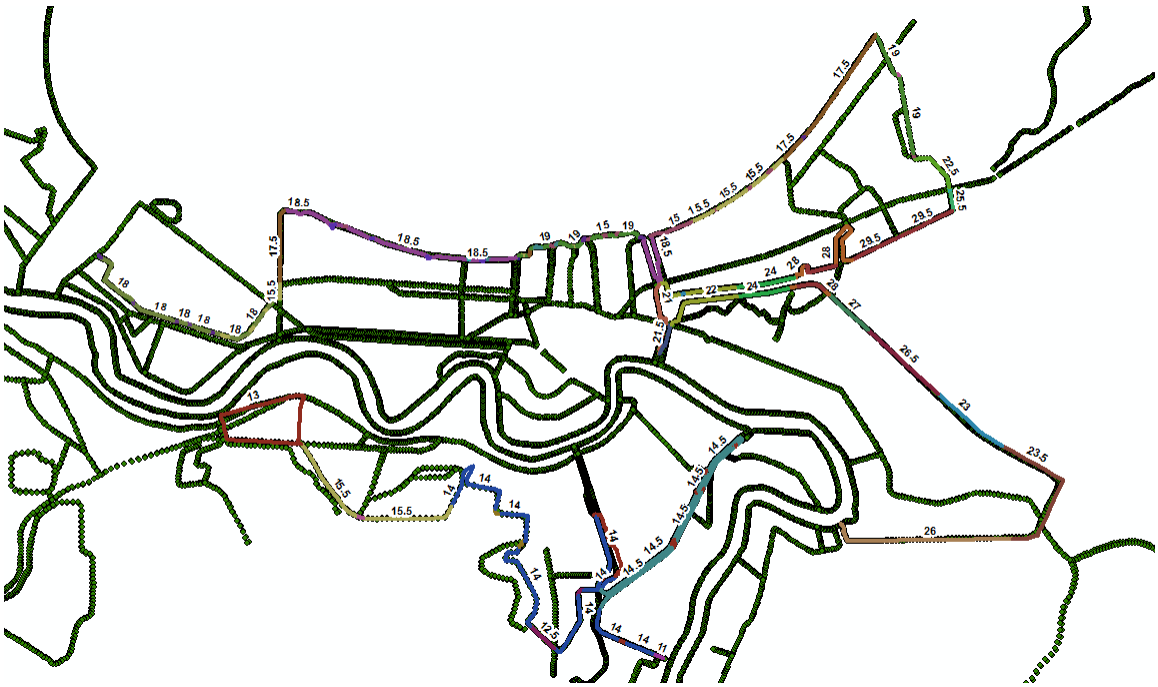

Figure 29 USACE 100 year levee heights as ADCIRC mesh boundaries

Table 13 Storm Design Values and Resulting Maximum Wind Speeds

Storm Number	MPI (mb)	Rmax (nm)	30 Min Avg Ws (m/s)	30 Min Avg Ws(mph)	1 Min Avg Ws(mph)	Category
27	900	21.8				
193	880	25.8				
870	870	25.8	62	139	172	5
850	850	25.8	65	144	179	5
830	830	25.8	67	150	186	5
800	800	25.8	70	157	194	5
881	880	35.6	59	133	164	5
871	870	6	61	137	170	5
851	850	6	64	143	177	5
882	880	45.6	58	130	161	5

All storms resulted in maximum wind speeds that fall in the Saffir-Simpson scale of Category 5 storms. The wind model used is a more recent version of what is called the TC-96 Planetary Boundary Layer (PBL) wind model (Thompson and Cardone, 1996) developed by the Corps of Engineers. This model was updated and enhanced by Ocean Weather Inc. (OWI) for modeling hurricanes and produced wind speed, wind direction, and atmospheric pressures to drive ocean response models. Winds produced by this PBL model are what are called 30-minute average wind speeds at the 10 meter level. These need to be converted to 1-minute average wind speeds in order to be categorized according to the Saffir-Simpson scale. A value of 1.24 was used as the conversion factor which is the approximate value most accepted in practice (Westerink, J., 2007, personnel communication). Additionally, a value of 1.09 was used to convert the PBL model winds to 10-minute average wind speeds required by ADCIRC. Storm 800 with an MPI of 800mb and a radius to max winds of 25.8 nautical miles produced the most extreme wind speed of 194 miles per hour. This is the most extreme 'hypercane' postulated to form

influenced by sea level temperature as high as 36 ºC which is one degree higher than shown in Table 5.2. Peak surge plots from these storms are shown below in Figures 30 to 37. These storms all follow Track 3 (T3 of Figure 15) to enable direct comparison of surge results to storms simulated given the present climate. The storms shown in Table 10 and 13 and the peak surges produced by those storms, are shown in Figures 30 through 37 and were simulated given abrupt climate change and increased sea surface temperatures.

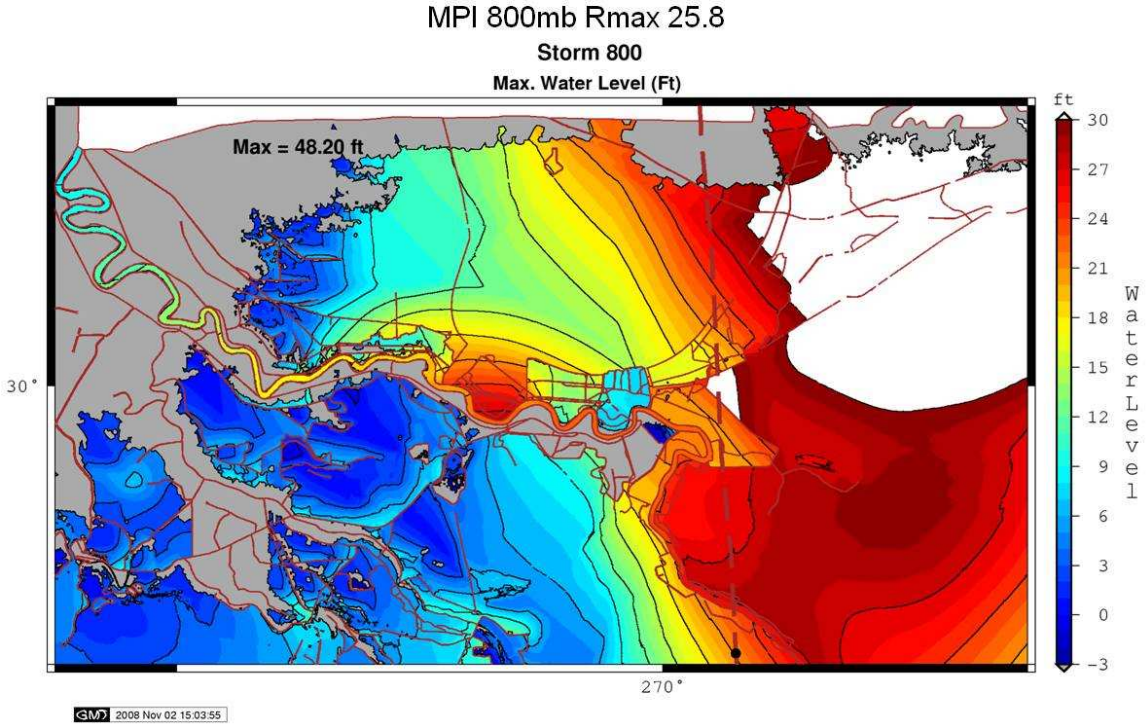

Figure 30 Storm 800 Peak Surges

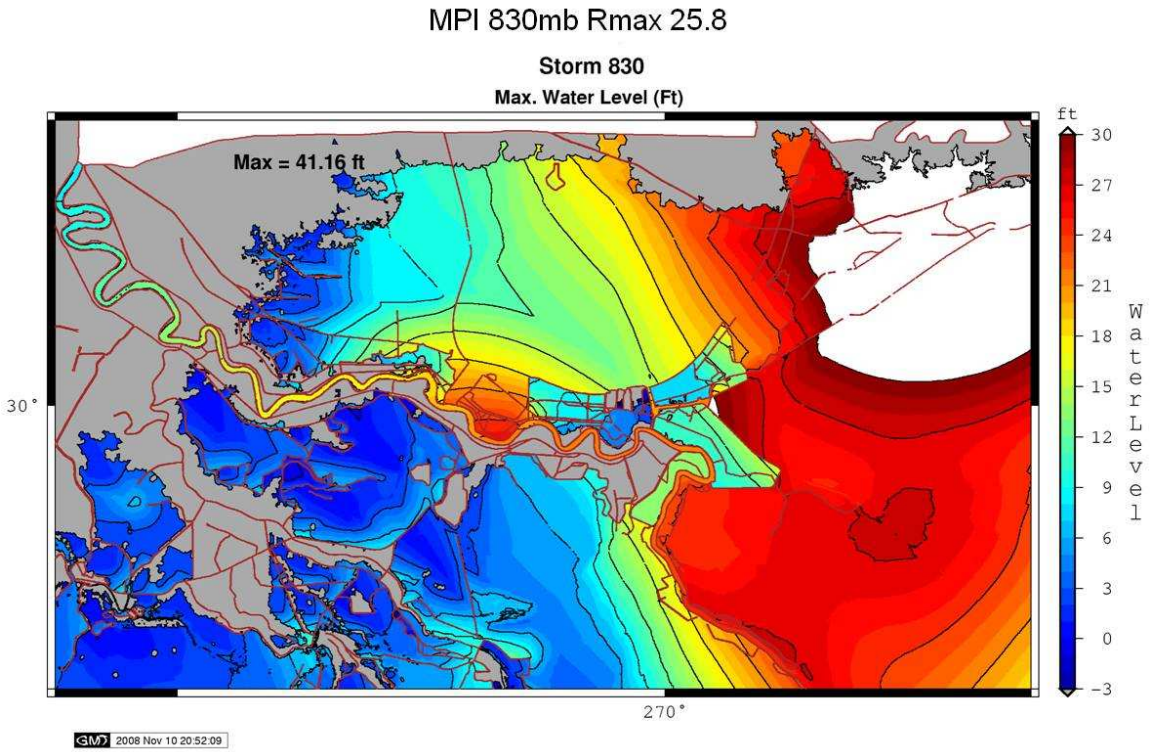

Figure 31 Storm 830 Peak Surges

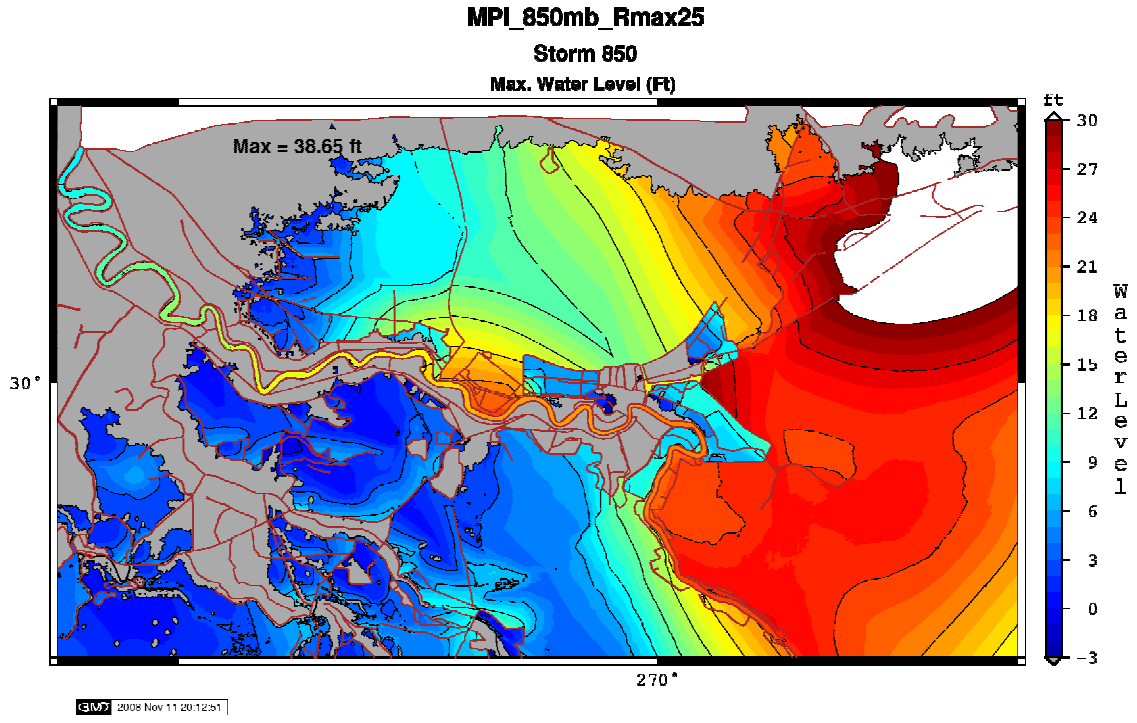

Figure 32 Storm 850 peak surges

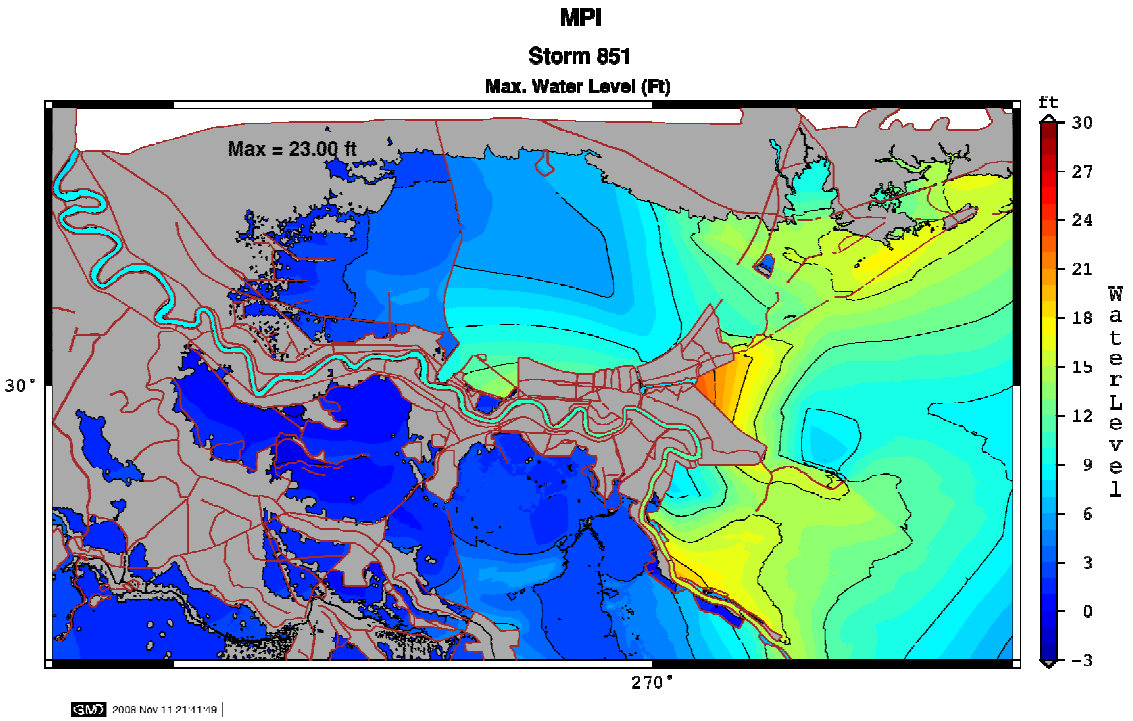

Figure 33 Storm 851 peak surges

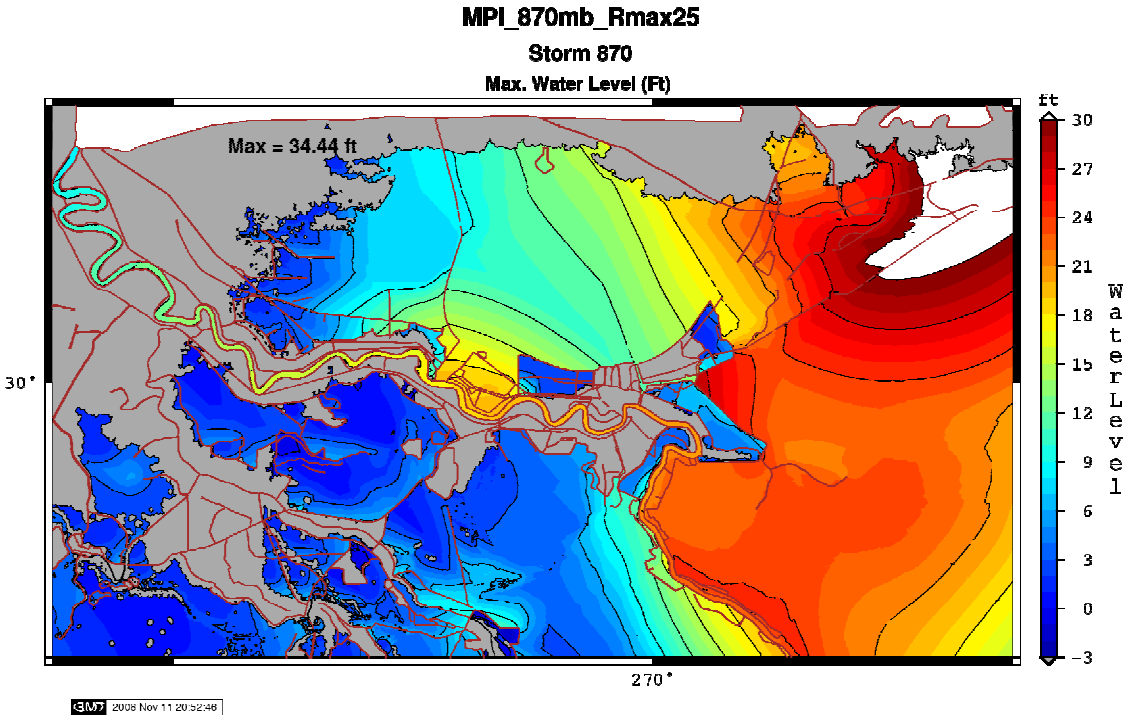

Figure 34 Storm 870 peak surges

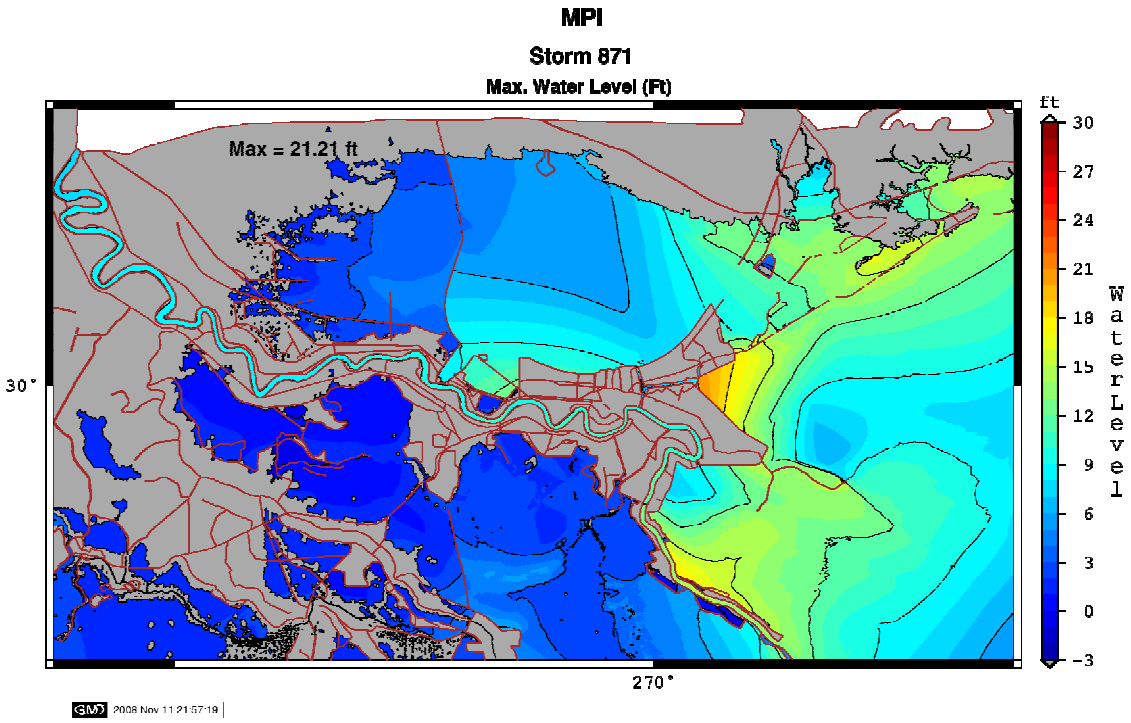

Figure 35 Storm 871 peak surges

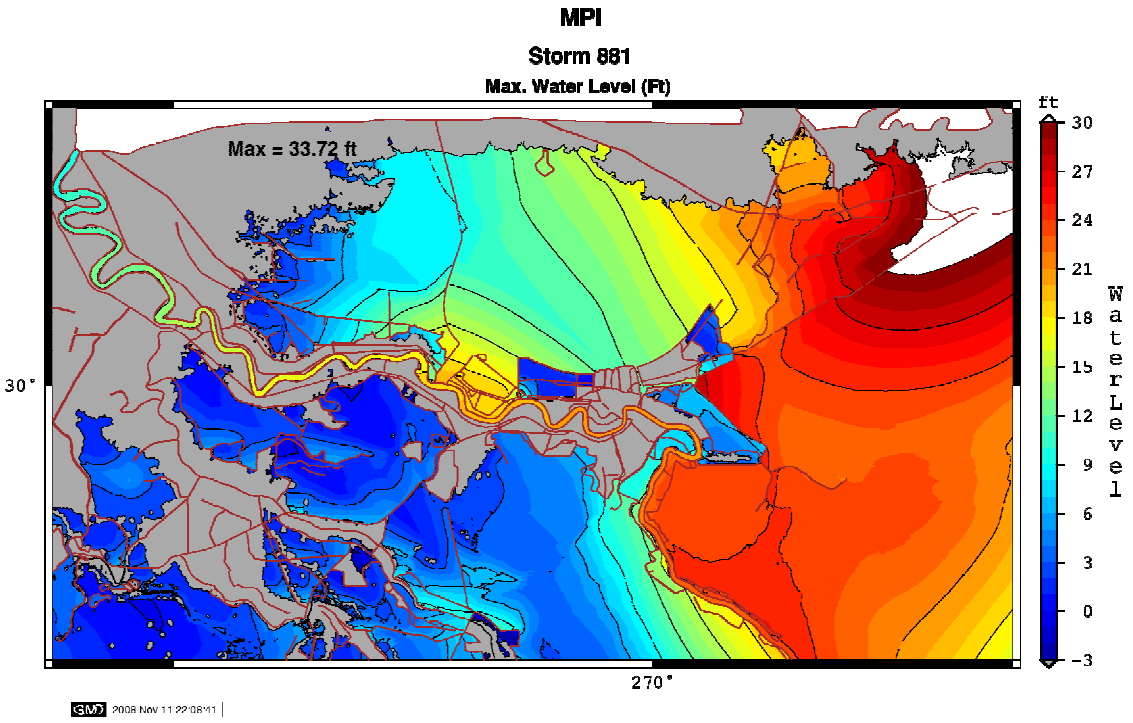

Figure 36 Storm 881peak surges

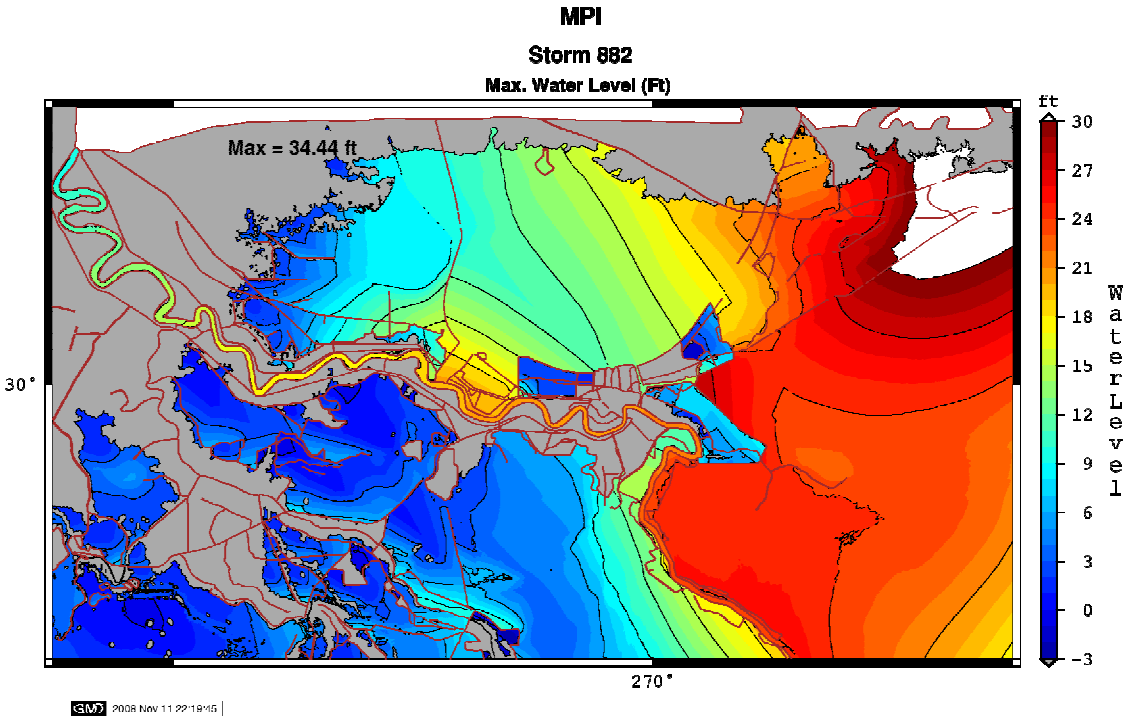

Figure 37 Storm 882 peak surges

One can progressively increasing storm surge heights corresponding with decreasing central pressures or increasing storm intensities. Table 14 provides a summary of maximum peak surges for the New Orleans area for selected modeled storms.

Table 14 Peak Storm Surge Results

Storm Number	MPI (mb)	Rmax (nm)	1 Min Avg Ws(mph)	Peak Surge (Ft)
27	900	21.8		26.80
193	880	25.8		34.67
870	870	25.8	172	34.45
850	850	25.8	179	38.65
830	830	25.8	186	41.14
800	800	25.8	194	48.19

Note that the surge values shown in Table 13 are for the entire storm simulation and are not located in the exact same location.

To quantify the increase in surge influenced by 1ºC of SST warming, Storm 027 peak surges were subtracted from Storm 193 peak surges and the results are shown in Figure 38. These surge differences show the increases from a very intense storm (027) reasonably possible given today's climate from surges produced by a storm influenced by 1ºC of SST warming (Storm 193). A mean difference of 2.1 feet was obtained for the study area.

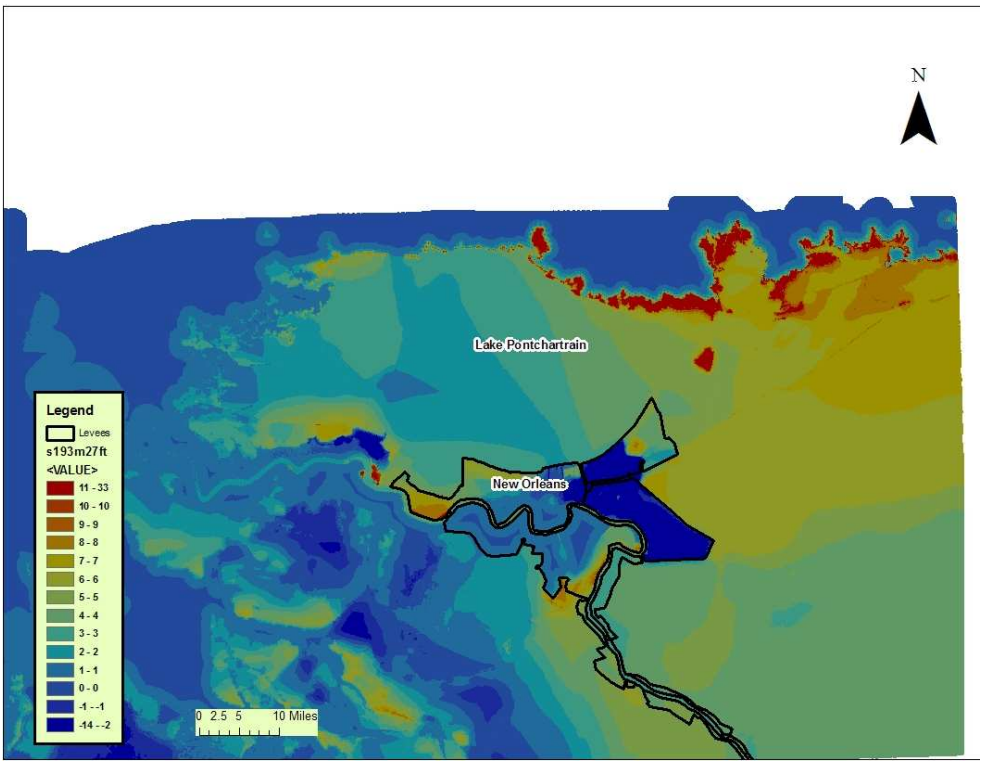

Figure 38 Increase in surges from 1ºC increase in SST computed by subtracting Storm 27 peak surges from Storm 193 peak surges (feet)

To obtain the increase in surges produced from storms influenced by 2ºC SST increase, peak surges from Storm 027 are subtracted from Storm 870 and shown in Figure 39. A mean of 2.0 feet was obtained for the study area.

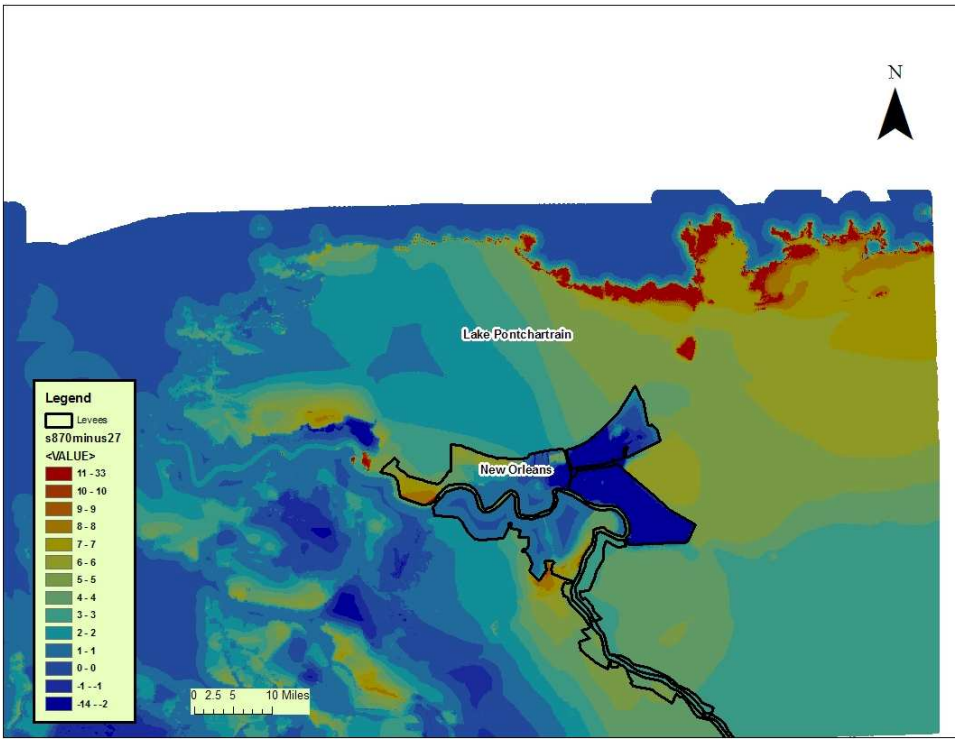

Figure 39 Increase in surges from 2ºC increase in SST computed by subtracting Storm 27 peak surges from Storm 870 (feet)

To obtain the increase in surges produced from storms influenced by 3ºC SST increase, peak surges from Storm 027 are subtracted from Storm 850 and shown in Figure 40. A mean of 3.2 feet was obtained for the study area.

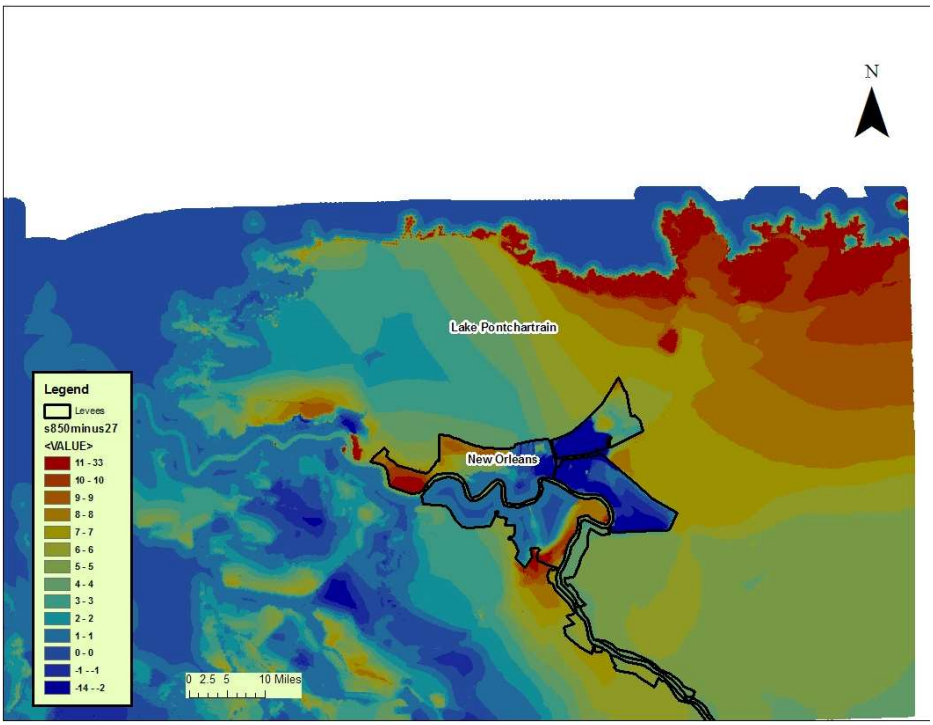

Figure 40 Increase in surges from 3ºC increase in SST computed by subtracting Storm 27 peak surges from Storm 850 peak surges (feet)

To obtain the increase in surges produced from storms influenced by 4ºC SST increase, peak surges from Storm 027 are subtracted from Storm 830 and shown in Figure 41. A mean of 4.2 feet was obtained for the study area.

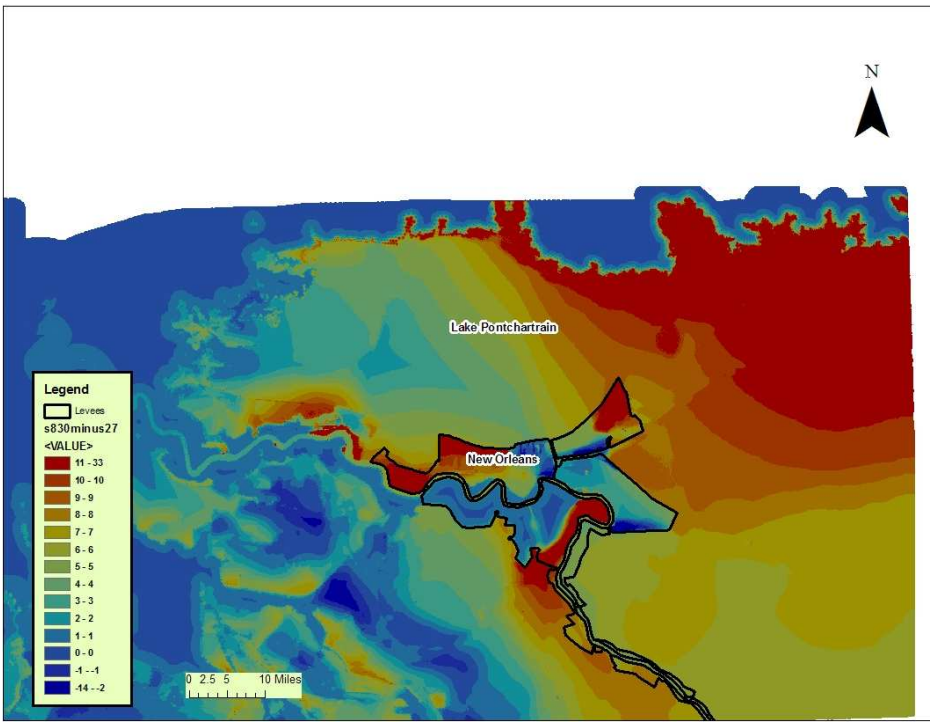

Figure 41 Increase in surges from 4ºC increase in SST computed by subtracting Storm 27 peak surges from Storm 830 peak surges (feet)

To obtain the increase in surges produced from storms influenced by 5 to 6ºC SST increase, peak surges from Storm 027 are subtracted from Storm 800 and shown in Figure 42. A mean of 6.1 feet was obtained for the study area.

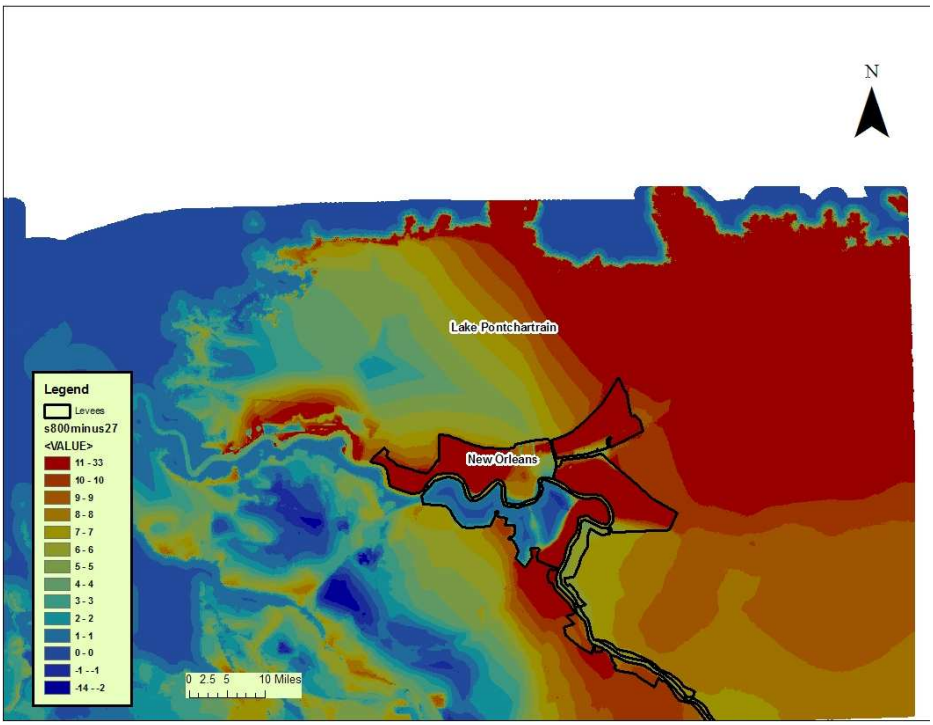

Figure 42 Increase in surges from 5 to 6ºC increase in SST computed by subtracting Storm 27 peak surges from Storm 800 peak surges (feet)

It is evident from the above simulations that these extreme storms generate even more extreme surges. With just a 1ºC increase in SST, peak differences range to 34 feet. The largest increases are for the 5 to 6ºC increase in SST up to 44 feet. However, the mean values start at 2 feet for the 1ºC increase in SST up to a maximum mean value of 6.1 feet. Table 14 tabulates percent increase in surges.

Table 15 Percent Storm surge Increase from present day climate.
Storm 27 is basis of comparison (present) and all storms were simulated using 2050 degraded coast.

Storm Number	MPI (mb)	Rmax(nm)	1 Min Avg Ws(mph)	Peak Surge (Ft)	% Surge Increase
27	900	21.8		26.80	
193	880	25.8		34.67	23%
870	870	25.8	172	34.45	22%
850	850	25.8	179	38.65	31%
830	830	25.8	186	41.14	35%
800	800	25.8	194	48.19	44%

Chapter 6 Frequency Analyses

6.1 Introduction

Hurricane frequency is now one of the most highly visible and debatable aspects of climate change. The issue of frequency is compounded by the fact that the time series of reliable tropical cyclone databases are simply too short for detecting trends in the frequency of extreme events (Landsea et al., 2006). Researchers have used the best available data on storm characteristics and observations and combined this with other factors which influence tropical cyclogenesis and storm intensity. Many methods of statistical analyses and procedures have been performed with the goal of quantifying the historic storm frequency, searching for trends, and then projecting future frequency influenced by global warming. These procedures analyze genesis location, storm track, and especially intensity. Results attempt to quantify not only the number of storms, but also wind speeds and the Saffir-Simpson scale category. However, the emphasis of this work is not specifically on quantifying hurricane frequencies, but to examine the frequency of hurricane storm *surges* (in terms of return period) produced by hurricanes under a global warming environment compared to previous efforts. Storm surge return periods were computed along the Louisiana coast during the late 1970's and early 1980's as part of FEMA's Flood Insurance Studies to produce Flood Insurance Rate Maps (FIRMS). Flood Hazard zones were delineated showing the 100 and 500 year return period. In 2007, the USACE completed a large effort to compute new storm surge return

period elevations for FEMA to update their FIRMS. Results of this work will be compared to these 2007 storm surge return periods.

6.2 Review of Existing Work

This section provides a very brief synopsis of previous efforts to quantify hurricane frequencies, both past and future. Following this synopsis, an overview of two storm surge frequency methodologies is discussed. The previous methodology employed by FEMA to produce FIRMS will be discussed along with the new methodology created by the Corps of Engineers along with FEMA and other agencies.

Frequency of extreme hurricanes has become so important not only because of the significant amount of potential damages and loss of life, but also because we are compelled to know if increases in intensities and/or frequencies are the result of anthropogenic forcing, natural variability, or both. Pielke et al. (2005) state that most research suggests future changes in hurricane frequency will be regionally dependent and there is no consistency among these studies on even the sign of the change in the total global number of storms (Henderson-Sellers et al. 1998; Royer et al. 1998; Sugi et al. 2002). One of the conclusions of the authors is ". . . peer-reviewed literature reflects that a scientific consensus exists that any future changes in hurricane intensities will likely be small in the context of observed variability (Henderson-Sellers et al. 1998; Knutson and Tuleya 2004), while the scientific problem of tropical cyclogenesis is so far from being solved that little can be said about possible changes in frequency . . ." (Pielke et al. 2005).

Knutson and Tuleya (2004) (see Chapter 1) performed a large set of simulations from nine different global climate models and using four different versions of the GFDL hurricane model in an effort to analyze any potential links between global warming and hurricane intensity. The results of their work show that an 80-year buildup of atmospheric carbon dioxide at 1% per year leads to roughly a ½ category increase in potential hurricane intensity on the Saffir-Simpson scale (Figure 43) and about a 20% increase in precipitation at the hurricane core. Although, as stated by the IPCC Special Report on Emissions Scenarios (Houghton et al. 2001), there is considerable uncertainty in projections of future radiative forcing of the Earth's climate.

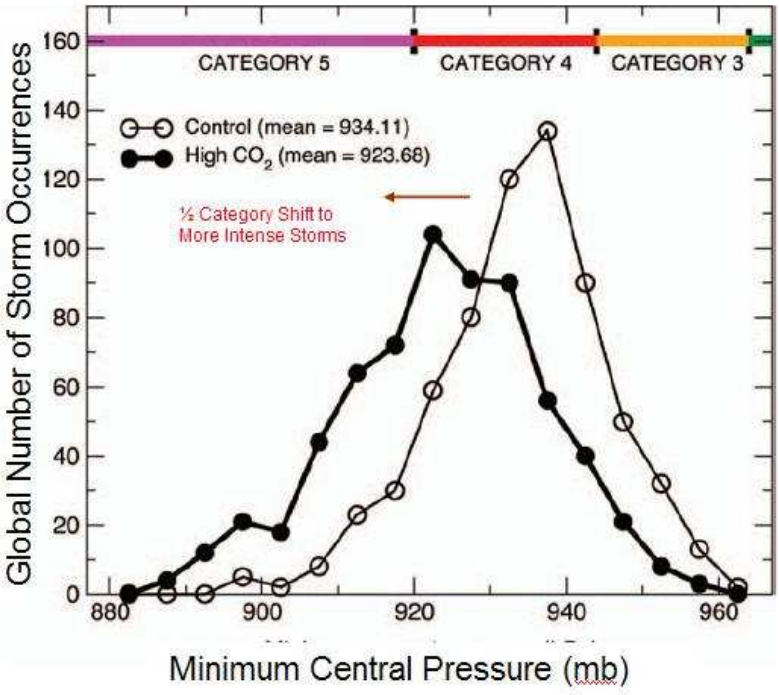

Figure 43 Number Of Hurricanes Present & Future Climate Conditions
Comparison of simulated hurricanes for present (thin line) and future (thick line) climate conditions from Knutson and Tuleya, 2004.

Emanuel (2005a) (See Chapter 1) astounded the world with his computations of tropical cyclone Power Dissipation Index (PDI) which doubled since about 1950 and correlated extremely well observed increases in SSTs over the past 30 years. Pielke (2005) criticized Emanuel's conclusions based upon statistics of hurricane damages. He contended that if hurricanes were becoming more destructive over the years then these trends would also be evident in damage statistics. However, he could find no such trends and postulated that Emanuel's PDI although realistic, was perhaps a weak indicator of hurricane destructiveness. But Emanuel (2005b) stood by his conclusions and stated that the trends were large and in all ocean basins, despite measurement techniques, and well correlated with SST which was a reliable well-observed data set. Emanuel accepted Landsea's (2005) corrections (see Chapter 1) to his bias-removal scheme for a portion of the historic Atlantic wind observations, but he still emphasized caution due to the high correlation of hurricane activity and SSTs, especially since the SST record is long enough to capture the influence of global warming. Emanuel (2005b) concluded that even with the arguments of Landsea and Pielke, the current levels of tropical storminess are unprecedented in the historical record and that a global-warming signal is now emerging in records of hurricane activity. Emanuel (2005a) also noted that his rate of increase of hurricane intensities (per degree Celsius of SST warming) is much greater than results from simulation projections by Knutson and Tuleya (2004).

Webster et al. (2005) published results from another study analyzing the changes in tropical cyclone number, duration, and intensity which caused more intense debate among scientists. The authors first completed a statistical assessment of tropical ocean

SST demonstrating SSTs have increased by about 0.5ºC between 1970 and 2004. An increase in SST should correspond to an increase in the intensity (wind speed is used as the metric of intensity in this analysis) of tropical storms. Webster et al. (2005) concluded that the total global number of hurricanes has remained the same but the number of category 4 and 5 hurricanes has almost doubled globally over the past 30 years (Figure 44). The authors show this is about an 80% increase in these intense storms due to the warming environment. In critique of this work, most scientists question the degree of data reliability and consistency across world ocean basins. Webster et al. (2005) do not mention nor attempt to quantify the uncertainty in their results and leading researchers point to the different wind observation methodologies and techniques that have evolved over the last 30 years.

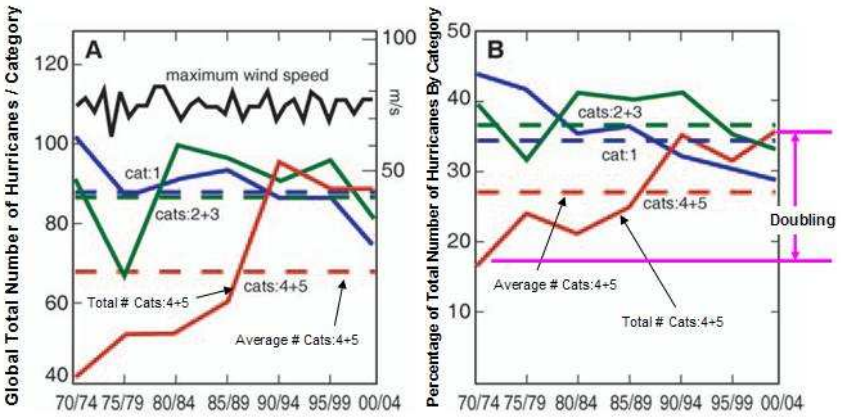

Figure 44 Number of Hurricanes / Category from Webster et. al. 2005
Intensity of hurricanes according to the Saffir-Simpson scale. (A) The total number of category 1 storm (blue), sum of category 2 and 3 (green), and the sum of categories 4 and 5 (red) in five year periods. Bold curve is max wind speed observed globally (m/s). Horizontal dashed line shows 1970-2004 average numbers in each category. (B) Same as (A), except the percentage of the total number of hurricanes in each category class. Dashed lines show average from Webster et al. 2005.

There are still many other efforts and approaches to assessing hurricane frequency and projection of future storm characteristics. These range from a combination of a statistical-deterministic approach (Emanuel et al. 2006; Vickery and Twisdale, 1995) to the entire field of paleotempestology. Proxy records from coastal lake and marsh sediments from four sites in Louisiana, Mississippi, Alabama, and Florida suggest that intense hurricane activity along the Gulf Coast varies significantly at the millennial timescale (Liu, 2004).

In light of the preceding discussion on increased frequency of intense storms, focus turns to past efforts to capture the frequency (in terms of return period) of storm surges produced by these intense hurricanes. As shown above, increases in more intense storms were not realized until most recently, especially with the impacts of Katrina and the 2005 Atlantic hurricane storm season. During the late 1950's and mid 1960's, there was an increase in the number of category 4 and 5 Atlantic storms and for the Gulf of Mexico these included the powerful hurricanes Audrey (1957), and Carla (1961). The "National Flood Insurance Act of 1968" established the National Flood Insurance program for insuring home owners and businesses against flood hazards including coastal flood hazards caused by hurricanes. The 1968 Act directed other agencies to cooperate with the Flood Insurance Agency (FIA), which later became FEMA, of the Department of Housing and Urban Development (HUD). In May of 1975, NOAA completed and published a report, NOAA Technical Report NWS 15 (Ho et al. 1975), which detailed frequency and return periods for several climatological characteristics of hurricanes along the Gulf and East coasts of the U.S. A smoothed frequency of tropical storms and

hurricanes entering and exiting the coast and passing within a band of 150 nautical miles during the period of 1871-1973 was used. Characteristics of minimum central pressure, radius to maximum winds, forward speed, and landfall direction were analyzed. The probability distribution of each factor was plotted and analyzed for each 50 nautical miles of the coast. The authors did perform some limited efforts to investigate joint probabilities and interrelations amongst the parameters, but ultimately concluded that a much larger data set was required for any meaningful or reliable result. But the results of this report and additional efforts were used in deriving storm surge return periods for the FIA and then FEMA. These early efforts primarily used the Joint Probability Method (JPM) in which probabilities of certain parameters are obtained before hand and then conditional probabilities are derived to ultimately compute final surge probabilities. The JPM was developed in the 1970's (Myers, 1975; Ho and Meyers, 1975) and subsequently extended by a number of investigators (Schwerdt *et al.*, 1979; Ho *et al.*, 1987) in an attempt to overcome problems related to limited historical records. In this approach, information characterizing a small set of storm parameters was analyzed from a relatively broad geographic area such as the study mentioned above for the Gulf and entire East U.S. coast. In applications of this method in the 1970's and 1980's, the JPM assumed that storm characteristics were constant along the entire section of coast from which the storm data were obtained. Recent analyses suggest that this assumption is inconsistent with the actual distribution of hurricanes along the east coast and within the Gulf of Mexico. The JPM used a set of parameters, including 1) central pressure, 2) radius of maximum wind speed, 3) storm forward speed, 4) storm landfall location, and 5) the angle of the storm track relative to the coast, to generate parametric wind fields. Initial applications of the

JPM assumed that the values of these five parameters varied only slowly in storms approaching the coast and thus, the values of these parameters at landfall could be used to estimate the surge at the coast. Recent data show that this is not a good assumption (Figure 45) due to the decay of intensity as the storm encounters the coastal area. Kimball (2006) has shown that such decay is consistent with the intrusion of dry air into a hurricane during its approach to land. Other mechanisms for decay might include lack of energy production from parts of the hurricane already over land and increased drag in these areas. In any event, the evidence appears rather convincing that major hurricanes begin to decay before they make landfall, rather than only after landfall as previously assumed.

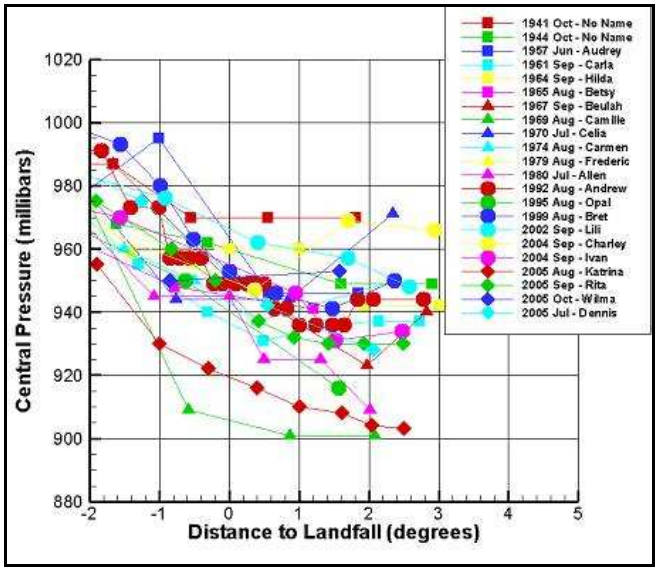

Figure 45 Storm decay approaching landfall from Resio et al. 2007

The conventional JPM used computer simulations of straight-line tracks with constant parametric wind fields to define the maximum surge value for selected combinations of the basic five storm parameters. Each of these maximum values was associated with a probability,

$p(c_p, R_{\max}, v_f, \theta_l, x)$

where

c_p is the central pressure,

$R_{\max}$ is the radius of maximum wind speed (6.1)

v_f is the forward velocity of the storm

θ_l is the angle of the track relative to the coast at landfall

x is the distance between the point of interest and the landfall location

These probabilities were treated as discrete increments and the CDF was defined as

$$F(x) = \sum p_{ijklm} \mid x_{ijklm} < x \qquad (6.2)$$

where the subscripts denote the indices of the 5 parameters from Equation 6.1 used to characterize the hurricanes. The conventional JPM included a range of parameter combinations that typically made extrapolation beyond the range of simulations unnecessary. A great advantage of the JPM over existing methods that depended heavily on historical storms was that the JPM considered storms that might happen and not just past events. Of course, the greater the number of possible combinations being considered increased the number of actual computations and simulations required. This became a very labor intensive effort when models such as SPLASH required both manual and computer assisted efforts. With the development of the SLOSH model and increased computer speed and power, the number of simulations required had less of an impact but was still an intensive effort.

One of the major issues associated with JPM methods used in the 70's and 80's was the exact definition and implementation of the 5 dimensional storm parameters within the joint-probability function (Resio et al. 2007). During this time and still relevant today, was the lack of reliable measured storm data especially for storms prior to

1950. This included minimum central pressure and storm size. Radius to the maximum wind was unavailable for most of these historical storms and a statistical estimate of Rmax as a function of latitude and central pressure was frequently used instead of actual values in the probability distribution. Another weakness was the inability to fully capture the important time varying properties of tropical storms. Surges derived from previous JPM applications were based on storm characteristics near the coast that were constant. Thus, these results may have been biased low since storms are now observed to be more intense offshore than near shore.

Following the devastating impacts of Katrina and the 2005 hurricane season, a team consisting of members of the Corps of Engineers, FEMA, NOAA, as well as private and academic researchers developed a new methodology for estimating hurricane inundation probabilities. This methodology is a modification of the JPM method with the goal of providing well defined estimates of surges using as small a number of dimensions as possible, while retaining the effects of additional dimensions by including an ε term within the CDF for surges (Resio et al. 2007). The method is now called the Joint Probability Method with Optimal Sampling (JPM-OS). The JPM-OS has several advantages over the previous JPM which include storm varying characteristics over spatial regions, winds are derived from a dynamic, physics-based, planetary boundary layer (PBL) wind model, pre and post landfall variations of central pressure, radius to maximum winds, and a wind 'peakedness' parameter (Holland B). Additionally, longer storm tracks are defined and derived from historical tracks, and the interdependencies between central pressure and radius to maximum winds are captured.

The numerical integration in the original JPM used what is equivalent to a "rectangular" or trapezoidal integration method where

$$F(S) = \sum_{n}\sum_{m}\sum_{k}\sum_{j}\sum_{i}\Delta P_{ijkmn} \text{ for all } \hat{S}_{ijkmn} > S \quad (6.3)$$

Where ΔP_{ijkmn} are the individual probabilities for each of the 5 primary parameters (direction, radius to maximum wind, minimum central pressure, forward speed, and distance from point of interest), $\hat{S}_{ijkm}$ are the respective surges produced given those specific parameter definitions, and F(S), the cumulative probability distribution.

In this method discrete increments of probability are assigned to the value of the simulated surge. Recently with the development of risk based applications, the concept of a "response surface" has been developed. In this approach and development of a response surface, it is assumed that response is a continuous function of the parameters used to discretize the probabilities. Thus, for this application, surge is assumed to be a continuous function of central pressure, radius to maximum wind (Rmax), angle of approach, forward storm velocity, and distance from location of maximum surge for a specific combination of the other parameters. The integration is now more aligned with a Gauss Quadrature integration method. Essentially a set of functional relations between surge and each of the 5 primary probability parameters is defined. Once defined, an interpolation can be performed without the need to perform additional simulations. Its accuracy is predicated on the ability to fit the response surface with an accurate set of functional relationships from the actual sampled storms. These functional relationships and their development are detailed by Resio et. al. (2007). Additionally, the estimation of the surge cumulative distribution function includes a "random" (ε) deviation term added

to the modeled values. This term includes the variations to all the neglected parameters which ultimately affect surge heights and include both surge-independent terms (tide and model error) and surge-dependent terms (Holland B parameter), etc.

All surge computations for this work were computed using a subset of the JPM-OS Louisiana synthetic storms and the physics-based numerical models used in the Joint FEMA and Corps of Engineers Coastal Storm Surge Study.

In view of the above, it is worth mentioning another methodology for modeling hurricane surge risk which uses the "Empirical Track Model". Vickery et al. (2000) presents this method which has been adopted for the development of wind speed maps within the U.S. ((American National Standards Institute (ANSI), ASCE 1990, 1996). This method uses a Monte Carlo approach to sample from empirically derived probability and joint probability distributions. The central pressure is modeled stochastically as a function of sea surface temperature along with storm heading, storm size, storm speed, and the Holland B parameter. This method has been validated for several regions along U.S. coastlines and provides a rational means for examining hurricane risks associated with geographically distributed systems such as transmission lines and insurance portfolios (Resio et. al., 2007). However, the Empirical Track Model is applied within a Monte Carlo framework and has the ability to efficiently execute storms over many, many years (20,000 years in the Vickery *et al.* (2000) application). This number of simulations can be readily performed using this PBL wind model. However, there is simply not enough time and power even using supercomputers today to run this many storms using large,

high-resolution ocean and coastal response models (wave models and surge models). For this reason, the Empirical Track Model was not considered for application to coastal storm surge probability computations. But this method does provide an excellent source for validating the statistical characteristics of the winds used for inundation modeling (Resio et al. 2007).

6.3 Surge Frequency Analyses

Most frequency analysis methods require a large data set and normally to obtain results for storm surge probabilities, a significant number of simulations are required. The emphasis of this work was not to specifically compute future storm surge probabilities but to determine the impacts of future storms. Only a small selection of storms were simulated which limits computations of storm surge probabilities from this data set alone. However, these results can be compared to existing storm surge return periods, specifically those computed using the JPM-OS methodology for the Joint FEMA and Corps of Engineers Coastal Storm Surge Study for the State of Louisiana and the Corps of Engineers Louisiana Coastal Protection and Restoration (LACPR) project. These projects produced a set of five levels of storm surge elevations which include the 50, 100, 500, 1000, and 2000 year return periods. Comparing future storm peak surges to these elevations quantifies where these results fit onto existing surge probabilities. Figure 46 shows Storm 870 peak surges minus the 1000 year storm surge elevations produced from the FEMA and LACPR projects. Storm 870 was modeled to have a minimum central pressure of 870 mb and radius to maximum winds of 25.8 nautical

miles. These values were attained approximately 90 miles off the coast and then as the storm moved closer to the coast and inland, decay rates were applied according to (Resio et al. 2007). Storm 870 produced a maximum wind speed of 172 miles per hour (1 minute average at the 10 meter level).

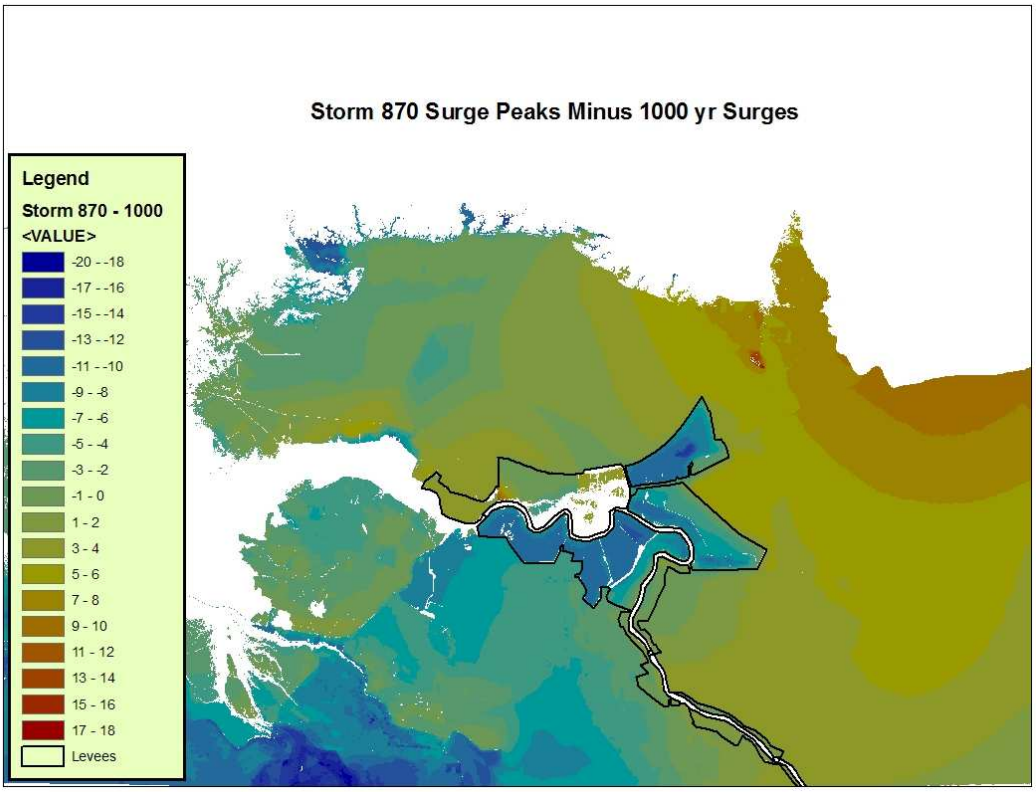

Figure 46 Surge differences between Storm 870 and 1000 year return levels (feet)

Storm 870 represents a potential storm influenced by 2ºC increase in SST. The surges from Storm 870 are both higher than today's 1000 year levels and in some locations lower. The highest surge is 18 feet above the 1000 year level. This is due to a small protected area located on the north shore of Lake Pontchartrain which had very low return elevations and there was significant inundation in this area by Storm 870. The

lowest values of around -20 feet because Storm 870 produced either little or no surge response, or drawdown occurred. Drawdown, or lowering of the water surface occurred primarily on the western side of the storm track and thus was evident on the west bank of the Mississippi River. The counterclockwise rotation of the winds resulted in winds from a northern direction driving inland water outward towards the coast. These locations were subsequently much lower than the 1000 year return levels. The mean difference between Storm 870 surges and the 1000 year return levels is -1.17 feet and thus below the 1000 year return period surge levels. However, as can be seen in Figure 43, Storm 870 surge levels are generally 1 to 3 feet higher than 1000 year levels at mid lake and then along the south shore of Lake Pontchartrain. These gradually increase to around 5 feet and higher near the area where Lake Pontchartrain eventually connects to the Gulf of Mexico which is called Rigolets Pass. Surges were also approximately 5 to 6 feet higher along the southwestern shore of Lake Pontchartrain near the Bonnet Carré spillway. Surge differences near the Louisiana and Mississippi State boundary, into the Pearl River Basin, range from 5 feet up to 9 feet along the Mississippi coast. These are primarily due to the track of Storm 870 for which the greatest surges were produced on the eastern side of the storm. Below New Orleans and on the west bank of the Mississippi River, Storm 870 surge levels were lower than the 1000 year levels primarily due to the storm track. The 1000 values were produced using the JPM-OS method which incorporated surges produced in this area by a large suite of storms along many tracks and directions.

Figure 47 shows Storm 850 peak surges minus the 1000 year storm surge elevations produced from the FEMA and LACPR projects. Storm 850 represents a

potential storm influenced by a 3ºC increase in SST. Storm 850 reached a minimum central pressure of 850 mb (Table 12) and a radius to maximum winds equal to Storm 870 of 25.8 nautical miles. The highest surge difference between Storm 850 and the 1000 year surge levels was 24 feet. This compares to 18 feet for Storm 870. But these values are in different locations from each storm. The largest differences from Storm 850 are within a protected close to the southwestern shore of Lake Pontchartrain. Surges from Storm 850 are a couple feet higher than those from Storm 870 near the south shore and the middle of Lake Pontchartrain. These surges are 10 to 11 feet higher than the 1000 year levels along the north shore of Lake Pontchartrain. The surges from Storm 850 are both higher than today's 1000 year levels and in some locations lower. The mean difference is -0.2 feet and the areas lower than the 1000 year levels are again below New Orleans on the west side of the Mississippi River.

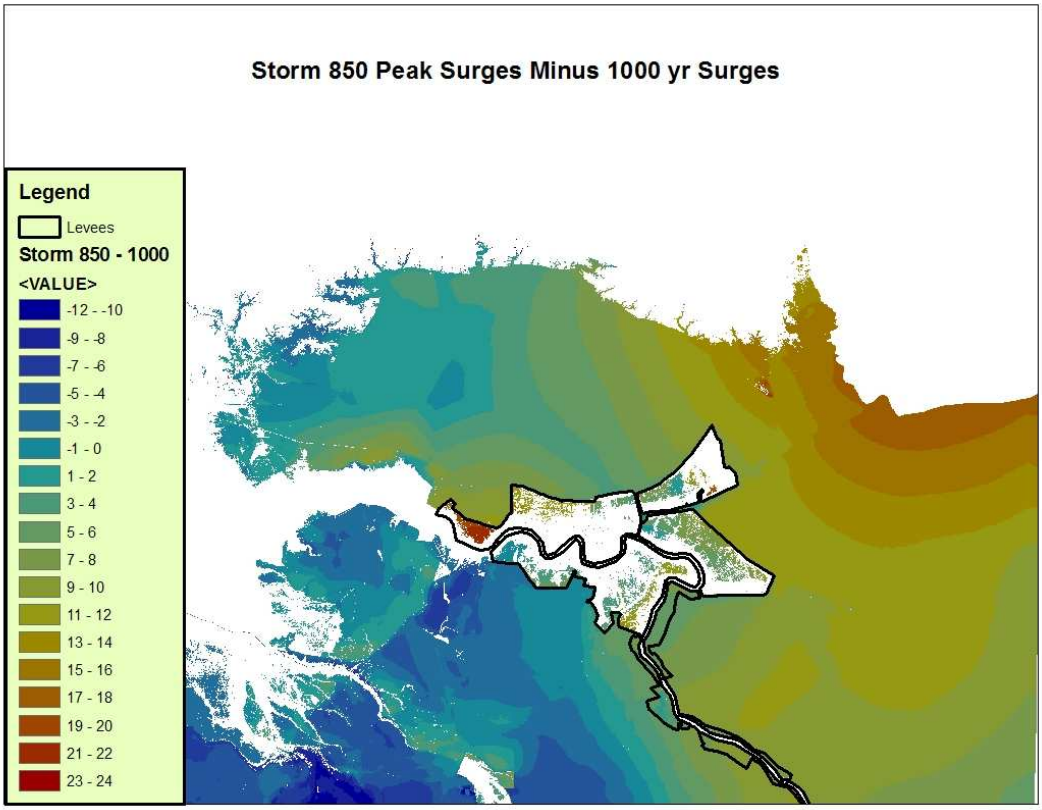

Figure 47 Surge differences between Storm 850 and 1000 year return levels (feet)

Generally both storms 870 and 850 produce surges near the current 1000 year return levels but as can be seen, one specific storm produces a wide range of surges, each with a different return period based on its specific location. Note that the 1000 year levels are chosen for comparison because the FEMA and LACPR projects did not produce 2000 year return period surge level surfaces.

Although it is difficult to ascertain surge probabilities, some estimates can be performed to compute probabilities of the storms. Using the results of Figure 43

(Knutson and Tuleya, 2004) a frequency curve was created giving the relative frequency of exceedence of a severe storm (category 3 or greater) as shown in Figure 48.

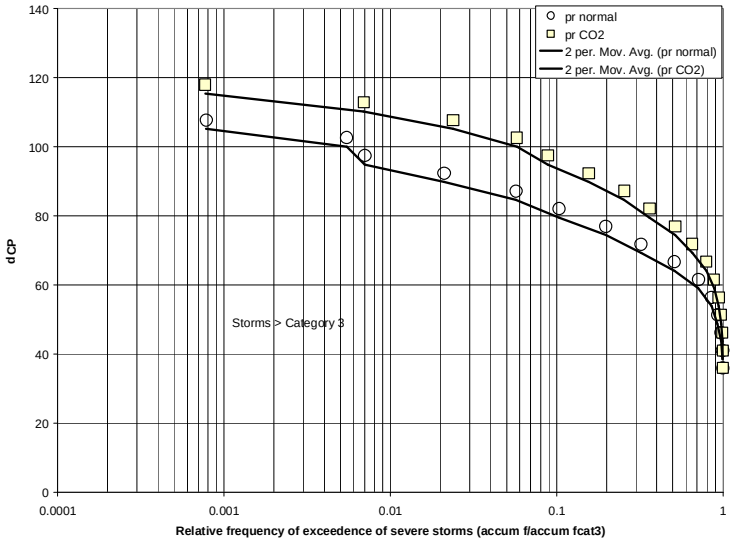

Figure 48 Relative frequency of exceedence of severe storms

This chart shows that the frequency of a central pressure reduction > 100 is about 10 times higher for the high CO_2 climate compared to the present-day climate. This implies that a 1:2000 event could become a 1:200 event. The ΔCP for the low frequency events is about 12 hPa which is about ½ of a Category which agrees with Knutson and Tuleya (2004). The results from a recent study computed specific return levels for minimum central pressure values within the Gulf of Mexico and are shown in Figure 49 (Levinson 2006).

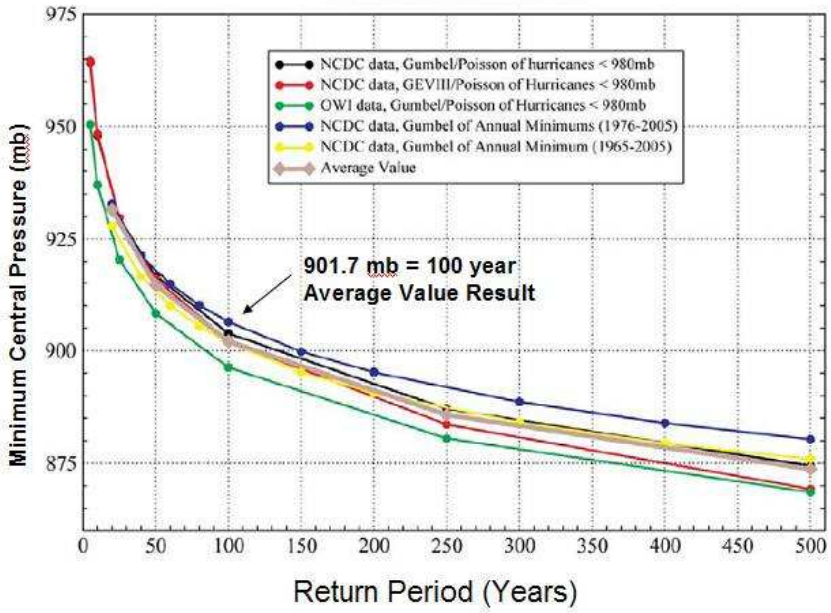

Figure 49 Central Pressure Return Values Gulf of Mexico (Levinson, 2006)
A comparison of the different return periods of the CPI determined independently in Zone B along the Central Gulf of Mexico coast. Each of the curves shown above corresponds to the GEV analysis technique applied and the period of record of the data. The grey line denotes the average of the 5 methods shown. (Levinson, 2006)

By combining these results, return periods for the storm central pressures created under abrupt climate change can be estimated. Storm 193 achieved a minimum central pressure of 880 mb and using the average Gumbel Extreme Value (GEV) curve from Figure 49, this is about a 400 year return period. Based on a 10 times greater frequency estimated using Figure 48 and derived from Knutson and Tuleya (2004), Storm 193 with a central pressure of 880 mb, would have a return period of 40 years in a doubled CO_2 climate, induced by abrupt climate change. Based on central pressure alone, Table 16 shows the shifts in frequency for each storm possible in a warmer high carbon climate.

Table 16 Future Storm Central Pressure Returns

Storm Number	MPI	Return Period (Yrs) Present	Return Period (Yrs) Future
27	900	120	12
193	880	400	40
870	870	700	70
850	850	1000	100

However, to compute the best probability estimate of a storm, all storm parameters should be used and a conditional probability distribution. For these future storms the other primary factor readily available in this study is the radius to maximum winds. Thus, a better estimate of the probability of Storm 193 and the others is given by

$$P(\text{storm}) = P(Cp) * P(Rm \mid Cp) \qquad (7.1)$$

where C*p* = minimum central pressure and R*m* = radius to maximum winds. Following (Resio et al. 2007) a computation of P(R*m* | C*p*) can be represented as

$$P(R_p \mid \Delta p) = \frac{1}{\sigma(\Delta p)\sqrt{2\pi}} e^{-\frac{x^2}{2}}$$

where (7.2 , 7.3)

$$x = \left(\frac{R_p - \bar{R}_p(\Delta p)}{\sigma(\Delta p)} \right)$$

In this equation a linear regression ($\bar{R}_p = 14. + 0.3*(110. - \Delta p)$ - with units for R_p and $\bar{R}_p$ in nautical miles and units for Δp in millibars implied) was used to represent the conditional mean for storm size and the standard deviation was taken as $\sigma(\Delta p) = 0.44\bar{R}_p(\Delta p)$ (Resio et al., 2007). Using this formulation for the conditional

probability of a storm based on both its central pressure and it's radius to maximum winds, Table 17 shows the probabilities computed for storms under present climate and also for future climate conditions.

Table 17 Future Abrupt Climate Change Storm Return Periods (RP)

Prob(Rp |Delta p)	Cp(mb)	Prob(Cp)	Prob(Cp & Rp)	Present RP(yrs)	Future RP(yrs)
0.00761	900	0.01000	0.00008	13135	1313
0.01177	880	0.00250	0.00003	33979	3398
0.01830	870	0.00143	0.00003	38246	3825
0.01658	850	0.00125	0.00002	48254	4825

Considering the conditional probability of both minimum central pressure and radius to maximum wind, the return period of Storm 870 is 38,000 years for present day climate and estimated to be 3,800 years in a future climate where SSTs are 2ºC higher than today. Of course these are only estimates and the total probability estimate should include other factors such as storm wind speed, and atmospheric influences of vertical wind sheer, and El Nino events.

Chapter 7 Discussion

7.1 Effect of Relative Sea Level Rise and Degradation of Coast on Surge Impacts

Results of simulations of high category 5 storms on the Louisiana coast for 50 years into the future show increased surge levels. The projected increases are on the magnitude of 3 to 5 feet and primarily in regions of projected high erosion and/or local subsidence. Storms were simulated on five different storm tracks and produced very large surges ranging to 30 feet or more. These storms characteristics were designed to model the most intense storm possible under today's climate and sea surface temperatures. Surges from these storms overtopped the New Orleans 100 year level protection. However, simulations of Katrina on a degraded 50 year projected coast did NOT overtop the New Orleans 100 year levee system.

As local subsidence, erosion, and sea level rise occur over specific regions along the coast, it is these regions which will feel the most impact and can expect higher future surges. Projections have been made (Barras et. al, 2004); however these are based on historic rates and capture results of recent extreme events (i.e. Hurricane Andrew) but do not take into consideration a changing climate and geomorphologoic response to climate change. Figure 50 shows the 2050 projected coast which includes land gain from state and federal protection and restoration projects. Land loss areas are shown in red and these are the locations which will most likely see higher changes in surge levels.

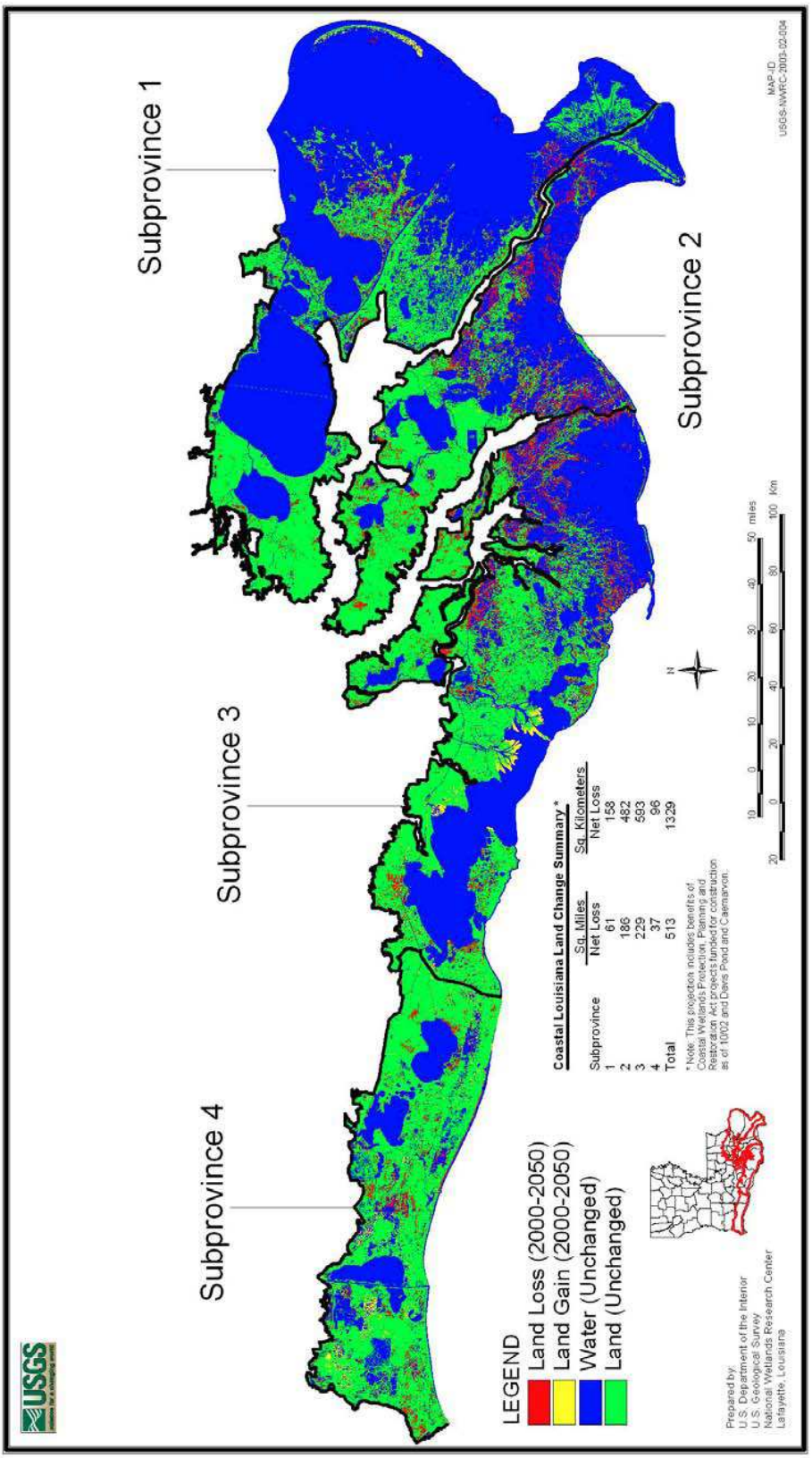

Figure 50 Projected 2050 Louisiana Coastal Land Changes from Barras et al. 2004

These 2050 projections were produced before the catastrophic hurricane season of 2005. As can be seen in Figure 50 barrier islands are projected to still exist. However, Katrina had a severe impact on the Chandeleur Islands along the east coast of Louisiana. The USGS has been actively surveying the islands for 3 years after Katrina and all surveys indicate a continued rate of erosion. The Chandeleur Islands in the Louisiana portion of the Gulf may erode all together in the near future (Sallenger, 2008). This has implications for other Louisiana barrier islands and the Mississippi River bird's foot delta. Extreme events such as Katrina and the storms possible with abrupt climate change may severely erode Louisiana barrier islands and initiate their degradation. The Mississippi delta may also feel the impacts of these storms but this depends on the amount of sediment that will be allowed to continue to flow into the Gulf. There are many large scale diversions alternatives currently being studied to divert this sediment away from the bird's foot delta.

AR4 projects global sea level rise as shown in Figure 51. Twilley and Doyle, (2007) have incorporated these projections into estimates of local relative sea level rise projections specifically for the Louisiana coast (Figure 52). These estimates also include local subsidence and the resultant range is 24 to 76 inches (2 to 6 feet) change in Relative Sea Level Rise by 2100 (Twilley and Doyle, 2007). Of critical importance in these computations and the future is how well the wetlands and marshes can keep pace with the changes in sea level. There are ongoing studies to further investigate these issues. However, the storms and simulations in this study did not account for sea level rise. Thus, if sea levels do continue to rise, impacts will most likely be even higher surges depending on the amount of relative sea level rise.

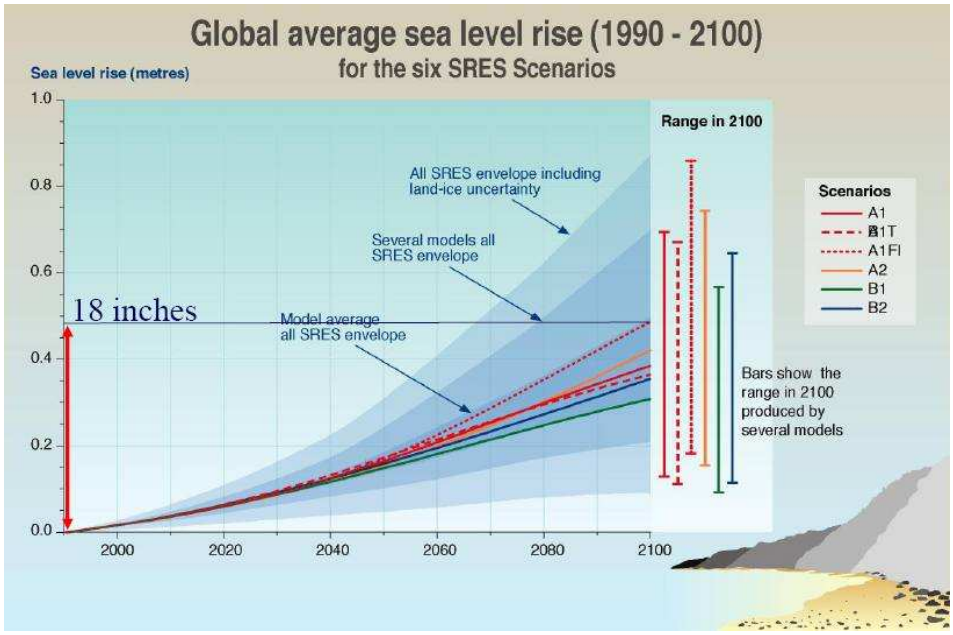

Figure 51 Global Sea Level Rise Projections (IPCC, 2007)

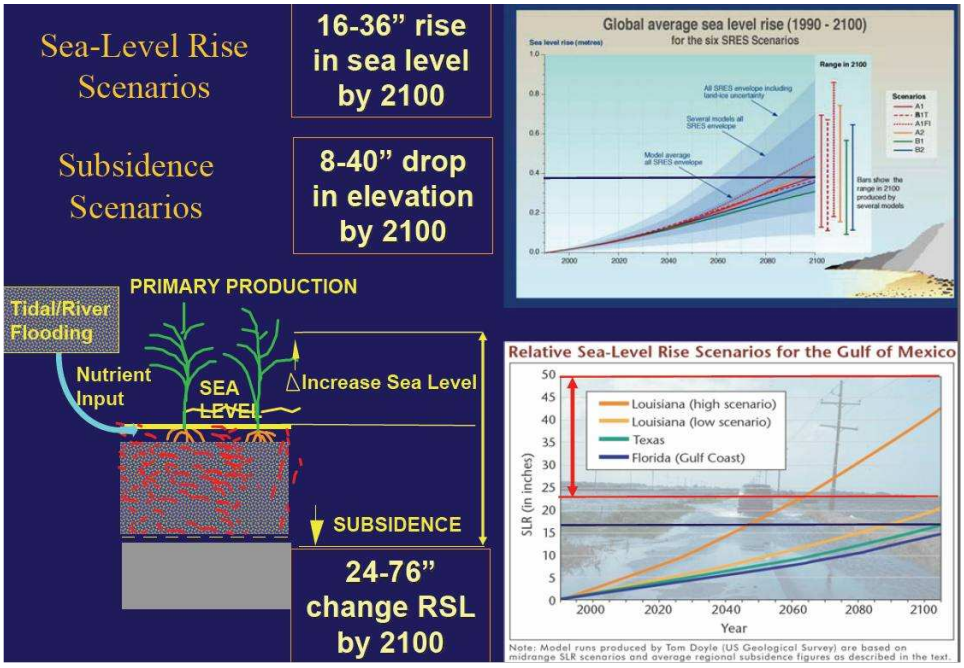

Figure 52 Relative Sea Level Rise Projections from Twilley and Doyle, (2007)

7.2 Effect of Abrupt Climate Change on Coast and Surge Impacts

Storms designed to represent plausible intense storms driven by abrupt climate change were simulated on the projected future coastline. These storms produced significant surges on the order of 30 to 40 feet in some locations. When comparing these surges to existing storm surge frequencies, the results indicate return periods ranging from current day 500 to over 1000 year return levels.

In light of these results there still could be many questions and much discussion on whether these storms and surges are really possible. The minimum central pressure and radius to maximum winds were adjusted, but how will future climatic affect the wind field distributions in storms? How will vertical wind shear change and reduce formation of new storms? How will ocean heat content and circulation patterns affect storm intensities?

A tremendous amount of effort has been expended over the years to advance understanding of the Earth's climate. We now understand more fully the physics of atmospheric and oceanic circulation and also better understand their interactions and complexities. We know many of the primary and secondary factors that affect storm surge and these include storm direction of approach, forward speed, minimum central pressure, distance from the eye-wall, radius to maximum wind, tides, slope of the coast, etc. However there are still many questions to answer and issues to address. In regards specifically to climate change and the influence on hurricanes, questions still remain. Several unresolved questions include quality and reliability of tropical cyclone databases. Also, the relative importance of thermodynamic state (e.g., potential intensity, SST, atmospheric temperature and moisture, ocean heat content, etc.) versus the role of

dynamic factors such as vertical wind shear in affecting frequency and formation of tropical cyclones.

7.3 Hurricane Frequencies and Surge Impacts in 2050

The results from hurricane frequency analyses indicate the possible increase in frequency and intensity under a warmer climate with higher carbon concentrations. The more extreme storms will produce higher storm surges and as shown in Figures 46 and 47. The highest surge increases will be in the regions susceptible to the most erosion and relative sea level rise. Along the Louisiana coast these are wetland areas but not necessarily developed urban areas. Damages will increase and be dependent on the level of protection, both manmade (levees) and natural (wetlands and barrier islands).

What is the likelihood of an increase or decrease in the frequency of these extreme events? Some research indicates very real possibilities (Knutson and Tulelya, 2004, Webster et al. 2005, Mann and Emanuel, 2006). The conclusions of AR4 (IPCC, 2007) answer an emphatic: "Yes, the type, frequency and intensity of extreme events are expected to change as the Earth's climate changes, and these changes could occur even with relatively small mean climate changes. Changes in some types of extreme events have already been observed, for example, increases in the frequency and intensity of heat waves and heavy precipitation events." AR4 identifies research efforts of Knutson and Tuleya, (2004) and others which show evidence that tropical cyclones can become more severe with greater wind speeds and more intense precipitation. AR4 also specifically addresses the question of "How likely are Major or Abrupt climate changes such as Loss of Ice Sheets or Changes in Global Ocean Circulation?" The authors state that these

changes are "not likely to occur in the 21st century" (IPCC, 2007). However, increased evidence of significant changes in glacier melting and sea formation since the publication of IPCC, 2007 have many scientists debating on the real possibilities of major changes in effect today.

To address the likelihood of climate change impacts on tropical storms, IPCC, 2007 specifically concludes that "increased tropical cyclone activity" is "Likely" (IPCC, 2007). This translates into a >66% probability of occurrence (Table 3).

7.4 Uncertainties

The importance of uncertainty cannot be overstated. Issues of data uncertainties are paramount in regards to the historic hurricane record and the need to be consistent for our current and future observations. Climate models are becoming extremely complex and we are building into these models more of the fundamental physics. But there are uncertainties in many of the parameterizations of specific components such as clouds and water vapor content.

There are uncertainties in the numerical storm surge and wave models, as well as the PBL wind models. All have to be validated against reliable, consistent, and valid measurements and observations. The ADCIRC storm surge model has been validated over the years performing hindcasts of many storms. Overall results from Katrina simulations are on the order of less than 1 foot. But can this be improved? And how much do these results depend upon the wind fields? How (un)certain are the "best" winds? One of the hardest pieces of data to collect are the wind speeds (averaged for how many seconds? minutes?) at the level of 10 meters during the lifetime an extremely

intense storm. These data are now mainly collected using dropsondes and remote devices. What are the uncertainties associated with this equipment?

In order to begin to assess uncertainties one must first identify the factors that contribute to uncertainty in the results. These can be:

- Inputs: solar energy, atmospheric composition – carbon, water vapor , methane, clouds, aerosols, etc., ocean - temperatures, salinity, etc.; landscape – deserts, forests, urban areas, etc.; cryosphere – ice sheets, glaciers, sea ice, snow, permafrost, etc. There are uncertainties in the measurements of each of the inputs to varying degrees.
- Drivers: solar energy, atmospheric circulation – jet streams, El Nino, La Nina, etc.; oceanic heat content and circulation patterns and meridional overturning current.
- Bathymetry, topography, vegetation – these uncertainties are also in the measurements, data accuracy, and how well the data represents actual conditions. Surveys have their inherent uncertainty and the physical geomorphology is constantly changing.
- Numerical models – uncertainties range from model formulation which depends not only on how well we understand the physics, but also how well the mathematical formulation and implementation can represent the physics. Other factors then include calibration and parametric implementation of some components, i.e., barotropic assumptions. Additional uncertainties arise when models are coupled together. Factors come into play such as transformation and re-griding of one model output to another model input formats as well as time step

issues such as between a storm surge model running at a 1 sec time step and a wave model running at a 30 minute time step. Additionally, uncertainty arises in scenarios where non-hydrostatic conditions affect flow and surge. ADCIRC represents ridges, roads, and levees as sub grid scale features and employs the standard weir equation to compute flows over these features. However, uncertainty can be reduced by using more accurate 3D Boussinesq models that better capture the physics of the conditions. Boussinesq models are required to capture local wave setup at critical structures and levee reachs. Additionally, the 2D Shallow Water Equations have limitations in that they do not allow bidirectional flow in the vertical and ignore density effects such as changes in salinity. These could be important in the near shore and also in the Gulf.

AR4 (IPCC, 2007) defines several classes of uncertainties. The two primary types are "value" and "structural". Value uncertainties are associated with incomplete determination of the values or results when data are inaccurate or do not fully represent the component of interest. For example, these are the uncertainties of measured observations and the quality of historic databases. Structural uncertainties are those associated with the incomplete understanding of the processes that control a particular value or result, or when the model used for a particular analysis does not fully capture the relevant processes or relationships. AR4 strives to be particularly transparent on all uncertainties and separates uncertainty from likelihood. Definitions for levels of confidence (uncertainties) are shown in Table 2 and likelihood levels (probabilities) are shown in Table 3. These definitions are very helpful to quantify

issues such as uncertainty in climate models due to parameterization of such components as clouds and water vapor processes. Skeptics have used the uncertainties in these parameterizations to formulate arguments which essentially say one can place no confidence in any of the climate models results.

The above is merely scratching the surface of the total uncertainties inherent in modeling our Earth system. But there are ongoing research efforts which are beginning to help and lay the ground work for assessing the total uncertainty in modeling complex systems. These efforts will eventually help us to further quantify uncertainty in our systems and quantify results with standard and accepted levels of confidence.

7.4 Recommendations

Results of this work can be used as a starting point for further research and study into hurricanes influenced by warming, potential abrupt climate change, and both storm and overall climate impacts. Work can be extended to further design time a suite of future possible time varying storms modeled to produce a large data set of storms, storm characteristics, and the resultant surges. This database can then be used for statistical analyses such as the JPM-OS. The JPM-OS would have to be modified using climate model projection results of future storm parameter probability distributions. These future distributions of factors such as minimum central pressure, forward speed, radius to maximum winds, etc. can then be incorporated into the JPM-OS to the produce probability distributions of future storm surges. Uncertainties can then be compiled for both the storm parameters as well as the resultant storm surges.

There are many possible metrics of intensity (maximum potential intensity, average intensity, average storm lifetime, maximum storm lifetime, average wind speed, maximum sustained wind speed, maximum wind gust, accumulated cyclone energy, power dissipation, etc.), and not all of these have been closely studied. This has been due to data limitations and other reasons. Additionally, most of the debate has tended to focus on SSTs although other environmental factors should be considered. For example, the tropical cyclone heat potential (a measure of the oceanic heat content from the sea surface to the depth of the 26 °C isotherm) may be a better indicator of the potential for hurricane intensification than SST (Scharroo et al. 2005).

With increasing temperatures and exacerbating affects of sea level rise, the coast of Louisiana is more vulnerable than ever to climate change impacts and especially extreme storm events. Along with the coastal zone, the people who populate the southern coast of Louisiana are also in peril. If storm power and frequency increase, so will damages and potentially loss of life within the coastal zone. These implications are relevant not only to Louisiana, but to all coastal areas surrounding the U.S. which are susceptible to the impacts of climate change.

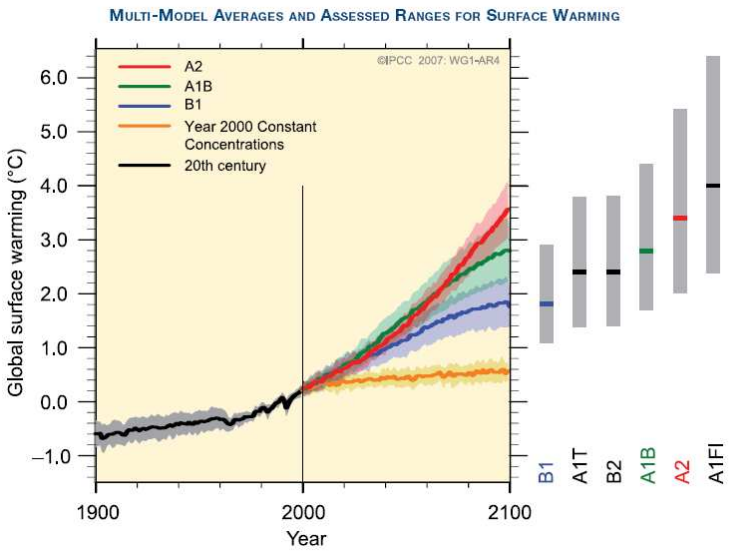

Figure 53 Global Surface Warming Projections
Solid lines are multi-model global averages of surface warming (relative to 1980–1999) for the scenarios A2, A1B and B1 shown as continuations of the 20th century simulations. Shading denotes the ±1 standard deviation range of individual model annual averages. The orange line is for the experiment where concentrations were held constant at year 2000 values. The grey bars at right indicate the best estimate (solid line within each bar) and the **likely** range assessed for the six SRES marker scenarios. The assessment of the best estimate and **likely** ranges in the grey bars includes the AOGCMs in the left part of the figure, as well as results from a hierarchy of independent models and observational constraints (IPCC, 2007).

Long-term studies and re-analysis of atmospheric and oceanic data sets will continue to be needed to address issues climate change and hurricanes. World wide efforts are ongoing and re-analysis for both historic hurricanes and for reconstruction of climate data for ready incorporation into new climate models are being performed. Additionally, improvements in modeling technology should provide new insights and advancements as well. For example, a model at NASA Goddard Space Flight Center called the Finite Volume General Circulation Model (fvGCM) that represents hurricanes and their behavior at unprecedented spatial resolutions for a GCM (Atlas et al. 2004). New satellite and enhanced in situ observing capabilities can provide new observational capabilities for hurricane internal and external environments that will increase our understanding of past and current events. This will also help in assessing the likelihood of

future projections. However, it seems for the Atlantic and Gulf of Mexico, regardless of whether the underlying cause of increased hurricane activity is a natural cycle, or by anthropogenic forcing, or a combination of the two, it appears likely that continued high levels of hurricane activity will continue as long as increased SSTs persist.

More research is needed from observations, theory, and modeling to address issues of the effect of global warming and abrupt climate changes on tropical storms.

Chapter 8 Summary and Conclusions

This work has provided a background on global climate change knowledge developed over the past few decades and the current state of climate models and their projections of future climate change. Within the context of global warming, abrupt climate change was defined and current research identified that demonstrated abrupt climate change has happened many times in the history of our planet, including as recent as 11,000 years ago. Records of these changes have been retrieved using all types of climate proxies form ice cores and tree rings to speleothems. These records hold clues not only to climate change but some also document the frequency of intense hurricanes during ancient and historic climates. Previous and current research searching for trends in hurricane frequencies, intensities, and genesis were presented which show that our databases are still too short and the data itself may not have enough quality to derive scientifically provable trends.

The objectives of this research were threefold: (1) Quantify storm surges for the Louisiana Coast with wetland loss as projected by the USGS in the year 2050; (2) Project the impacts of abrupt climate change through creation and modeling of storms of increasing maximum intensities possible under such change to estimate future surge levels; and (3) Estimate frequencies of future storms based upon minimum central pressure and radius to maximum wind, and compare surge results obtained from these future storms, to published storm surge return period levels.

The first objective was met by simulating the most intense storm possible given today's climate using a topography representative of the landscape 50 years from the present. The conclusion drawn from this objective is that if the Louisiana coast continues

to degrade through erosion processes and subsidence, the results will be higher surges which will depend on the storm intensity, direction, minimum central pressure and other atmospheric parameters as previously discussed. Surge heights ranged from 1 to 3 feet higher for the storms simulated and specific future surges will additionally depend on the degree of local subsidence and relative sea level rise. Additionally, the New Orleans 100 year level of protection will protect against a Katrina–like storm 50 years form now. However, overtopping will occur for more intense storms that are possible given our present climate.

To meet the second objective, results form current research was used to create possible storms characteristic of future conditions influenced from 1 to 6ºC of average global warming. Storm surges produced by these storms were quantified and differences between surges of these future storms were compared to surges of comparable present day storms. Surges can be significantly higher along many areas of the coast. Lake Pontchartrain surges increases ranged from 2 feet to over 10 feet higher for each degree increase in SST. IPCC 'A1F1' high emission scenario results in an estimated 2ºC increase in global mean temperature by 2050, and 4ºC by 2100. Realization of these temperatures will result in 2 feet to 7 feet higher surges depending on storm intensity, direction, forward speed, and other atmospheric conditions. New Orleans levees will offer some protection from more intense storms that may potentially form influenced by global warming and increased sea surface temperatures, but overtopping will occur.

The third objective was met by comparing future storm surges against storm surge return levels, specifically for the 1000 year return period, produced from current present coastal storm surge analyses. Additionally, estimates of the probabilities of these

future storms were computed along with shifts in the frequencies of these events given abrupt climate change realization. There is no doubt our climate is warming and this warming is having impacts regionally and globally. Whether the cause of this warming is human induced or not is still open for debate. However, based on the results of these storm simulations, for each 1ºC rise in average SSTs, surges from extreme storms will increase on the order of at least 1 to 3 feet or more depending on other atmospheric and oceanic conditions. Table 16 summarizes probabilities of future extreme events and the potential shifts in frequencies from present climate conditions. A storm with a probability of 1:10000 years may become a storm of 1:1000 years return period. Figure 53 shows IPCC projections for global average temperatures for six SRES scenarios with the highest estimate of 4ºC with the likely range of up to 6 ºC by 2100. If temperatures reach these limits, future storms may potentially be very similar to the storms designed in this study along with the high surges produced by these powerful events. These are extreme storms and from basis statistical reasoning, a small shift in the mean of a primary variable (i.e. average temperature) can result in substantial changes in the frequency of the extremes. Extremes are the infrequent events at the high and low end of the range of possible values for a particular variable. An increase in the frequency of one extreme (e.g. the number of hot days) can be accompanied by a decline in the opposite extreme (in this case the number of cold days). Ultimately, the result is an increase in the number of extremes (hot days or severe storms). Within the next 50 years, the amount of increased warming will determine the realization of the exact number of these extreme events.

References

Alley, R.B, and P.U. Clark. 1999. The deglaciation of the Northern Hemisphere: A global perspective. Annual Reviews of Earth and Planetary Sciences 27:149-182.

Alley, R. B., 2000. The Younger Dryas cold interval as viewed from central Greenland. *Quartenary Science Reviews* 19:213-226.

Alley, R. B., 2003. Abrupt Climate Change Inevitable Surprises, National Research Council

ASCE, 1990. Minimum design loads for buildings and other structures, ASCE 7-88, New York.

ASCE 1996. Minimum design loads for buildings and other structures, ASCE 7-95, New York.

Atlas, R., et al., 2004. Hurricane forecasting with the high-resolution NASA finite volume general circulation model. *Geophysical Research Letters* 32, pp. L03807, doi:10.1029/2004GL021513.

Barnett, T.P., Pierce, D.W., Schnur, R., 2001. Detection of Anthropogenic climate change in the world's oceans. Science 292: 270–274.

Brohan P., et al., 2006. Uncertainty estimates in regional and global observed temperature changes: A new data set from 1850. *J. Geophys. Res.*, **111**, D12106, doi:10.1029/2005JD006548.

Barras, J., Beville, S., Britsch, D., Hartley, S., Hawes, S., Johnston, J., Kemp, P., Kinler, Q., Martucci, A., Porthouse, J., Reed, D., Roy, K., Sapkota, S., and Suhayda, J., 2003. Historical and projected coastal Louisiana land changes: 1978-2050: USGS Open File Report 03-334, 39 p. (Revised January 2004).

Britsch, L.D., Dunbar, J.B., 1993. Land-loss rates: Louisiana coastal plain: Journal of Coastal Research, v. 9, p. 324-338.

Bryden, Longworth, H.L., Hannah R., Cunningham, S. A., 2005. Slowing of the Atlantic meridional overturning circulation at 25° N, *Nature*, **438**, 655-657.

Dickson et al., 2002. Rapid freshening of the deep North Atlantic Ocean over the past four decades, *Nature*, **416**, 832-836.

Camp Dresser & McKee, Inc., Study to Revise and Update FEMA's Storm Surge Model. Federal Emergency Management Agency, Washington, D.C., 1985.

Conner, W.C., Kraft, R.H., Harris, D.L., Empirical Methods for Forecasting the Maximum Storm Tide Due to Hurricanes and Other Tropical Storms, Monthly Weather Review 85(4):113-116, 1957.

Dansgaard, W., et al., 1984. North Atlantic climatic oscillations revealed by deep Greenland ice cores. In: *Climate Processes and Climate Sensitivity* [Hansen, J.E., and T. Takahashi (eds.)]. American Geophysical Union, Washington, DC, pp. 288–298.

Dansgaard, W., et al., 1993. Evidence for general instability of past climate from a 250-kyr ice-core record. *Nature*, **364**, 218–220.

Dietrich, J.C., Kolar, R., Luettich, R., 2005. "Assessment of ADCIRC's Wetting and Drying Algorithm." School of Civil Engineering and Environmental Science, University of Oklahoma, Norman, Oklahoma

Harris, D.L., 1963. Characteristics of the Hurricane Storm Surge, U.S. Department of Commerce Weather Service Technical Paper No. 48.

Dowdeswell, Julian A., 2006. "The Greenland Ice Sheet and Global Sea-Level Rise", Science 311: 963-964.

Emanuel, K. 1987 . The dependence of hurricane intensity on climate. Nature 326, pp. 483–485.

Emanuel, K. 1998. “The power of a hurricane: An example of reckless driving on the information superhighway.” *Weather* 54, 107-108.

Emanuel, K. 2005. Increasing destructiveness of tropical cyclones over the past 30 years. Nature 436:686-688.

——. 2000. A statistical analysis of tropical cyclone intensity. *Monthly Weather Review* 128, pp. 1139–1152.

——. 2005a. Increasing destructiveness of tropical cyclones over the past 30 years. *Nature* 436, pp. 686–688.

——. 2005b. Emanuel replies. *Nature* 438, pp. E13.

Emanuel, K., Ravela S., Vivant, E., Risi, C., 2006. A Statistical Deterministic Approach to Hurricane Risk Assessment. Bulletin of the American Meteorological Society, DOI:10.1175/BAMS-87-3-299

Flather, R. A., 1988. “A numerical model investigation of tides and diurnal-period continental shelf waves along Vancouver Island,” *Journal of Physical Oceanography* 18, 115-139.

Fleitman, 2008. Quarternary Science Reviews, Vol 26, pp. 170-188.

Frappier, A., Knutson T., Liu, K-B., Emanuel, K., 2007. Perspective: Coordinating Paleoclimate Research on Tropical Cyclones with Hurricane-Climate Theory and Modeling, Tellus 59A.

Geerts, B., 1999. Trends in atmospheric science journals. *Bull. Am. Meteorol. Soc.*, **80**, 639–652.

Gregory, J.M., Dixon, K.W., Stouffer, R.J., Weaver, A.J., Driesschaert, E., Eby, M., Fichefet, T., Hasumi, H., Hu, A., Jungclaus, J.H., Kamenkovich, I.V., Levermann, A., Montoya, M., Murakami, S., Nawrath, S., Oka, A., Sokolov, A.P., Thorpe, R.B., 2005. "A Model Intercomparison of Changes in the Atlantic Thermohaline Circulation in Response to Increasing Atmospheric CO2 Concentration", *Geophysical Research Letters*, Vol. 32, L12703.

Hansen, J., A. Lacis, R. Ruedy, and M. Sato, 1992. Potential climate impact of Mount-Pinatubo eruption. *Geophys. Res. Lett.*, **19**, 215–218.

Henderson-Sellers, A., et al., 1998. Tropical cyclones and global climate change: a post-IPCC assessment. *Bulletin of the American Meteorological Society* 79, pp. 19–38.

Houghton, J.T., et al. (Eds), 2001. Climate change 2001: The Scientific Basis: contributions of working group I to the third assessment report of the intergovernmental panel on climate change. Cambridge, UK: Cambridge University Press.

Holland, J.G., 1997. “The Maximum Potential Intensity of Tropical Cyclones”, *Journal Of the Atmospheric Sciences* 54:2519-2541.

IPCC, 1990. *Climate Change: The IPCC Scientific Assessment* [Houghton, J.T., G.J. Jenkins, and J.J. Ephraums (eds.)]. Cambridge University Press, Cambridge, United Kingdom and New York, NY, USA, 365 pp.

IPCC, 1992. *Climate Change 1992: The Supplementary Report to the IPCC Scientific Assessment* [Houghton, J.T., B.A. Callander, and S.K. Varney (eds.)]. Cambridge University Press, Cambridge, United Kingdom and New York, NY, USA, 200 pp.

IPCC, 1995. *Climate Change 1994: Radiative Forcing of Climate Change and an Evaluation of the IPCC IS92 Emission Scenarios* [Houghton, J.T., et al. (eds.)]. Cambridge University Press, Cambridge, United Kingdom and New York, NY, USA, 339 pp.

IPCC, 1996. *Climate Change 1995: The Science of Climate Change* [Houghton, J.T., et al. (eds.)]. Cambridge University Press, Cambridge, United Kingdom and New York, NY, USA, 572 pp.

IPCC, 2001a. *Climate Change 2001: The Scientific Basis. Contribution of Working Group I to the Third Assessment Report of the Intergovernmental Panel on Climate*

Change [Houghton, J.T., et al. (eds.)]. Cambridge University Press, Cambridge, United Kingdom and New York, NY, USA, 881 pp.

IPCC, 2001b. *Climate Change 2001: Synthesis Report. A contribution of Working Groups I, II, and III to the Third Assessment Report of the Intergovernmental Panel on Climate Change* [Watson, R.T., et al. (eds.)]. Cambridge University Press, Cambridge, United Kingdom and New York, NY, USA, 398 pp.

Jelesnianski, C.P., 1972, SPLASH (Special Program to List Amplitudes of Surges From Hurricanes) I. Landfall Storms, U.S. Department of Commerce NOAA Technical Memorandum NWS TDL-46.

Jelesnianski, C.P., Chen, J., Shaffer, W.A., 1992, SLOSH: Sea, Lake, and Overland Surges from Hurricanes, U.S. Department of Commerce NOAA Technical Report NWS 48.

Kerr, R. 2006. "A Tempestuous Birth for Hurricane Climatology" *Science* 312: 676-678.

Knutson,T. R., et al., 2001. Impact of CO2-induced warming on hurricane intensities as simulated in a hurricane model with ocean coupling. *Journal of Climate* 14 (11), pp. 2458–2468.

Knutson T.R. and R.E. Tuleya, 2004. Impact of CO2-induced warming on simulated hurricane intensity and precipitation: Sensitivity to the choice of climate model and convective parameterization. Journal of Climate 17: 3477–3495.

Knutson,T. R., et al., 2006. Assessment of twentieth-century regional surface temperature trends using the GFDL CM2 coupled models. *Journal of Climate* 19 (9), pp. 1624–1651.

Kolar, R. L., Gray, W. G., Westerink, J. J., and Luettich, R. A., 1993. "Shallow water modeling in spherical coordinates: Equation formulation, numerical implementation, and application," Journal of Hydraulic Research.

Kolar, R.L., Westerink, J.J., 2000. "A Look Back at 20 Years of GWC-Based Shallow Water Models," *Computational Methods in Water Resources XIII, Vol. 2*, Bentley et al., eds. 899-906, Balkema.

Landsea, C.W., et al., 1999. Atlantic basin hurricanes: indices of climatic changes. *Climatic Change* 42, pp. 89–129.

Landsea,T. R., 2005. Hurricanes and global warming. *Nature* 438, pp. E11–E12.

Landsea, T. R., et al., 2006. Can we detect trends in extreme tropical cyclones? *Science* 313, pp. 452–454.

Levenson, D., 2006. Update to the Standard Project Hurricane, NOAA, National Climatic Data Center

Liu, K-b., 2004. *Paleotempestology: Principles, methods, and examples from Gulf coast lake sediments*. In Hurricanes and Typhoons: Past, Present, and Future. Eds. Murnane, R.J and Liu, K., Columbia University Press, New York, 13–57pp.

Luettich, R. A., Jr., Westerink, J. J., 2004. Formulation and Numerical Implementation of the 2D/3D ADCIRC Finite Element Model Version 44.XX

Luettich, R. A., Jr., Westerink, J. J., and Scheffner, N. W., 1992. "ADCIRC: An advanced three-dimensional circulation model for shelves, coasts, and estuaries," Technical Report DRP-92-6, U.S. Army Engineer Waterways Experiment Station, Vicksburg, MS.

Luettich, R.A., Westerink, J.J., 1999. "Elemental wetting and drying in the ADCIRC hydrodynamic model: upgrades and documentation for ADCIRC version 34.XX." *Contractors Report*, U.S. Army Corps of Engineers.

Lynas, M., 2008, Six Degrees, National Geographic Society

Mercer, J.H., 1978. West Antarctic ice sheet and CO2 greenhouse effect: a threat of disaster. *Nature*, **271**, 321–325.

Massey, W.G., Gangai, J.W., Drei-Horgan, E., Slover, K.J., Dewberry, 2007. History of Coastal Innundation Models, Marine Technology Society Journal, Vol.41 No.1.

Mann, M. E., and Emanuel, K.A., 2006. Atlantic hurricane trends linked to climate change. *Eos, Transactions American Geophysical Union* 87, pp. 233–244.

National Research Council (NRC), 1998. Decade-to-Century Scale Climate Variability and Change: A Science Strategy. National Academy Press, Washington D.C.

National Oceanic and Atmospheric Asssociation (NOAA), 2006. Global Surface Temperature Anomalies. Asheville, NC: NOAA/National Climatic Data Center. Online at http:/www.ncdc.noaa.gov/oa/climate/research/anomalies/ Accessed April 2006.

Pielke, R.A. Jr., 2005. Are there trends in hurricane destruction? *Nature* 438, pp. E11.

Pielke, R.A. Jr., et al., 2005. Hurricanes and global warming. *Bulletin of the American Meteorological Society* 86, pp. 1571–1575.

Resio D. T., Boc S.J., Borgman, L., Cardone, V.J., Cox A., Dally W.R., Dean R.G., Divoky, D., Hirsh, E., Irish, J.L., Levinson, D., Niedororda, A., Powell, M.D., Ratcliff, J.J., Stutts, V., Suhada, J., Toro, G.R., Vickery, P.J., Westerink, J.J., 2007. White Paper on Estimating Hurricane Inundation Probabilities. USACE-ERDC

Sallenger, A., 2008. Extreme Storm Impacts, Severe Storm Prediction, Education and Evacuation from Disasters Conference

Schade, L. 2000. "Tropical Cyclone Intensity and Sea Surface Temperature" Journal of the Atmospheric Sciences, Volume 57

Scharroo, R., Smith,W. H. F., and Lillibridge, J. L., 2005. Satellite altimetry and the intensification of Hurricane Katrina. *Eos, Transactions American Geophysical Union* 86 (40), p. 366

Schiermeier, Q. 2005. "Trouble brews over contested trend in hurricanes." *Nature* 2005.

Shepherd J, Knutson T., 2007. "The Current Debate on the Linkage Between Global Warming and Hurricanes." Geography Compass January 2007.

Stanhill, G., 2001: The growth of climate change science: A scientometric study. *Climate Change*, **48**, 515–524.

Stefensen, J.P., Andersen, K.K., Bigler, M., Clausen, H.B., Dahl-Jensen, D., Fischer, H., Goto-Azuma, K., hansson, M., Johnsen, S.J., Jouzel, J., Masson-Delmotte, V. Popp, T., Rasmussen, S.O., Rothlisberger, R., Ruth, U. Stauffer, B. Siggaard-Andersen, M., Sveinbjornsdottir, A.E., Svensson, A., White, J.W., 2008, High Resolution Greenland Ice Core Data Show Abrupt Climate Change Happens in Few Years, Science 321, 680 (2008); DOI: 10.1126/science.1157707

Suhayda, J.N. 1997. Modeling impacts of Louisiana barrier islands on wetland hydrology. Journal of Coastal Research 13: 686-693

Thompson, E. F., Cardone, V. J., 1996. Practical Modeling of Hurricane Surface Wind Fields, Journal of Waterway, Port, Coastal, and Ocean Engineering

TIME, August 29, 2005. Is Global Warming Fueling Katrina?

Tonkin H., Holland G., Holbrook N., Henderson-Sellers A., 2000. An Evaluation of Thermodynamic Estimates of Climatological Maximum Potential Tropical Cyclone Intensity. AMS Monthly Weather Review, Volume 128

Trenberth, K. 2005. Uncertainty in Hurricanes and Global Warming. Science 308: 1753–1754.

Twilley R., Doyle, T., 2007. Is it Doable: Rising Sea Levels and the Challenges of Restoring Coastal Louisiana, Forum for Global Climate Change

Twilley R., Couvillion B., Hossain I., Kaiser C., Owens A., Steyer G., Visser J., 2008. Coastal Louisiana Ecosystem Assessment and Restoration Program: The Role of Ecosystem Restoration Planning in the Mississippi River Deltaic Plain. American Fisheries Society Symposium 64:29-46

Vickery, P.J., Twisdate, L.A., 1995. Prediction of Hurricane Wind Speeds in the United States. Journal of Structural Engineering, Vol. 121, No. 11

Vickery, P.J., Skerjl, P.F., L.A. Twisdale, 2000: Simulation of hurricane risk in the U.S. using empirical track model, *J.Struct. Engr.*, 1222-1237.

Walshaw, D., 2000. Modeling Extreme Wind Speeds in Regions Prone to Hurricanes. Applied Statistics, Vol 49 Part 1, pp. 51-62

Webster, P.J., Holland, G.J., Curry, J.A. and H.-R. Chang. 2005. Changes in tropical cyclone number, duration, and intensity in a warming environment. Science 309:1844-1846.

Westerink, J.J. 1993. “Tidal prediction in the Gulf of Mexico/Galveston Bay using model ADCIRC-2DDI,” Contractors Report to the U.S. Army Engineer Waterways Experiment Station, Vicksburg, Mississippi.

Westerink, J.J., Luettich, R.A., Feyen, J.C., Atkinson, J.H., Dawson, C., Roberts, H.J., Powell, M.D., Dunion, J.P., Kubatko, E.J., Pourtaheri, H.P., (2008), A Basin to Channel Scale Unstructured Grid Hurricane Storm Surge Model Applied to Souhern Louisiana, Monthly Weather Review, 136, *3, 833-8*64

US Army Corps of Engineers (USACE), New Orleans District, January 2004, Review of the Application of the Numerical Model “ADCIRC” For Storm Surge Predictions in the New Orleans, LA Vicinity, Report Prepared By: Technical Review Committee: Robert G. Dean, Mark Powell, Robert O’Reid.

U.S. Army Corps of Engineers. 2007. “Performance Evaluation of the New Orleans and Southeast Louisiana Hurricane Protection System. Final Report of the Interagency Performance Evaluation Task Force; Volume IV – The Storm.” 26 March.

Vita

Jay Ratcliff was born in New Orleans, Louisiana and received his B.S. in Civil Engineering from Tulane University in May of 1979. He continued his studies in this field and received his M.E. from the University of New Orleans in May of 1994.